Oncology and Translational Medicine

Volume 9 • Number 2 • April2023

Oncology and Translational Medicine Volume 9 • Number 2 • April 2023 pp 49-98

邮发代号：38-121
ISSN 2095-9621

GENERAL INFORMATION
≫otm.tjh.com.cn

ISSN 2095-9621
CN 42-1865/R

Oncology and Translational Medicine

肿瘤学与转化医学（英文）

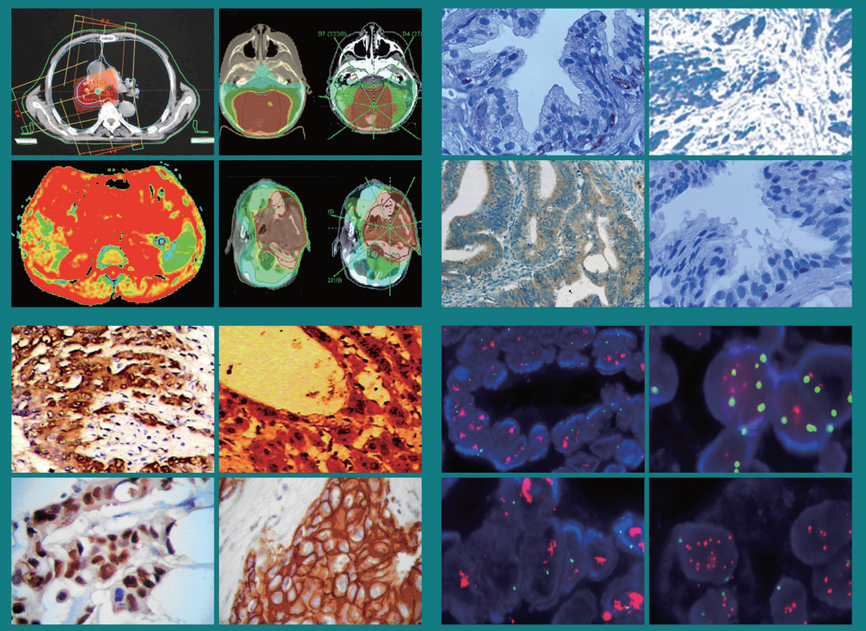

Volume 9
Number 2
April 2023

OTM

Oncology and Translational Medicine
April 2023 Volume 9 Number 2

Contents

中国抗癌协会系列期刊
JOURNAL OF THE CHINA ANTICANCER ASSOCIATION

Oncology and Translational Medicine

Oncology and Translational Medicine

Editors

Oncology and Translational Medicine
DOI 10.1007/s10330-023-0642-2
April 2023, Vol. 9, No. 2, 49–55

REVIEW ARTICLE

Research progress on immunotherapy targeting the tumor immune microenvironment for cholangiocarcinoma*

Tianyin Ma[1, 2], Zhang Chen (Co-first author)[1, 2], Yibo Chai[1, 2], Xiangdong Gongye[1, 2], Peng Xia[1, 2], Chenming Qu[1, 2], Ming Tian[1, 2] (✉), Yufeng Yuan[1, 2, 3] (✉)

[1] Department of Hepatobiliary and Pancreatic Surgery, Zhongnan Hospital of Wuhan University, Wuhan 430071, China
[2] Clinical Medicine Research Center for Minimally Invasive Procedure of Hepatobiliary & Pancreatic Diseases of Hubei Province, Wuhan 430071, China
[3] TaiKang Center for Life and Medical Sciences, Wuhan University, Wuhan 430071, China

Abstract

Cholangiocarcinoma (CCA) is the second most common hepatobiliary cancer, and its incidence has increased significantly in recent years. CCA has poor prognosis owing to the limited diagnosis and treatment options. The tumor immune microenvironment (TIME), which comprises immune cells, cytokines, and chemokines, plays a significant role in cancer progression, the evasion of immune surveillance, and therapeutic responses. Immunotherapeutic strategies targeting the TIME offer the potential for the recognition and eradication of CCA. This review discusses the cellular and molecular components of the TIME in CCA and immunotherapeutic strategies targeting it.

Received: 18 April 2023
Revised: 23 April 2023
Accepted: 29 April 2023

Key words: Cholangiocarcinoma; Tumor Immune Microenvironment; Tumor-Associated Macrophages; Tumor-Infiltrating Lymphocytes; Adoptive T-cell Transfer; Immune Checkpoint Inhibitors; Immunotherapy

Cholangiocarcinoma (CCA), a malignant tumor originating from the biliary duct, has poor prognosis because of limited diagnostic and treatment options [1, 2]. Current treatment options for CCA include surgery, chemotherapy, and radiotherapy. However, delayed diagnosis, high recurrence rates, and a lack of effective systemic therapies compromise the prognosis [3]. The tumor immune microenvironment (TIME) is a multifaceted system comprising immune cells, cytokines, and chemokines that actively interact with neoplastic cells. These intricate interactions critically affect cancer progression, the evasion of immune surveillance, and responses to therapeutic interventions [4]. By modulating host immunity to recognize and eradicate malignant cells, immunotherapy targeting the TIME is a potential therapeutic strategy against several cancers, including CCA [5].

Cellular and molecular components of TIME in CCA

Tumor-associated macrophages (TAMs) and their roles in promoting tumor growth and metastasis

TAMs are abundant in the CCA tumor microenvironment and contribute to tumor progression, angiogenesis, and metastasis by secreting growth factors, cytokines, and chemokines. These key TIME components contribute to disease progression [6]. They also suppress T cells and promote the expansion of immunosuppressive

✉ Correspondence to: Ming Tian. E-mail: Tianm131@163.com; Yufeng Yuan. E-mail: yuanyf1971@whu.edu.cn
* Supported by grants from the Research Fund of the Health Commission of Hubei Province (No. WJ2021M255); Cancer Research and Translational Platform Project of Zhongnan Hospital of Wuhan University (No. ZLYNXM202004); Key Research and Development Program of Hubei Province (No. 2021BCA114); the Research Fund from the Medical Sci-Tech Innovation Platform of Zhongnan Hospital of Wuhan University (No. PTXM2021022); and the Outstanding Doctoral (Postdoctoral) Program of Zhongnan Hospital of Wuhan University (No. ZNYB2021021).

cells, such as regulatory T cells (Tregs) and myeloid-derived suppressor cells (MDSCs) [7]. TAMs are characterized by their remarkable ability to adjust and transform, allowing them to perform pro-tumoral or anti-tumoral actions, as influenced by stimuli within their immediate environment [8]. Their high plasticity renders them important for promoting or suppressing tumor growth. In CCA, TAMs promote tumor growth and metastasis through various mechanisms [6, 9].

First, they promote CCA progression through the expression of immune checkpoint molecules, such as signal regulatory protein alpha (SIRPα) and programmed cell death protein 1 (PD1). Elevated SIRPα and PD1 expression in TAMs is associated with poor prognosis in patients with intrahepatic CCA, suggesting a potential role for these immune checkpoint molecules in immune evasion and tumor progression [9].

Second, TAMs secrete various cytokines and chemokines that promote tumor cell proliferation, angiogenesis, and tissue remodeling [8]. Physiologically, TAMs overexpress matrix metalloproteinase 1 (MMP1), a protein-digesting enzyme that participates in the breakdown of extracellular matrices and facilitates tumor infiltration into surrounding tissues [10]. TAMs can also suppress anti-tumor immune responses by interacting with other immune cells, such as MDSCs and Tregs, within the TIME [8]. This immunosuppressive environment enables tumor cells to escape immune surveillance and promote tumor growth and metastasis. Thus, given the significance of TAMs in the promotion of CCA development, therapies targeting them are being considered as potential therapeutic options for this malignancy [6, 9].

Tumor-infiltrating lymphocytes (TILs) and their roles in tumor immunity

TILs, including $CD4^+$ helper T cells, $CD8^+$ cytotoxic T cells, Tregs, B cells, and natural killer (NK) cells, are essential components of CCA TIME. They infiltrate tumor tissues and play pivotal roles in tumor immunity [2, 11, 12]. Their presence within the TIME influences cancer progression, immune surveillance, and therapeutic responses [4, 13]. $CD4^+$ helper T cells and $CD8^+$ cytotoxic T cells are key players in anti-tumor immune responses as they can recognize and bind tumor antigens to induce tumor cell killing. Patients with CCA tend to exhibit better treatment outcomes when their tumors are infiltrated by a high density of TILs, particularly $CD8^+$ T cells [11, 12]. The LEL subtype of Epstein-Barr virus-associated intrahepatic cholangiocarcinoma is linked with good survival outcomes, possibly due to the activation of tumor-infiltrating B and $CD8^+$ T cells [14]. However, immunosuppressive factors in the TIME can suppress the activity of these T cells, resulting in immune evasion and tumor progression [2].

Tregs are a subset of TILs that suppress anti-tumor immune responses by inhibiting effector T cell functions, leading to a pro-tumorigenic environment [12]. Tregs are strongly associated with poor prognosis in all types of CCA [15]. Owing to their potentially important role in tumor progression, especially in lymph node metastasis, the $FoxP3^+/CD8^+$ ratio is considered an important marker of the immune environment in intrahepatic cholangiocarcinoma (ICC) [16, 17].

B cells and NK cells also contribute to tumor immune responses. B cells produce tumor-specific antibodies and serve as antigen-presenting cells, whereas NK cells are innate immune cells that kill tumor cells without prior sensitization. However, their roles in CCA have not been fully elucidated [2].

Overall, TILs play crucial roles in shaping anti-tumor immune responses, and their presence within the TIME is vital. The elucidation of their complex interplay and function will aid the development of novel immunotherapeutic strategies for the treatment of this disease. By investigating the multifaceted roles of TILs in CCA, valuable insights that can ultimately lead to improved treatment outcomes using immunotherapy may be gained [2, 11].

MDSCs and their immunosuppressive effects

MDSCs accumulate in the TIME of CCA and contribute to immunosuppression by inhibiting the activation and functioning of effector T cells, promoting tumor growth and immune evasion [4]. MDSCs are a heterogeneous population of immature myeloid cells that expand in response to tumor-derived factors. They suppress immune responses by inhibiting the functions of T cells, NK cells, and dendritic cells, thereby promoting tumor progression and metastasis. The gut microbiome regulates hepatocytes to form an immunosuppressive environment through the accumulation of $CXCR2^+$ polymorphonuclear MDSCs to promote CCA [18]. Although the significance of MDSCs in CCA are yet to be conclusively determined, they can be regulated by cancer-associated fibroblasts to enhance cancer stemness [19].

Immune checkpoint molecules and their roles in immune evasion

Immune checkpoint molecules play a crucial role in regulating the immune system and maintaining self-tolerance. However, these molecules can be exploited by cancer cells, including CCA cells, to evade immune surveillance and promote tumor progression. In CCA, immune checkpoints such as programmed death-1 (PD-1), programmed death ligand-1 (PD-L1), and cytotoxic T-lymphocyte-associated protein 4 (CTLA-4) play significant roles in immune evasion [20].

PD-1 is a receptor on activated T cell surfaces, whereas PD-L1 is a ligand on tumor and antigen-presenting cells. Interactions between PD-1 and PD-L1 suppress T cell activation and proliferation, thereby dampening anti-tumor immune responses [20]. In extrahepatic CCA, PD-L1, TILs, and human leukocyte antigen have shown potential for immunotherapy [21].

CTLA-4, an immune checkpoint molecule, is expressed on T cells and competes with the co-stimulatory molecule CD28 to bind B7 ligands (CD80 and CD86) on antigen-presenting cells. This competition results in the inhibition of T cell activation and the suppression of immune responses against cancer cells [22]. Thus, targeting immune checkpoint molecules is a promising therapeutic strategy for CCA. Immune checkpoint inhibitors (ICIs) such as anti-PD-1, anti-PD-L1, and anti-CTLA-4 antibodies have shown great potential in preclinical studies and clinical trials, providing a rationale for further investigation of their use for patients with CCA [22–24].

Cytokines and chemokines in the TIME and their effects on tumor progression and immune responses

Cytokines and chemokines, including transforming growth factor-beta (TGF-β), interleukin-6 (IL-6), and chemokine (C-C motif) ligand 2 (CCL2), play vital roles in shaping the TIME in CCA. They regulate immune cell recruitment, infiltration, and activation, thereby influencing tumor progression and the overall immune response. Chemokine (C-C motif) ligand 20 (CCL20), a crucial player in CCA cell migration, promotes tumor progression [25]. Similarly, CXCL12 expression in intrahepatic CCA is associated with metastasis and a poor prognosis [26]. These chemokines attract immune cells to tumor sites and modulate immune responses.

Cytokines, such as interleukins and interferons, also play essential roles in the TIME. They promote or suppress tumor growth and modulate immune responses against cancer cells. Pro-inflammatory cytokines stimulate immune cell activation and enhance anti-tumor responses, whereas anti-inflammatory cytokines suppress immune cell functions and promote tumor immune evasion. According to Guo *et al.*, the absence of AT-rich interactive domain 1A (ARID1A) within the SWItch/sucrose nonfermentable (SWI/SNF) complex impairs TGF-β signaling activation in biliary epithelial cells. These alterations lead to the development of CCA, originating from biliary cells [27]. Elucidating the roles of specific cytokines and chemokines in the TIME in CCA will aid the development of immunotherapeutic strategies to improve patient outcomes. Li *et al.* showed that the cGGNBP2-184aa protein, produced by the IL-6-induced *cGGNBP2* gene, promotes ICC progression through a positive feedback loop. Therefore, cGGNBP2-184aa can be used as an auxiliary treatment for clinical interventions targeting IL-6/STAT3 signaling in ICC [28].

Immunotherapeutic strategies targeting the TIME in CCA

Modulation of TAMs to enhance anti-tumor immune responses

Targeting TAMs is a promising strategy for enhancing anti-tumor immune responses in CCA. Inhibiting TAM recruitment or polarization towards the immunosuppressive phenotype or promoting their reprogramming towards a pro-inflammatory, anti-tumor phenotype might improve the efficacy of immunotherapy in CCA [7]. One approach to modulate TAMs is to block the colony-stimulating factor 1 receptor (CSF1R), which is involved in TAM recruitment and survival. The inhibition of CSF1R reduces TAM infiltration in various tumor models, leading to suppressed tumor growth and enhanced anti-tumor immune responses [29, 30]. However, the efficacy of CSF1R blockade could depend on the tumor model and the timing of treatment [31].

Combination therapies targeting TAMs and other immune cells have shown promising outcomes for CCA. Loeuillard *et al.* reported that targeting TAMs and granulocytic-MDSCs improved the efficacy of PD-1 blockade in CCA, leading to enhanced tumor control and improved survival outcomes [32]. This demonstrates the potential of combining TAM-targeting strategies with other immunotherapies, such as immune checkpoint inhibitors, to achieve better therapeutic outcomes in CCA. In summary, the modulation of TAMs is a potential approach for enhancing anti-tumor immune responses in CCA. Further studies and clinical trials are needed to optimize TAM-targeting strategies and explore their potential when combined with other immunotherapies.

Adoptive T-cell transfer and its potential for targeting TILs

Adoptive T cell transfer (ACT) is a promising immunotherapeutic strategy for CCA that involves the isolation, expansion, and reinfusion of tumor-specific T cells into patients to enhance anti-tumor immune responses. The use of chimeric antigen receptor (CAR) T cells is a novel cellular therapeutic approach in which autologous T cells are harvested from a patient and genetically modified to express CARs. CAR-T cell therapy is thus a type of adoptive T-cell transfer with great potential for CCA treatment [33, 34].

Anti-mucin 1 (MUC1) CAR T cells have been developed for adoptive T cell therapy for CCA. They have been shown to exert cytotoxic effects against MUC1-expressing CCA cells *in vitro* [35]. The anti-MUC1 CAR T cells expressing a PD-1-CD28 switch receptor exhibited

enhanced cytotoxicity against CCA cells, overcoming the immunosuppressive effects of PD-1 signaling [36].

Another promising target for CAR T cell therapy in CCA is CD133, a cancer stem cell marker. Fourth-generation CAR T cells targeting CD133 exhibit anti-tumor effects against CCA cells *in vitro* and *in vivo* [37]. Further, T cells secreting αCD133-αCD3 bispecific T cell engager (BiTE) have anti-tumor activities against CCA, with the potential to redirect T cells to target CD133-positive tumor cells [38].

To overcome the challenge of instability of T lymphocyte cytotoxicity on combining gemcitabine with cytotoxic T lymphocytes, Methi *et al*. developed a recombinant PD-L1xCD3 BiTE, and the results showed that the combination of gemcitabine and PD-L1xCD3 BiTE could promote T lymphocyte cytotoxicity against CCA cells *in vitro*, suggesting potential synergistic effects between chemotherapy and immunotherapy [39]. However, CAR T immunotherapy targeting human epidermal growth factor receptor 2 (HER2) in patients with advanced CCA only led to disease stabilization in four of nine patients [40].

Tumor vaccines induce immune activation through tumor antigens

Tumor vaccines are designed to stimulate immune responses against tumor-specific antigens, thereby promoting tumor-specific T cell activation and expansion. Messenger RNA (mRNA) vaccines have gained significant attention because of their potential for precise and personalized cancer immunotherapy [41]. These vaccines deliver mRNA encoding tumor-associated antigens, which are then translated into proteins by host cells. These antigens are then presented to the immune system, activating immune responses against the tumor cells expressing them [42].

In CCA, studies have aimed to identify tumor antigens and immune subtypes suitable for mRNA vaccine development. Huang *et al*. identified 13 CCA-specific antigens and three immune subtypes that can be targeted by personalized mRNA vaccines [43]. Tang *et al*. proposed a precise pipeline for mRNA vaccine development for CCA, including tumor antigen identification, the design of mRNA constructs, and assessments of vaccine efficacy in preclinical models [41].

Studies on bile duct cancer vaccines have also included DNA and protein vaccines [44, 45], with one study noting that protein vaccines could downregulate PD-L1 gene expression and suppress CCA carcinogenesis, relative to the effects of DNA vaccines [45]. Although CCA vaccines are in the early developmental stages, studies highlight the potential of mRNA vaccines to target tumor antigens and induce immune activation against CCA cells. Studies and clinical trials should be performed to assess the safety, efficacy, and optimal combination of tumor antigens for personalized mRNA vaccines in patients with CCA.

ICIs target immune checkpoints in CCA

ICIs are promising immunotherapeutic agents for CCA that target immune checkpoints to enhance anti-tumor immune responses. Immune checkpoints such as PD-1, PD-L1, and CTLA-4 play critical roles in tumor cell immune evasion [20]. ICIs block these checkpoints, enabling the immune system to effectively recognize and attack tumor cells [23].

Nivolumab, an anti-PD-1 antibody, is a potential treatment option for biliary tract cancers, including CCA [23]. A single-center study found that both pembrolizumab and nivolumab exert effective anticancer effects when combined with lenvatinib [46]. Durvalumab, an anti-PD-L1 antibody, is also a potential therapeutic option for CCA [24]. TOPAZ-1, the first phase 3 trial, which involved 685 patients with inoperable, locally advanced, recurrent, or metastatic biliary tract cancer who were randomized to receive durvalumab or a placebo, showed the benefits of immunotherapy for improved overall survival, in combination with chemotherapy, creating a new standard of care [47]. Clinical and molecular analyses of advanced biliary tract cancers treated with immune checkpoint blockade have shown that elevated PD-L1 expression, TILs, and microsatellite instability are potential markers of the response to ICIs [21, 48]. Ipilimumab, an anti-CTLA-4 antibody, binds to the CTLA-4 antigen, resulting in anti-tumor immune responses. This allows the body to attack cancerous cells, and it is less likely to harm healthy tissues. A phase 2 clinical trial found that a combination of nivolumab and ipilimumab could improve therapeutic outcomes in patients with advanced biliary tract cancers [49]. However, the addition of nivolumab to chemotherapy or ipilimumab did not improve the 6-month progression free survival (PFS) [50].

Various clinical trials have investigated the efficacy and safety of combining ICIs with other targeted therapies or chemotherapies for CCA treatment [22, 51]. The combination of MEK inhibitors and ICIs has shown promising activity against various solid tumors, especially in the presence of KRAS or p53 mutations [52, 53]. These combination therapies enhance the anti-tumor effects of ICIs and improve patient outcomes [51]. In summary, ICIs that target immune checkpoints are potential therapeutic strategies for CCA. Clinical trials should be performed to determine the optimal patient population, combination therapies, and biomarkers for predicting responses to these treatments.

Bifunctional fusion proteins inhibit TGF-β and enhance anti-PD-L1 outcomes

Bifunctional fusion proteins that target TGF-β and PD-L1 have been developed to enhance the efficacy of anti-PD-L1 treatment [54]. High expression is associated with CCA invasion and metastasis [55]. By inhibiting TGF-β1-mediated mesenchymalization, these fusion proteins can modulate the immunosuppressive effects of TGF-β in the TIME while enhancing anti-tumor immune responses through PD-L1 blockade [56]. Inhibiting TGF-β has the ability to rejuvenate exhausted cytotoxic T cells, augmenting the efficacy of anti-PD-L1 treatment [57]. Bintrafusp alfa (M7824) is an innovative and unique protein consisting of a human anti-PD-L1 IgG1 monoclonal antibody and two extracellular domains of TGF-β receptor II. It is considered the first bifunctional fusion protein in its class. Preclinical studies have shown promising results [54, 56] and long-term follow-up safety and efficacy data for bintrafusp alfa in patients with pretreated CCA have been reported [58]. Currently, two newly developed drugs, SHR-1701 and YM101 [59, 60], have been designed to target PD-L1 and TGF-β in cancer treatment. Clinical studies have reported that SHR-1701 has a favorable therapeutic effect on solid tumors, such as CCA [61]. In contrast, YM101 is used in conjunction with other drugs to reduce immune exclusion in tumors and enhance their therapeutic effects against cancer [62]. While similar drugs, such as JS201, GS-19, PM8001, and NRT6003, are still in the preclinical research stage, further studies and clinical trials should be performed to assess the potential of bifunctional fusion proteins for CCA treatment [4].

Conclusions and perspectives

Immunotherapy targeting the TIME is a promising therapeutic approach for CCA treatment. The cellular and molecular components of the TIME, such as TAMs, TILs, MDSCs, Tregs, immune checkpoint molecules, and cytokines/chemokines, play critical roles in tumor progression, immune evasion, and therapeutic responses. Various immunotherapeutic strategies, including the modulation of TAMs, ACT, tumor vaccines, ICIs, and bifunctional fusion proteins, have shown great potential for CCA therapy in preclinical studies and clinical trials.

However, overall response rates to immunotherapies remain modest, and some patients experience immune-related adverse events. Studies should aim to optimize treatment regimens, identify predictive biomarkers of treatment responses, and develop rational combination therapies that enhance the efficacy of immunotherapy while minimizing toxicity. In addition, an elucidation of the complex interactions among tumor cells, immune cells, and the TIME is essential for the development of novel therapeutic strategies and personalized treatment approaches for patients with CCA [4, 5, 63].

In conclusion, studies on immunotherapy targeting the TIME in CCA have provided valuable insights and promising therapeutic strategies that can potentially improve the outcomes of patients with CCA. As the understanding of the TIME and its components continues to grow, we anticipate the development of more effective and personalized immunotherapeutic approaches. Researchers and clinicians should continue to collaborate in designing and executing well-conducted preclinical studies and clinical trials, with the goal of improving the prognosis and quality of life of patients with CCA [4, 5, 63].

Acknowledgements

Not applicable.

Funding

This work was supported by the Research Fund of the Health Commission of Hubei Province (No. WJ2021M255); Cancer Research and Translational Platform Project of Zhongnan Hospital of Wuhan University (No. ZLYNXM202004); Key Research and Development Program of Hubei Province (No. 2021BCA114); the Research Fund from the Medical Sci-Tech Innovation Platform of Zhongnan Hospital of Wuhan University (No. PTXM2021022); and the Outstanding Doctoral (Postdoctoral) Program of Zhongnan Hospital of Wuhan University (No. ZNYB2021021).

Conflicts of interest

The authors declare that they have no conflicts of interest.

Author contributions

All authors contributed to data acquisition and interpretation and reviewed and approved the final version of this manuscript.

Data availability statement

Not applicable.

Ethical approval

Not applicable.

References

1. Cholangiocarcinoma. Nature Reviews. Disease Primers. 2021;7(1):66.
2. Fabris L, Sato K, Alpini G, et al. The Tumor Microenvironment in Cholangiocarcinoma Progression. Hepatology (Baltimore, Md.). 2021;73 Suppl 1(Suppl 1):75-85.
3. Roskoski R. Futibatinib (Lytgobi) for cholangiocarcinoma. Trends Pharmacol Sci. 2023;44(3):190-191.
4. Charalampakis N, Papageorgiou G, Tsakatikas S, et al.

Immunotherapy for cholangiocarcinoma: a 2021 update. Immunotherapy. 2021;13(13):1113-1134.
5. Fabris L, Perugorria MJ, Mertens J, et al. The tumour microenvironment and immune milieu of cholangiocarcinoma. Liver Int. 2019;39 Suppl 1:63-78.
6. Xu L, Yan M, Long J, et al. Identification of macrophage correlated biomarkers to predict the prognosis in patients with intrahepatic cholangiocarcinoma. Front Oncol. 2022;12:967982.
7. Yu Q, Liu C, Pillai A, et al. Twenty years of radiation therapy of unresectable intrahepatic cholangiocarinoma: internal or external? A systematic review and Meta-analysis. Liver Cancer. 2021;10(5): 433-450.
8. Li W, Wang F, Guo R, et al. Targeting macrophages in hematological malignancies: recent advances and future directions. J Hematol Oncol. 2022 ;15(1):110.
9. Yang H, Yan M, Li W, et al. SIRPα and PD1 expression on tumor-associated macrophage predict prognosis of intrahepatic cholangiocarcinoma. J Transl Med. 2022;20(1):140.
10. Murray G I, Duncan M E, O'Neil P, et al. Matrix metalloproteinase-1 is associated with poor prognosis in oesophageal cancer. J Pathol. 1998;185(3):256-261.
11. Vita F, Olaizola I, Amato F, et al. Heterogeneity of cholangiocarcinoma immune biology. Cells. 2023;12(6):846.
12. Cao H, Huang T, Dai M, et al. Tumor microenvironment and its implications for antitumor immunity in cholangiocarcinoma: future perspectives for novel therapies. Int J Biol Sci. 2022;18(14):5369-5390.
13. Jakubowski C D, Azad N S. Immune checkpoint inhibitor therapy in biliary tract cancer (cholangiocarcinoma). Chin Clin Oncol (Chinese). 2020;9(1):2.
14. Huang YH, Zhang CZ, Huang QS, et al. Clinicopathologic features, tumor immune microenvironment and genomic landscape of Epstein-Barr virus-associated intrahepatic cholangiocarcinoma. J Hepatol. 2021;74(4):838-849.
15. Xia T, Li K, Niu N, et al. Immune cell atlas of cholangiocarcinomas reveals distinct tumor microenvironments and associated prognoses. J Hematol Oncol. 2022;15(1):37.
16. Fluxá P, Rojas-Sepúlveda D, Gleisner MA, et al. High $CD8^+$ and absence of $Foxp3^+$ T lymphocytes infiltration in gallbladder tumors correlate with prolonged patients survival. BMC cancer. 2018;8(1): 243.
17. Konishi D, Umeda Y, Yoshida K, et al. Regulatory T cells induce a suppressive immune milieu and promote lymph node metastasis in intrahepatic cholangiocarcinoma. Br J Cancer. 2022;127(4):757-765.
18. Zhang Q, Ma C, Duan Y, et al. Gut microbiome directs hepatocytes to recruit MDSCs and promote cholangiocarcinoma. Cancer Discov. 2021;11(5):1248-1267.
19. Lin Y, Cai Q, Chen Y, et al. CAFs shape myeloid-derived suppressor cells to promote stemness of intrahepatic cholangiocarcinoma through 5-lipoxygenase. Hepatology. 2022;75(1): 28-42.
20. Rizzo A, Ricci A D, Brandi G. PD-L1, TMB, MSI, and other predictors of response to immune checkpoint inhibitors in biliary tract cancer. Cancers. 2021;13(3): 558.
21. Yu F, Gong L, Mo Z, et al. Programmed death ligand-1, tumor infiltrating lymphocytes and HLA expression in Chinese extrahepatic cholangiocarcinoma patients: Possible immunotherapy implications. Biosci Trends. 2019;13(1):58-69.
22. Vogel A, Bathon M, Saborowski A. Immunotherapies in clinical development for biliary tract cancer. Expert Opin Investig Drugs. 2021;30(4):351-363.
23. Di Federico A, Rizzo A, Ricci A D, et al. Nivolumab: an investigational agent for the treatment of biliary tract cancer. Expert Opin Investig Drugs. 2021;30(4): 325-332.
24. Rizzo A, Ricci A D, Brandi G. Durvalumab: an investigational anti-PD-L1 antibody for the treatment of biliary tract cancer. Expert Opin Investig Drugs. 2021;30(4):343-350.
25. Win Maung HM, Chan-On W, Kunkeaw N, et al. Common transcriptional programs and the role of chemokine (C-C motif) ligand 20 (CCL20) in cell migration of cholangiocarcinoma. EXCLI J. 2020;19:154-166.
26. Miyata T, Yamashita YI, Yoshizumi T, et al. CXCL12 expression in intrahepatic cholangiocarcinoma is associated with metastasis and poor prognosis. Cancer Sci. 2019;110(10):3197-3203.
27. Guo B, Friedland SC, Alexander W, et al. Arid1a mutation suppresses TGF-β signaling and induces cholangiocarcinoma. Cell Rep. 2022; 40(9):111253.
28. Li H, Lan T, Liu H, et al. IL-6-induced cGGNBP2 encodes a protein to promote cell growth and metastasis in intrahepatic cholangiocarcinoma. Hepatology. 2022;75(6):1402-1419.
29. Kumar V, Donthireddy L, Marvel D, et al. Cancer-associated fibroblasts neutralize the anti-tumor effect of CSF1 receptor blockade by inducing PMN-MDSC infiltration of tumors. Cancer Cell. 2017; 32(5):654-668.
30. O'Brien SA, Orf J, Skrzypczynska KM, et al. Activity of tumor-associated macrophage depletion by CSF1R blockade is highly dependent on the tumor model and timing of treatment. Cancer Immunol Immunother. 2021;70(8):2401-2410.
31. Zhu Y, Knolhoff BL, Meyer MA, et al. CSF1/CSF1R blockade reprograms tumor-infiltrating macrophages and improves response to T-cell checkpoint immunotherapy in pancreatic cancer models. Cancer Res. 2014;74(18):5057-5069.
32. Loeuillard E, Yang J, Buckarma E, et al. Targeting tumor-associated macrophages and granulocytic myeloid-derived suppressor cells augments PD-1 blockade in cholangiocarcinoma. J Clin Invest. 2020;130(10):5380-5396.
33. Feng KC, Guo YL, Liu Y, et al. Cocktail treatment with EGFR-specific and CD133-specific chimeric antigen receptor-modified T cells in a patient with advanced cholangiocarcinoma. J Hematol Oncol. 2017;10(1):4.
34. Mao R, Hussein MS, He Y. Chimeric antigen receptor engineered T cells and their application in the immunotherapy of solid tumours. Expert Rev Mol Med. 2022;24:e7.
35. Supimon K, Sangsuwannukul T, Sujjitjoon J, et al. Anti-mucin 1 chimeric antigen receptor T cells for adoptive T cell therapy of cholangiocarcinoma. Sci Rep. 2021;11(1):6276.
36. Supimon K, Sangsuwannukul T, Sujjitjoon J, et al. Cytotoxic activity of anti-mucin 1 chimeric antigen receptor T cells expressing PD-1-CD28 switch receptor against cholangiocarcinoma cells. Cytotherapy. 2023;25(2):148-161.
37. Sangsuwannukul T, Supimon K, Sujjitjoon J, et al. Anti-tumour effect of the fourth-generation chimeric antigen receptor T cells targeting CD133 against cholangiocarcinoma cells. Int Immunopharmacol. 2020;89:107069.
38. Sangsuwannukul T, Supimon K, Chieochansin T, et al. Antitumor activity of T cells secreting αCD133-αCD3 bispecific T-cell engager against cholangiocarcinoma. PloS One. 2022;17(3): e0265773.
39. Wathikthinnakon M, Luangwattananun P, Sawasdee N, et al. Combination gemcitabine and PD-L1xCD3 bispecific T cell engager (BiTE) enhances T lymphocyte cytotoxicity against cholangiocarcinoma cells. Sci Rep. 2022;12(1):6154.

40. Feng K, Liu Y, Guo Y, et al. Phase I study of chimeric antigen receptor modified T cells in treating HER2-positive advanced biliary tract cancers and pancreatic cancers. Protein Cell. 2018;9(10):838-847.
41. Tang TY, Huang X, Zhang G, et al. mRNA vaccine development for cholangiocarcinoma: a precise pipeline. Mil Med Res. 2022;9(1):40.
42. Miao L, Zhang Y, Huang L. mRNA vaccine for cancer immunotherapy. Mol Cancer. 2021;20(1):41.
43. Huang X, Tang T, Zhang G, et al. Identification of tumor antigens and immune subtypes of cholangiocarcinoma for mRNA vaccine development. Mol Cancer. 2021;20(1):50.
44. Pan YR, Wu CE, Chen MH, et al. Comprehensive evaluation of immune-checkpoint DNA cancer vaccines in a rat cholangiocarcinoma model. Vaccines. 2020;8(4):703.
45. Pan YR, Wu CE, Huang WK, et al. Chimeric immune checkpoint protein vaccines inhibit the tumorigenesis and growth of rat cholangiocarcinoma. Front Immunol. 2022;13:982196.
46. Lin J, Shi W, Zhao S, et al. Lenvatinib plus checkpoint inhibitors in patients (pts) with advanced intrahepatic cholangiocarcinoma (ICC): Preliminary data and correlation with next-generation sequencing. J Clin Oncol. 2018;36: 500.
47. Oh DY, Ruth HA, Qin S, et al. Durvalumab plus gemcitabine and cisplatin in advanced biliary tract cancer. NEJM Evid. 2022;1(8): EVIDoa2200015.
48. Li J, Wei Q, Wu X, et al. Integrative clinical and molecular analysis of advanced biliary tract cancers on immune checkpoint blockade reveals potential markers of response. Clin Transl Med. 2020;10(4): e118.
49. Klein O, Kee D, Nagrial A, et al. Evaluation of combination nivolumab and Ipilimumab Immunotherapy in patients with advanced biliary tract cancers: subgroup analysis of a phase 2 nonrandomized clinical trial. JAMA Oncol. 2020;6(9):1405-1409.
50. Sahai V, Griffith KA, Beg MS, et al. A randomized phase 2 trial of nivolumab, gemcitabine, and cisplatin or nivolumab and ipilimumab in previously untreated advanced biliary cancer: BilT-01. Cancer. 2022; 128(19):3523-3530.
51. Chakrabarti S, Kamgar M, Mahipal A. Targeted therapies in advanced biliary tract cancer: an evolving paradigm. Cancers. 2020;12(8):2039.
52. Ribas A, Algazi A, Ascierto PA, et al. PD-L1 blockade in combination with inhibition of MAPK oncogenic signaling in patients with advanced melanoma. Nat Commun. 2020;11(1):6262.
53. Lee JW, Zhang Y, Eoh KJ, et al. The Combination of MEK inhibitor with immunomodulatory antibodies targeting programmed death 1 and programmed death ligand 1 results in prolonged survival in Kras/p53-Driven lung cancer. J Thorac Oncol. 2019;14(6):1046-1060.
54. Lan Y, Zhang D, Xu C, et al. Enhanced preclinical antitumor activity of M7824, a bifunctional fusion protein simultaneously targeting PD-L1 and TGF-β. Sci Transl Med. 2018;10(424):5488.
55. Chen Y, Ma L, He Q, et al. TGF-β1 expression is associated with invasion and metastasis of intrahepatic cholangiocarcinoma. Biol Res. 2015;48(1):26.
56. David JM, Dominguez C, McCampbell KK, et al. A novel bifunctional anti-PD-L1/TGF-β Trap fusion protein (M7824) efficiently reverts mesenchymalization of human lung cancer cells. Oncoimmunology. 2017;6(10):1349589.
57. Ferris RL, Lenz HJ, Trotta AM, et al. Rationale for combination of therapeutic antibodies targeting tumor cells and immune checkpoint receptors: Harnessing innate and adaptive immunity through IgG1 isotype immune effector stimulation. Cancer Treat Rev. 2018;63:48-60.
58. Yoo C, Oh DY, Choi HJ, et al. 73P Long-term follow-up of bintrafusp alfa, a bifunctional fusion protein targeting TGF-β and PD-L1, in patients with pretreated biliary tract cancer. J Immunother Cancer. 2020;8(1):e000564..
59. Cheng B, Ding K, Chen P, et al. Anti-PD-L1/TGF-βR fusion protein (SHR-1701) overcomes disrupted lymphocyte recovery-induced resistance to PD-1/PD-L1 inhibitors in lung cancer. Cancer Commun. 2022;42(1):17-36.
60. Yi M, Zhang J, Li A, et al. The construction, expression, and enhanced anti-tumor activity of YM101: a bispecific antibody simultaneously targeting TGF-β and PD-L1. J Hematol Oncol. 2021;14(1):27.
61. Liu D, Zhou J, Wang Y, et al. Bifunctional anti-PD-L1/TGF-βRII agent SHR-1701 in advanced solid tumors: a dose-escalation, dose-expansion, and clinical-expansion phase 1 trial. BMC Med. 2022; 20(1):408.
62. Yi M, Niu M, Wu Y, et al. Combination of oral STING agonist MSA-2 and anti-TGF-β/PD-L1 bispecific antibody YM101: a novel immune cocktail therapy for non-inflamed tumors. J Hematol Oncol. 2022;15(1):142.
63. Gutiérrez-Larrañaga M, González-López E, Roa-Bautista A, et al. Immune checkpoint inhibitors: the emerging cornerstone in cholangiocarcinoma therapy? Liver Cancer. 2021;10(6):545-560.

DOI 10.1007/s10330-023-0642-2
Cite this article as: Ma TY, Chen Z, Chai YB, et al. Research progress on immunotherapy targeting the tumor immune microenvironment for cholangiocarcinoma. Oncol Transl Med. 2023;9(2):49-55.

Oncology and Translational Medicine
DOI 10.1007/s10330-023-0625-5

April 2023, Vol. 9, No. 2, 56–65

REVIEW ARTICLE

Role of miRNA-21 in radiation-induced heart disease

Zhijie Fan, Motuma Yigezu Daba, Lingyan Xiao, Xianglin Yuan(✉)

Department of Oncology, Tongji Hospital, Tongji Medical College, Huazhong University of Science and Technology, Wuhan 430030, China

Abstract

Radiation-induced heart disease (RIHD) is a potentially fatal clinical complication of chest radiotherapy (RT). RIHD is detrimental to the long-term health of post-RT survivors and limits the dose and intensity of RT required to effectively kill tumor cells. However, the cellular and molecular mechanisms underlying these effects remain largely unknown. MicroRNAs (miRNAs) are highly conserved, non-coding, single-stranded, small molecular RNAs that regulate gene expression and participate in cellular proliferation, apoptosis, differentiation, and disease development. MicroRNA-21 (miRNA-21) has become one of the most intensively studied miRNAs in the fields of cancer and cardiovascular disease in recent years. miRNA-21 plays an important role in RIHD progression. This article reviews the origin and function of miRNA-21 in the cardiovascular system and its role in RIHD pathogenesis. In addition, the potential role of miRNA-21 as a new target for predicting and treating RIHD is also discussed.

Received: 3 February 2023
Revised: 26 February 2023
Accepted: 3 March 2023

Key words: microRNA-21 (miRNA-21); radiation-induced heart disease (RIHD); biomarkers; targeted therapy; fibrosis

Despite the increased overall survival rate in patients receiving radiation therapy, its side effects and sequelae have become major obstacles to the patients' quality of life in long-term survival, and radiation-induced heart disease (RIHD) is one of these vital detrimental factors [1]. When patients receive chest radiotherapy (RT), the heart is almost inevitably exposed to radiation, thus causing serious health complications that lead to RIHD [2]. In recent decades, RT techniques have been developed in a way that reduces such complications. However, these methods do not prevent exposure to cardiac radiation [3]. It may take decades for patients to manifest obvious RIHD symptoms after exposure to radiation [4]. Cardiomyopathy, pericarditis, coronary artery atherosclerosis, valvular disease, and conduction defects are common clinical presentations of RIHD [5]. The damage to the cardiovascular system caused by radiation is widely recognized and proved by numerous epidemiological, clinical, and preclinical studies [6, 7]. Nonetheless, owing to the complexity of the cardiovascular system and post-radiation effects, the mechanisms underlying RIHD still remain unknown.

MicroRNAs (miRNAs) are highly conserved non-coding single-stranded small molecular RNAs that mediate post-transcriptional gene silencing by binding to the 3' untranslated region (UTR) of target genes [8]. miRNAs are closely involved in regulating general cellular processes, such as cell proliferation and differentiation, which makes them highly associated with disease onset [9]. A recent study showed differential expression levels of miRNAs in different pathological conditions, including RIHD [10].

miRNA-21 is a widely studied miRNA that is expressed in the majority of human cells, including macrophages, monocytes, myocardial cells, and dendritic cells [11]. The studies of miRNA-21 are mainly involved with its epigenetics function in oncology and cardiology. The expression of miRNA-21 is maintained through transcription and post-transcriptional regulation [12]. Non-transcriptional upregulation of miRNA-21 has also been proposed as a supplement [13, 14]. Radiation leads to increased miRNA-21 expression levels. Kwon *et al.* [15] found increased miRNA-21 levels in irradiated sites in mice. Similar findings in the serum of patients with breast cancer who underwent RT were reported by Halimi *et al* [16], suggesting that serum miRNA-21 may be utilized as a biomarker to identify patients exposed to ionizing radiation. Additionally, fibrosis may result from the persistent overexpression of miRNA-21 [17]. According to Lin *et al* [18], miRNA-21 upregulates SIRT1 and is involved

✉ Correspondence to: Xianglin Yuan. Email: yuanxianglin@hust.edu.cn

with the process of fibrosis via TGF- β1 pathway.

In the pathogenesis of RIHD, the role of miRNA-21 remains unknown. Previous scientific studies have reported the involvement of miRNA-21 in the pathology of cardiovascular disease and cancer; however, few have focused on the effects of irradiation on the cardiac system and the mechanisms involving miRNA-21 in such processes. Herein, we summarize the basic biology and mechanisms underlying miRNA-21 involvement in RIHD and the cardiovascular system and discuss its potential as a biomarker and future therapeutic target.

Biogenesis of miRNA-21

miRNA-21 is one of the first miRNAs to be discovered, and the human miRNA-21 gene is located in the intergenic region on the 3' UTR end of transmembrane protein 49 (TMEM 49), which is also known as protein with human vacuolar membrane 1 (VMP1), on chromosome 17q23.2 [19]. The miRNA-21 gene has a total of 3433 nucleotides, and there are two transcription sites within the locus: one major transcription site approximately 3.5 kb in size and one minor transcription site approximately 4.3 kb in size. In the nucleus, these transcription sites are initiated by RNA Polymerase II (RNAP II) to synthesize pri-miRNA-21 [20]. After transcription, pri-miRNA-21 is processed by Drosha endonuclease (an RNase III) and dgcr8 (a dsRNA-binding protein) into pre-miRNA-21 72 bases in size (precursor miRNA-21), which is transported from the nucleus to the cytoplasm by exportin 5 [21]. The pre-miRNA-21 structure's last loop is cut by cytoplasmic Dicer (an RNase III endonuclease), and the nucleotide sequence is processed into a mature single-stranded nucleotide sequence, miRNA-21, with a length of 22 nucleotides. Mature miRNA-21 is associated with the RNA-induced silencing complex (RISC), a cytoplasmic protein complex [22]. The domain at the 5' end of miRNAs in this miRNA-RISC complex targets the 3' UTR of the target mRNAs. RISC promotes protein downregulation by inhibiting or degrading mRNA after binding to their UTR in a complementary base-pairing manner [23].

In combination with RNAP II, the miRNA-21 gene in the nucleus is transcribed into pri-miRNA, which is the most primitive form of miRNA-21. Pri-miRNA-21 is further processed by Drosha (an RNase III endonuclease) and DGCR8 (a dsRNA-binding protein) to become pre-miRNA-21, which is the miRNA precursor, approximately 70–90 bases in size. This precursor is transferred from the nucleus to the cytoplasm through exportin 5 (Exportin 5). The circular structure of pre-miRNA-21 is removed after digestion with the Dicer (an RNAse III endonuclease) in the cytoplasm to form mature miRNA (miRNA/miRNA duplex) in a double-stranded structure. After processing by Dicer, transactivation response RNA binding protein (TRBP), and protein kinase RNA activator (PACT), these miRNA duplexes unwind into single strands, and some of these miRNAs may become circulating miRNAs after secretion. However, miRNAs that remain in the cell participate in the formation of the RISC, which can combine with mRNA or target genes to play a regulatory role in translation (Fig.1).

miRNA-21 in the cardiovascular system

miRNA-21 primarily contributes to cardiovascular disease by controlling the expression of its downstream target genes. Target genes that have been extensively studied include programmed cell death protein 4 (PDCD4) [24], sprouty1 (SPRY1), sprouty2 [25] and phosphatase and tensin homolog deleted from chromosome 10 (PTEN) [26]. In addition, some target genes have also been considered as specific binding sites of miRNA-21 in recent decades, including peroxisome proliferator-activated receptor alpha (PPAR-α) [27], factor related apoptosis ligand [28], a-kinase anchoring protein 8 (Akap8), BRCA1 associated RING domain 1 (Bard1) [29], Jagged 1 [30], and hypoxia inducible factor-1 alpha (HIF-1α) [31].

In the cardiovascular environment, the role of miRNA-21 in the PTEN pathway is of primary concern, and most studies have focused on apoptosis of cardiomyocytes in this pathway. miRNA-21, through the inhibition of the PTEN pathway, protects the heart from apoptosis [32]. One study demonstrated that miRNA-21 is involved in regulating pathological symptoms and cardiomyocyte apoptosis in hypertensive rats through the PTEN/PI3K/Akt/mTOR signaling pathway [33]. Furthermore, miRNA-21 is a central regulator of cardiac fibrosis [34]. Previous *in vivo* and *in vitro* experiments have focused on miRNA-21 inhibition to regulate the PTEN pathway, which shows a protective effect of miRNA-21 against pathological injury and aging. Bei Y *et al*. showed that inhibiting miRNA-21 had the same protective effect against d-galactose-induced cardiac alterations and doxorubicin-induced cardiomyocyte senescence by targeting PTEN [35]. In an *in vitro* model of myocardial I/R injury, Huang J *et al*. demonstrated that miRNA-21 mediates the protective effects of kaempferol against hypoxia/reoxygenation-induced H9c2 cell injury by promoting the Notch/PTEN/Akt signaling pathway [36].

Similarly, miRNA-21 inhibits the pro-apoptotic effect of PDCD4, showing the protective effects of miRNA-21 in heart cardiomyopathy. Xiao J *et al*. indicated that exosomal miRNA-21 prevents cardiomyocyte apoptosis by targeting PDCD4 [37]. Overexpression of miRNA-21 inhibits PDCD4, suppresses activator protein-1 (AP-1) inhibition by PDCD4, and leads to the upregulation of AP-1. AP-1, being a transcription factor, is able to directly promote miRNA-21 expression, thus forming a

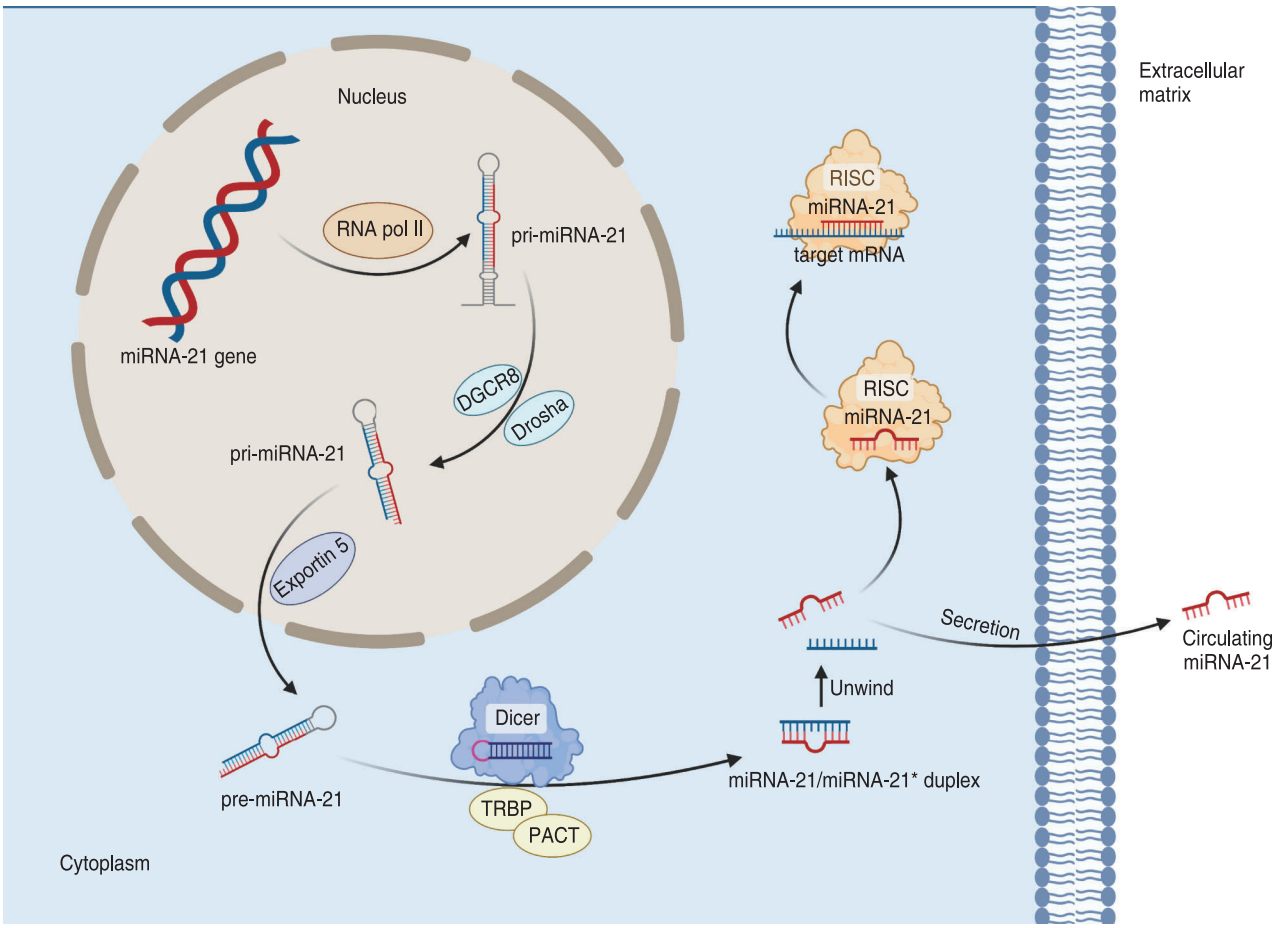

Fig. 1 miRNA-21 biogenesis of miRNA-21.

positive feedback loop in this pathway [38] Recent scientific reports on mice also confirmed that the suppression of miRNA-21 prevents hypertrophic stimulation-induced cardiac remodeling by regulating PDCD4, AP-1, and TGF-β1 signaling pathway [39].

However, in the Smad7/Smad2/3 pathway, miRNA-21 has an inhibitory effect on Smad7, thereby increasing collagen deposition, inducing the TGF-β1 pathway, and leading to α-smooth muscle actin and filamentous actin polymerization, which in turn promotes the development of myocardial fibrosis [40]. Similar pro-fibrotic effects of miRNA-21 have been reported in the spry/ERK/mTOR pathway [41]. Li X *et al.* found that miRNA-21 knockout DM mice had reduced cardiac hypertrophy and cardiac dysfunction compared to wild-type diabetes mellitus (DM) mice and concluded that miRNA-21 overexpression reduced autophagy by inhibiting the spry1/ERK/mTOR pathway and aggravated fibrosis in miRNA-21 knockout DM mice [42].

Some relatively novel miRNA-21 specific binding sites have also been reported in recent research. Peroxisome proliferators-activated receptors (PPARs) are ligand activated receptors in the nuclear hormone receptor family, of which PPARα isoforms are highly expressed in the heart and are one of the key receptors involved in regulating fatty acid metabolism. Chuppa S *et al.* used next-generation mRNA sequencing to identify novel molecular mediators in a 5/6 nephrectomy rat model of chronic kidney disease, and the results revealed that miRNA-21-5p suppression altered gene expression in PPARα regulated pathways in the left ventricle, which identified PPARα as a potential therapeutic target for CKD-related cardiac dysfunction [27].

The rat cardiomyocytes study by Shen H *et al.* identified that miRNA-21 significantly enhanced hypoxia/reoxygenation-induced apoptosis, indicating that miRNA-21 is directly targeted to the 3' UTR of Akap8 and Bard1 mRNA. miRNA-21 exerts protective effects against H/R-induced apoptosis and reactive oxygen species (ROS) production in cardiomyocytes via this mechanism [29]. Zhou XL *et al.* found that miRNA-21 targeted the 3' UTR end of Jagged1 and promoted the transformation of rat cardiac fibroblasts to myofibroblasts. TGF-β1 also induced miRNA-21 expression and inhibited Jagged1

expression. While by targeting Jagged1, miRNA-21 in turn influenced TGF-β1 on the transformation of rat cardiac fibroblasts into myofibroblasts and resulted in cardiac fibrosis [43]. Cao, W *et al.* concluded that tumor suppressor cell adhesion molecule 1 (CADM1) is regulated by miRNA-21, which promotes cardiac fibrotic remodeling and fibroblast proliferation by targeting CADM1 [44].

miRNA-21 and RIHD

Radiation damage to the heart mainly manifests as the production of free radicals, leading to the development of inflammatory processes [45]. Radiation exposure also leads to significant changes in the expression of many proteins, including prostaglandins, prostacyclins, thromboxanes and leukotriene [46]. These inflammatory factors contribute widely to vasodilation, vasoconstriction, increased microvascular permeability, and thrombosis in patients with RIHD. Irradiation can damage the capillary endothelium, resulting in decreased myocardial perfusion and ischemia [47].

About 150–200 miRNAs are expressed in cardiac myocytes [23], many of which are dynamically regulated in response to cardiovascular toxicity following irradiation. miRNAs participate in the pathological processes of radiation-induced myocardial fibrosis, including DNA damage, oxidative stress, inflammation, endothelial dysfunction, hypertrophy, and fibrosis [48].

Kura B *et al.* indicated that miRNA-21 is widely involved in the pathological processes of RIHD, including oxidative stress, fibrosis, hypertrophy, ischemia, preconditioning, and inflammation [49]. After chest irradiation, miRNA-21 was upregulated in cardiomyocytes, where it acted as a regulator of growth factors secretion in cardiac fibroblasts, their survival, and the ERK/MAPK pathway, eventually leading to myocardial hypertrophy and myocardial fibrosis [50]. PDCD4 is also considered a potential target of miRNA-21, along with other cardiac protective mediators related to miRNA-21, such as AP-1, heat shock protein-70, endothelial nitric oxide synthase, and heat shock transcription factor-1 [51].

Prognosis

Ionizing radiation stimulates miRNA-21 expression in various mammalian cell types, including cardiomyocytes, fibroblasts and macrophages [45]. This significant upregulation in cardiomyocytes after irradiation indicates that miRNA-21 has the potential to become a predictive tool for RIHD.

After administering a single dose of 25 Gy radiation to the mediastinum, Kura B. *et al.* [48] discovered that myocardial miRNA-1 was downregulated, whereas miRNA-21 was upregulated after 6 weeks. These findings were supported by further research published in 2019, which showed that miRNA-21 was upregulated in the left ventricle of rats following mediastinal irradiation with 10 Gy [52].

According to a study by Slezak J *et al.*, the expression of microRNA-21 in rat hearts increased approximately 10-fold after 6 weeks of 25 Gy mediastinal irradiation, indicating a compensatory/protective impact in the myocardium 6 weeks after radiation [45]. Similar findings were reported by Viczenczova C *et al.* [50], where an increase in miRNA-21 expression was closely associated with an increase in Cx43 expression in the irradiated rat heart. In addition, under diverse oxidative stress situations, the expression of miRNA-21 increased in human fibroblasts [53].

Kwon OS *et al.* discovered that radiation raised the expression of miRNA-21 in a mouse model [15]. Similar findings were reported in the serum of irradiated patients by Halimi M *et al.* [16], indicating that human miRNA-21 is a possible biomarker for radiation exposure. Experimental data from rats showed that 8 Gy of total body irradiation led to cardiac fibrosis, which was related to miRNA-21 upregulation. The hearts of rats in the control group showed reduced collagen and fibrosis [54].

Many studies reported the upregulation of miRNA-21 expression after cardiac irradiation, where the key pathway regulated by miRNA-21 is tightly related to the cardiac pathogenesis, such as in cardiac fibrosis. However, because miRNA-21 is widely present in human cells and miRNA expression is regulated by a complicated mechanism, consistent results from studies with various samples from different individuals are still missing. Other studies were not limited to using miRNA-21 as a single biomarker but attempted to find a combination of miRNAs that can be used as specific biomarkers for cardiovascular disease [55, 56]. To obtain consistent outcomes, several significant clinical investigations are needed, and the potential of miRNA-21 as a biomarker for the early detection of heart disease and RIHD remains controversial.

Mechanism

Radiation exposure affects cardiac capillary endothelial cells, causing proliferation, damage, swelling, and degeneration of endothelial cells and a significant decrease in the number of capillaries [57]. Radiation-induced endothelial cell injury is the primary cause of myocardial injury following radiation exposure [58]. This kind of reduction causes chronic hypoxia that is also a cause of fibrosis via stabilizing hypoxia-inducible factor 1α (HIF-1α) [59], which was reported as one of the targets of miRNA-21 [31]. HIF-1α can directly or indirectly facilitate fibrosis by stimulating various pro-fibrotic mediators in the cardiovascular system, such as TGF-β, endothelin-1, connective tissue growth factor, as well

as vascular endothelial growth factor (VEGF) [60]. In a guinea pig experiment, the expression of miRNA-21 was confirmed to be positively correlated with VEGF and HIF-1 [61]. Similar conclusions have been reached in patients with neoplasms [62]. According to Mace, T.A. *et al.*, hypoxia in pancreatic cancer cells induces miRNA-21 via the overexpression of HIF-1α [63], which showed that miRNA-21 has an anti-apoptotic effect in HIF-induced hypoxia environment. *In vitro*, RT-PCR results showed that miRNA-21 can target PTEN, activate the AKT and ERK1/2 signal transduction pathways, and increase the expression of HIF-1 and VEGF. HIF- 1α is the primary downstream target of miRNA-21, which controls angiogenesis [64].

Monocyte migration to the intima is also a result of radiation damage. Radiation damage with a dose ≥ 2 Gy in endothelial cells can stimulate the expression of inflammatory factors, such as vascular cell adhesion molecule-1, intercellular adhesion molecule-1, and E-selectin. These factors increase the invasiveness of monocytes in tissues [65]. Monocytes gradually transform into activated macrophages and secrete a large amount of TGF-β during the process of recruitment to the intima, inducing smooth muscle cells to differentiate into myofibroblasts and produce a large amount of type IV collagen [66]. The profibrotic effect of miRNA-21 in cardiac fibroblasts is inextricably linked to TGF-β, which induces the process of epithelial-mesenchymal transition [67, 68]. Cardiovascular fibroblasts treated with miRNA-21 mimics can produce and secrete a large amount of TGF-β1, and in a similar way, cardiac fibroblasts transfected with TGF-β1 enhance miRNA-21 expression [69]. Additionally, by suppressing Smad7 expression, miRNA-21 lessens the Smad7 pathway's inhibitory influence on TGF-β1, which greatly contributes to the development of cardiac fibrosis [40].

As another major pathological mechanism of RIHD, irradiation induces the superoxide overproduction and cardiomyocyte apoptosis of intracellular ROS in cardiomyocytes [70]. Pro-oxidant enzymes, particularly NADPH oxidases, are heavily controlled by a variety of growth factors and cytokines, including TGF-β, and irradiation can also result in an aberrant increase in these enzymes [71]. ROS can encourage the initiation and continuation of the pro-fibrotic process through TGF-β1. ROS acts as an intracellular second messenger that can also regulate the nuclear factor-κB (NF-κB) pathway to mediate epigenetic regulation of fibroblasts and induce fibroblast to myofibroblast differentiation [72, 73]. By specifically targeting the PDCD4 gene, miRNA-21 shields cardiomyocytes from myocardial infarction and injury caused by ROS [74, 75]. In cardiac myocytes overexpressed with ROS, miRNA-21 can directly target PDCD4, which also proves that NF-κB can promote cell death by regulating the excessive production of miRNA-21 [76].

Bax, a member of the Bcl-2 family, is also a target of miRNA-21 via various apoptotic pathways [77]. Exposure to radiation increases Bax expression and activation, which causes it to move and insert into the outer mitochondrial membrane [78, 79]. This regulation accelerates the opening of mitochondrial voltage-dependent anion channels, thereby increasing mitochondrial membrane permeability, and finally, swelling of the mitochondrial membrane leads to apoptosis [80]. Overexpression of miRNA-21 downregulates PTEN, which activates the PI3K/Akt pathway and subsequently inhibits the pro-apoptotic function [81], promoting the survival and proliferation of myocardial cells through anti-apoptotic effects.

By activating the ERK/MAP kinase pathway, radiation also inhibits PPAR-α to lower energy production from fatty acids [82]. When 8 or 16 Gy of single dose cardiac radiation were administered to C57BL/6 mice, the activated phospho-ERK phosphorylated PPAR-α, which resulted in a protein conformational change and subsequent inactivation of PPAR-α complex. This process leads to abnormal myocardial lipid metabolism and mitochondrial function damage that triggers the process of cell apoptosis [83]. Inhibiting the expression of miRNA-21-5p could upregulate the gene expression in the PPAR-α pathway [27], and PPAR-α downregulation could weaken the impact of miRNA-21-5p gene knockdown, including cell growth and infiltration[84].

miRNA-21 plays a dual role in RIHD. miRNA-21 inhibits the PPAR-α pathway to achieve an anti-apoptotic effect, reflecting the protective role of miRNA-21 against radiation, which can promote the inhibition of ERK/MARK pathway and PPAR-α, leading to cell apoptosis through the mitochondrial pathway. miRNA-21 also affects the Bcl-2/Bax/caspase-3 signaling pathway by targeting PTEN and regulating apoptosis. Similarly, miRNA-21 inhibits the expression of PDCD4 to protect myocardial cells from apoptosis. ROS produced during RT mediates the NF-κB pathway to directly promote the overexpression of miRNA-21, which antagonizes ROS-induced apoptosis. In addition, PDCD4 inhibits the upregulation of AP-1, and AP-1 can, in turn, directly promote the expression of miRNA-21, forming a positive feedback loop between miRNA-21 and AP-1. In contrast, miRNA-21 enables promotion of myocardial fibrosis mainly by regulating the Smad7/Smad2/3 pathway. Radiation can stimulate various types of cardiac cells to produce inflammatory factors, such as TGF-β1, VCAM, ICAM and E-selection, which enhance the expression of the smad2/3 pathway and further promote myocardial fibrosis. RIHD, peroxisome proliferator-activated receptor alpha(PPAR-α), Extracellular signal-regulated kinase (ERK) mitogen-activated protein

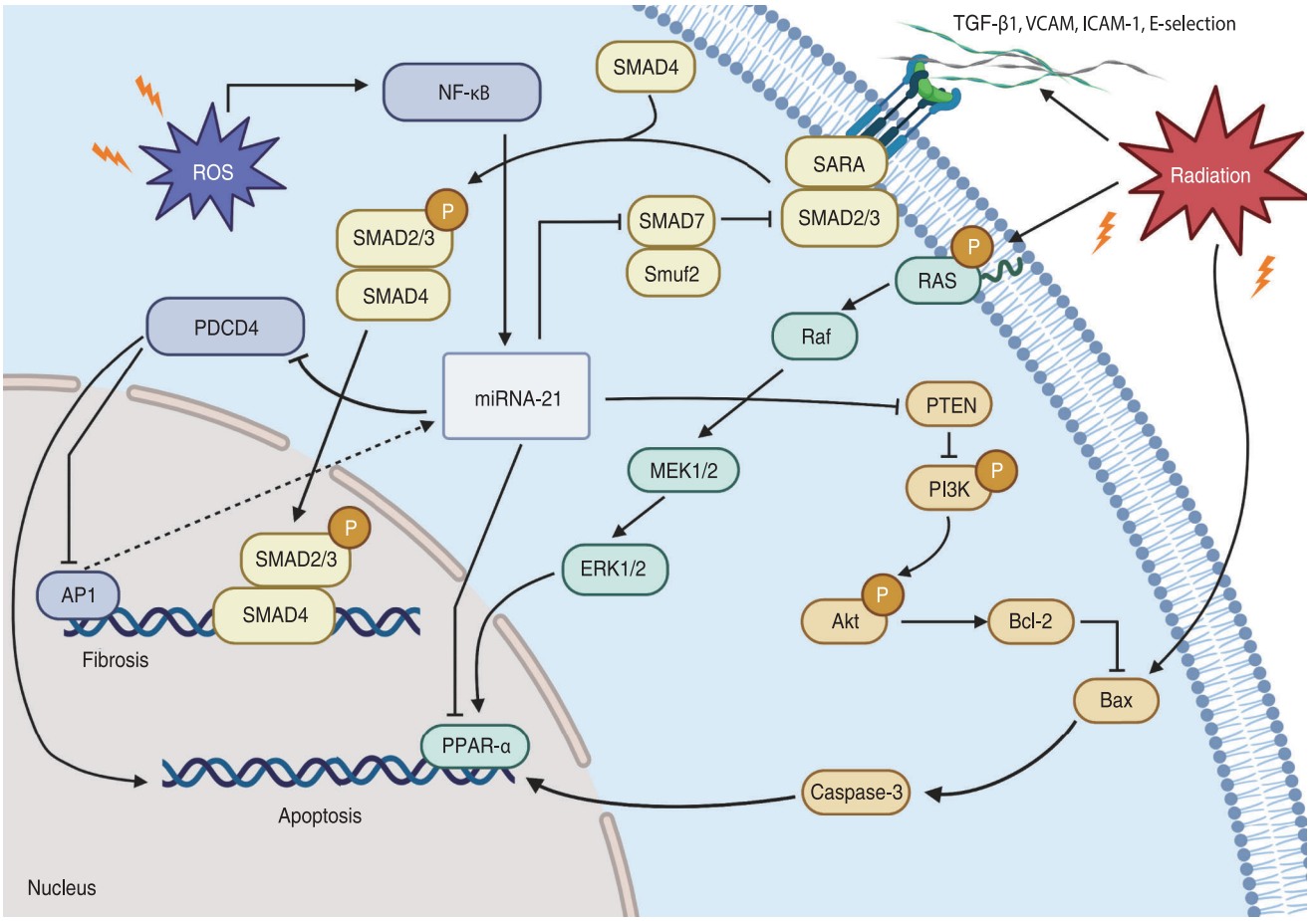

Fig. 2 The molecular mechanisms of miRNA-21 in RIHD.

kinase (MARK), B-cell lymphoma 2 (Bcl-2), bcl-2-like protein 4 (Bax), Phosphatase and tensin homolog deleted from chromosome 10 (PTEN), Programmed Cell Death 4 (PDCD4), Reactive oxygen species (ROS), Nuclear factor kappa-B (NF-κB), Activator protein-1 (AP-1), SMAD Family Member2/3/4/7 (Smad2/3/4/7), Transforming growth factor-β1 (TGF-β1)), Vascular cell adhesion molecule (VCAM), and Intercellular cell adhesion molecule (ICAM). This Figure was created using Biorender.com (Fig.2).

Therapy

In recent years, miRNA-based drugs have become popular owing to their high biological stability and advantage of being potential biomarkers [85]. There are currently three types of miRNA-based drugs [86]: AntagomiRs, which bind to the target miRNAs to specifically inhibit their function, resulting in reduced activation of RISC and upregulation of genes and production of proteins [87, 88]; synthetic miRNA mimics is an approach for gene silencing [89]. This kind of generated artificial double-stranded miRNA-like RNA fragments can target mRNA and activate RISC, which leads to their suppression and the reduction of overexpressed miRNAs in disease conditions [90]. Another lesser known approach involves miRNA sponges, masks, and erasers [91]. miRNA sponges are competitive inhibitors of miRNA target genes, which can engulf miRNAs-of-interest inside the cell, similar to water absorption by a sponge, leading to blocking of the activity of miRNAs [92, 93]. Erasers are oligonucleotides complementary to specific miRNAs that inhibit their function [94]. miRNA-masks are antisense chains that are completely complementary to the binding sites of miRNA and target mRNA; hence, they can form a complex with the target mRNA and act as a target protector to conceal the binding sites, thus interfering with the binding of the corresponding miRNA and target mRNA [95]. Lu YJ *et al.* proposed multi-target anti-miRNA antisense nucleotide inhibitors [96].

miRNA-21 is considered a potential therapeutic target for cardiomyopathy. One study demonstrated that miRNA-21 is a mediator involved in the pathogenesis of cardiac fibrosis, and using locked nucleic acid (LNA) anti-miRNA-21 can cause miRNA-21 inhibition, leading

to a reduction in collagen expression and alleviation of cardiac fibrosis [67]. Certain drug studies have focused on inducing or inhibiting the expression of miRNA-21 at the transcriptional level. By using melatonin (MET) entrapped poly nanoparticles (MET/PLGANPS), Wang S *et al*. proved the therapeutic effect of MET/PLgANPS in RT, and MET/PLGANPS may inhibit the miRNA-21/TGF- β1/Smad3 pathway to reduce the injury after radiation [97]. Kura B *et al*. showed that Enbrel and tadalafil changed miRNA expression values of irradiated rats to those of non-irradiated controls, thus contributing to the alleviation of radiation-induced toxicity [48]. Another study indicated that molecular hydrogen is a potential therapeutic agent that decreases myocardial miRNA-21 levels after irradiation by affecting the intracellular ROS levels [52]. Promotors such as AP-1, STAT3, Ras, ERK1/2, and EGFR can effectively induce miRNA-21 expression [98–101]. In contrast, some transcriptional suppressors, such as NFI, C/EBP, Gfi1, and estrogen receptors, have also been reported to repress miRNA-21 transcription [102, 103].

However, the main drawback of using miRNAs for diagnosis or therapy is that they target and affect the expression of multiple genes. Therefore, their targeting may also have an impact on other pathways in the organism [104]. MiRNA-21 is not necessarily a cell type-specific miRNA and hence is problematic for targeted therapy, and application of the miRNA-21 expression pattern in cardiomyopathies for repression or restoration is challenging [105].

Conclusion and perspective

The etiology and mechanism of occurrence after RIHD are not fully defined. Besides cardiomyocytes, some other cardiac cells also participate in the occurrence and development of this type of cardiomyopathy, such as endothelial cells, smooth muscle cells, fibroblasts, and immune cells [106]. Similarly, noncardiomyocytes play important roles in cardiomyocyte apoptosis, cardiac fibroblast activation, and immune cell infiltration [107]. Expression profiles of miRNAs may differ in cells of diverse origins [108, 109]. miRNA-21 has different expression characteristics and functions in various cardiac cell s [110]. Though miRNA-21 plays an important role in radiation-induced cardiac injury, the regulatory details of miRNA-21 in the processes of biogenesis, secretion, and degradation remain unclear. The use of miRNA-21 as an independent biomarker for diagnosis or prognosis persists to be challenging. Further research is required to determine the pathogenesis and mechanism of action of miRNA-21 in RIHD. With miRNA-21, there are still many other kinds of miRNAs that have been reported in the field of RIHD, such as miRNA-1 and -15b [52], miRNA-22, miRNA-24, miRNA-29, miRNA-133 [111], miRNA-208, miRNA-29, miRNA-199b, miRNA-221, miRNA-222, and the miRNA-15 family [49]. miRNA-15b is a regulator of cardiac hypertrophy and fibrosis as it inhibits the TGF-β Signal pathway after irradiation [112]. The miRNA-29 family targets mRNAs of various types of elastin, fibrin, and collagen (including type I and type III collagen) involved in fibrosis, which is a key pathological change related to RIHD in irradiated rats [45]. Cardiac specific miRNA-208 has been proved to be crucial to cardiac hypertrophy, fibrosis, and the expression of β-myosin heavy chain [113].

In conclusion, miRNA-21 is a critical miRNA that is involved in RIHD. Specific miRNA-21 studies have revealed the cellular and molecular mechanisms of RIHD, and its potential therapeutic role is still promising based on further animal experiments and clinical trials.

Acknowledgments

Not applicable.

Funding

This study did not receive any specific grants from funding agencies in public, commercial, or non-profit sectors.

Conflicts of interest

The authors indicated no potential conflicts.

Author contributions

Zhijie Fan prepared the manuscript draft and created the figures, Motuma Yigezu Daba prepared the manuscript draft, Lingyan Xiao polished the manuscript, and Xianglin Yuan revised the manuscript. All the authors have read and approved the final manuscript.

Data availability statement

Not applicable.

Ethical approval

Not applicable.

References

1. McGale P, Darby SC, Hall P, et al. Incidence of heart disease in 35,000 women treated with radiotherapy for breast cancer in Denmark and Sweden. Radiother Oncol. 2011;100(2):167-175.
2. Stewart JR, Fajardo LF. Radiation-induced heart disease: an update. Prog Cardiovasc Dis. 1984;27(3):173-194.
3. Wang KX, Ye C, Yang X, et al. New Insights into the Understanding of Mechanisms of Radiation-Induced Heart Disease. Curr Treat Options Oncol. 2023;24(1):12-29
4. Nielsen KM, Offersen BV, Nielsen HM, et al. Short and long term radiation induced cardiovascular disease in patients with cancer. Clin Cardiol. 2017;40(4):255-261.
5. Wang H, Wei J, Zheng Q, et al. Radiation-induced heart disease: a

review of classification, mechanism and prevention. Int J Biol Sci. 2019;15(10):2128-2138.
6. Stewart FA, Seemann I, Hoving S, et al. Understanding radiation-induced cardiovascular damage and strategies for intervention. Clin Oncol (R Coll Radiol). 2013;25(10):617-624.
7. Yusuf SW, Venkatesulu BP, Mahadevan LS, et al. Radiation-induced cardiovascular disease: a clinical perspective. Front Cardiovasc Med. 2017;4:66.
8. Cho WC. OncomiRs: the discovery and progress of microRNAs in cancers. Mol Cancer. 2007;6:60.
9. Jin C, Shi Z, Lin K, et al. Predicting miRNA-disease association based on neural inductive matrix completion with graph autoencoders and self-attention mechanism. Biomolecules. 2022;12(1):64.
10. Yu L, Zheng Y, Gao L. MiRNA-disease association prediction based on meta-paths. Brief Bioinform. 2022;23(2):bbab571.
11. McCall MN, Illei PB, Halushka MK. Complex sources of variation in tissue expression data: analysis of the GTEx lung transcriptome. Am J Hum Genet. 2016;99(3):624-635.
12. Haverty PM, Fridlyand J, Li L, et al. High-resolution genomic and expression analyses of copy number alterations in breast tumors. Genes Chromosomes Cancer. 2008;47(6):530-542.
13. Cai X, Hagedorn CH, Cullen BR. Human microRNAs are processed from capped, polyadenylated transcripts that can also function as mRNAs. RNA. 2004;10(12):1957-1966.
14. Davis BN, Hilyard AC, Lagna G, et al. SMAD proteins control DROSHA-mediated microRNA maturation. Nature. 2008;454(7200):56-61.
15. Kwon OS, Kim KT, Lee E, et al. Induction of MiR-21 by stereotactic body radiotherapy contributes to the pulmonary fibrotic response. PLoS One. 2016;11(5):e0154942.
16. Halimi M, Parsian H, Asghari SM, et al. Clinical translation of human microRNA 21 as a potential biomarker for exposure to ionizing radiation. Transl Res. 2014;163(6):578-584.
17. Roy S, Khanna S, Hussain SR, et al. MicroRNA expression in response to murine myocardial infarction: miR-21 regulates fibroblast metalloprotease-2 via phosphatase and tensin homologue. Cardiovasc Res. 2009;82(1):21-29.
18. Lin Q, Geng Y, Zhao M, et al. MiR-21 Regulates TNF-α-Induced CD40 Expression via the SIRT1-NF-κB Pathway in Renal Inner Medullary Collecting Duct Cells. Cell Physiol Biochem. 2017;41(1):124-136.
19. Lagos-Quintana M, Rauhut R, Lendeckel W, et al. Identification of novel genes coding for small expressed RNAs. Science. 2001;294(5543):853-858.
20. Lee Y, Kim M, Han J, et al. MicroRNA genes are transcribed by RNA polymerase II. EMBO J. 2004;23(20):4051-4060.
21. Yi R, Qin Y, Macara IG, Cullen BR. Exportin-5 mediates the nuclear export of pre-microRNAs and short hairpin RNAs. Genes Dev. 2003;17(24):3011-3016 .
22. Kawamata T, Seitz H, Tomari Y. Structural determinants of miRNAs for RISC loading and slicer-independent unwinding. Nat Struct Mol Biol. 2009;16(9):953-960.
23. Condorelli G, Latronico MV, Dorn GW 2nd. microRNAs in heart disease: putative novel therapeutic targets? Eur Heart J. 2010;31(6):649-658.
24. Spinetti G, Sangalli E, Tagliabue E, et al. MicroRNA-21/PDCD4 proapoptotic signaling from circulating CD34+ cells to vascular endothelial cells: a potential contributor to adverse cardiovascular outcomes in patients with critical limb ischemia. Diabetes Care. 2020;43(7):1520-1529.
25. Ghafouri-Fard S, Hussen BM, Mohaqiq M, et al Interplay between non-coding RNAs and programmed cell death proteins. Front Oncol. 2022;12:808475.
26. Cheng Y, Zhang C. MicroRNA-21 in cardiovascular disease. J Cardiovasc Transl Res. 2010;3(3):251-255.
27. Chuppa S, Liang M, Liu P, et al. MicroRNA-21 regulates peroxisome proliferator-activated receptor alpha, a molecular mechanism of cardiac pathology in Cardiorenal Syndrome Type 4. Kidney Int. 2018;93(2):375-389.
28. Wang K, Li PF. Foxo3a regulates apoptosis by negatively targeting miR-21. J Biol Chem. 2010;285(22):16958-16966.
29. Shen H, Yao Z, Zhao W, et al. miR-21 enhances the protective effect of loperamide on rat cardiomyocytes against hypoxia/reoxygenation, reactive oxygen species production and apoptosis via regulating Akap8 and Bard1 expression. Exp Ther Med. 2019;17(2):1312-1320.
30. Liu C, Wu M, Qu J, et al. JNK and Jag1/Notch2 co-regulate CXCL16 to facilitate cypermethrin-induced kidney damage. Ecotoxicol Environ Saf. 2022;238:113582.
31. Varghese E, Liskova A, Kubatka P, et al. Anti-angiogenic effects of phytochemicals on miRNA regulating breast cancer progression. Biomolecules. 2020;10(2):191.
32. Tu Y, Wan L, Fan Y, et al. Ischemic postconditioning-mediated miRNA-21 protects against cardiac ischemia/reperfusion injury via PTEN/Akt pathway. PLoS One. 2013;8(10):e75872.
33. Shi YJ, Xu W, Han YF, et al. Effects of miR-21 on hypertensive rats through PTEN/PI3K/Akt/mTOR signaling pathway. Eur Rev Med Pharmacol Sci. 2019;23(11):4924-4931.
34. Bauersachs J. miR-21: a central regulator of fibrosis not only in the broken heart. Cardiovasc Res. 2012;96(2):227-9; discussion 230-233.
35. Bei Y, Wu X, Cretoiu D, et al. miR-21 suppression prevents cardiac alterations induced by d-galactose and doxorubicin. J Mol Cell Cardiol. 2018;115:130-141.
36. Huang J, Qi Z. MiR-21 mediates the protection of kaempferol against hypoxia/reoxygenation-induced cardiomyocyte injury via promoting Notch1/PTEN/AKT signaling pathway. PLoS One. 2020;15(11):e0241007.
37. Xiao J, Pan Y, Li XH, et al. Cardiac progenitor cell-derived exosomes prevent cardiomyocytes apoptosis through exosomal miR-21 by targeting PDCD4. Cell Death Dis. 2016;7(6):e2277.
38. Fujita S, Ito T, Mizutani T, et al. miR-21 Gene expression triggered by AP-1 is sustained through a double-negative feedback mechanism. J Mol Biol. 2008;378(3):492-504.
39. Watanabe K, Narumi T, Watanabe T, et al. The association between microRNA-21 and hypertension-induced cardiac remodeling. PLoS One. 2020;15(2):e0226053.
40. Yuan J, Chen H, Ge D, et al. Mir-21 promotes cardiac fibrosis after myocardial infarction via targeting Smad7. Cell Physiol Biochem. 2017;42(6):2207-2219.
41. Adam O, Löhfelm B, Thum T, et al. Role of miR-21 in the pathogenesis of atrial fibrosis. Basic Res Cardiol. 2012;107(5):278.
42. Li X, Meng C, Han F, et al. Vildagliptin attenuates myocardial dysfunction and restores autophagy via miR-21/SPRY1/ERK in diabetic mice heart. Front Pharmacol. 2021;12:634365.
43. Zhou XL, Xu H, Liu ZB, et al. miR-21 promotes cardiac fibroblast-to-myofibroblast transformation and myocardial fibrosis by targeting Jagged1. J Cell Mol Med. 2018;22(8):3816-3824.
44. Cao W, Shi P, Ge JJ. miR-21 enhances cardiac fibrotic remodeling and fibroblast proliferation via CADM1/STAT3 pathway. BMC Cardiovasc Disord. 2017;17(1):88.
45. Slezak J, Kura B, Ravingerová T, et al. Mechanisms of cardiac radiation injury and potential preventive approaches. Can J Physiol

Pharmacol. 2015;93(9):737-753.
46. Sárközy M, Varga Z, Gáspár R, et al. Pathomechanisms and therapeutic opportunities in radiation-induced heart disease: from bench to bedside. Clin Res Cardiol. 2021;110(4):507-531.
47. Wijerathne H, Langston JC, Yang Q, et al. Mechanisms of radiation-induced endothelium damage: Emerging models and technologies. Radiother Oncol. 2021;158:21-32.
48. Kura B, Yin C, Frimmel K, et al. Changes of microRNA-1, -15b and -21 levels in irradiated rat hearts after treatment with potentially radioprotective drugs. Physiol Res. 2016;65 Suppl 1:S129-137.
49. Kura B, Babal P, Slezak J. Implication of microRNAs in the development and potential treatment of radiation-induced heart disease. Can J Physiol Pharmacol. 2017;95(10):1236-1244.
50. Viczenczova C, Szeiffova Bacova B, Egan Benova T, et al. Myocardial connexin-43 and PKC signalling are involved in adaptation of the heart to irradiation-induced injury: Implication of miR-1 and miR-21. Gen Physiol Biophys. 2016;35(2):215-222.
51. Kura B, Kalocayova B, Devaux Y, et al. Potential clinical implications of miR-1 and miR-21 in heart disease and cardioprotection. Int J Mol Sci. 2020;21(3):700.
52. Kura B, Kalocayova B, LeBaron TW, et al. Regulation of microRNAs by molecular hydrogen contributes to the prevention of radiation-induced damage in the rat myocardium. Mol Cell Biochem. 2019;457(1-2):61-72.
53. Simone NL, Soule BP, Ly D, et al. Ionizing radiation-induced oxidative stress alters miRNA expression. PLoS One. 2009;4(7):e6377.
54. Ma C, Fu Z, Guo H, et al. The effects of radix angelica sinensis and radix hedysari ultrafiltration extract on X-irradiation-induced myocardial fibrosis in rats. Biomed Pharmacother. 2019;112:108596.
55. Jin ZQ. MicroRNA targets and biomarker validation for diabetes-associated cardiac fibrosis. Pharmacol Res. 2021;174:105941.
56. Henning RJ. Cardiovascular exosomes and MicroRNAs in cardiovascular physiology and pathophysiology. J Cardiovasc Transl Res. 2021;14(2):195-212.
57. Darby SC, Cutter DJ, Boerma M, et al. Radiation-related heart disease: current knowledge and future prospects. Int J Radiat Oncol Biol Phys. 2010;76(3):656-665.
58. Boerma M, Sridharan V, Mao XW, et al. Effects of ionizing radiation on the heart. Mutat Res Rev Mutat Res. 2016;770(Pt B):319-327.
59. Yarnold J, Brotons MC. Pathogenetic mechanisms in radiation fibrosis. Radiother Oncol. 2010;97(1):149-161.
60. Ruthenborg RJ, Ban JJ, Wazir A, et al. Regulation of wound healing and fibrosis by hypoxia and hypoxia-inducible factor-1. Mol Cells. 2014;37(9):637-643.
61. Liu L, Zhu D, Ding W, et al. MiRNA-21-HIF-1α-VEGF axis Is associated with myopic choroidal neovascularization in guinea pigs. Ophthalmic Res. 2022;65(5):493-505.
62. Sabry D, El-Deek SEM, Maher M, et al. Role of miRNA-210, miRNA-21 and miRNA-126 as diagnostic biomarkers in colorectal carcinoma: impact of HIF-1α-VEGF signaling pathway. Mol Cell Biochem. 2019;454(1-2):177-189.
63. Mace TA, Collins AL, Wojcik SE, et al. Hypoxia induces the overexpression of microRNA-21 in pancreatic cancer cells. J Surg Res. 2013;184(2):855-860.
64. Liu LZ, Li C, Chen Q, et al. MiR-21 induced angiogenesis through AKT and ERK activation and HIF-1α expression. PLoS One. 2011;6(4):e19139.
65. Stewart FA, Hoving S, Russell NS. Vascular damage as an underlying mechanism of cardiac and cerebral toxicity in irradiated cancer patients. Radiat Res. 2010;174(6):865-869.
66. Cuomo JR, Javaheri SP, Sharma GK, et al. How to prevent and manage radiation-induced coronary artery disease. Heart. 2018;104(20):1647-1653.
67. Nonaka CKV, Sampaio GL, Silva KN, et al. Therapeutic miR-21 silencing reduces cardiac fibrosis and modulates inflammatory response in chronic chagas disease. Int J Mol Sci. 2021;22(7):3307.
68. Lamouille S, Xu J, Derynck R. Molecular mechanisms of epithelial-mesenchymal transition. Nat Rev Mol Cell Biol. 2014;15(3):178-196.
69. Surina S, Fontanella RA, Scisciola L, et al. miR-21 in human cardiomyopathies. Front Cardiovasc Med. 2021;8:767064. .
70. Farhood B, Ashrafizadeh M, Khodamoradi E, et al. Targeting of cellular redox metabolism for mitigation of radiation injury. Life Sci. 2020;250:117570.
71. Mortezaee K, Goradel NH, Amini P, et al. NADPH oxidase as a target for modulation of radiation response; implications to carcinogenesis and radiotherapy. Curr Mol Pharmacol. 2019;12(1):50-60.
72. Weintraub NL, Jones WK, Manka D. Understanding radiation-induced vascular disease. J Am Coll Cardiol. 2010;55(12):1237-1239.
73. Wei J, Wang B, Wang H, et al. Radiation-induced normal tissue damage: oxidative stress and epigenetic mechanisms. Oxid Med Cell Longev. 2019;2019:3010342.
74. Gu H, Liu Z, Li Y, et al. Serum-derived extracellular vesicles protect against acute myocardial infarction by regulating miR-21/PDCD4 signaling pathway. Front Physiol. 2018;9:348.
75. Cheng Y, Liu X, Zhang S, et al. MicroRNA-21 protects against the H(2)O(2)-induced injury on cardiac myocytes via its target gene PDCD4. J Mol Cell Cardiol. 2009;47(1):5-14.
76. Wei C, Li L, Kim IK, et al. NF-κB mediated miR-21 regulation in cardiomyocytes apoptosis under oxidative stress. Free Radic Res. 2014;48(3):282-291.
77. Kroemer G, Galluzzi L, Brenner C. Mitochondrial membrane permeabilization in cell death. Physiol Rev. 2007;87(1):99-163.
78. An J, Li P, Li J, et al. ARC is a critical cardiomyocyte survival switch in doxorubicin cardiotoxicity. J Mol Med (Berl). 2009;87(4):401-410.
79. Salata C, Ferreira-Machado SC, De Andrade CB, et al. Apoptosis induction of cardiomyocytes and subsequent fibrosis after irradiation and neoadjuvant chemotherapy. Int J Radiat Biol. 2014;90(4):284-290.
80. Sridharan V, Aykin-Burns N, Tripathi P, et al. Radiation-induced alterations in mitochondria of the rat heart. Radiat Res. 2014;181(3):324-334.
81. Ma N, Bai J, Zhang W, et al. Trimetazidine protects against cardiac ischemia/reperfusion injury via effects on cardiac miRNA-21 expression, Akt and the Bcl-2/Bax pathway. Mol Med Rep. 2016;14(5):4216-4222.
82. Livingston K, Schlaak RA, Puckett LL, et al. The Role of mitochondrial dysfunction in radiation-Induced heart disease: from bench to bedside. Front Cardiovasc Med. 2020;7:20.
83. Azimzadeh O, Sievert W, Sarioglu H, et al. PPAR alpha: a novel radiation target in locally exposed Mus musculus heart revealed by quantitative proteomics. J Proteome Res. 2013;12(6):2700-2714.
84. Guan CY, Tian S, Cao JL, et al. Down-regulated miR-21 in gestational diabetes mellitus placenta induces PPAR-α to inhibit cell proliferation and infiltration. Diabetes Metab Syndr Obes. 2020;13:3009-3034.
85. Jung M, Schaefer A, Steiner I, et al. Robust microRNA stability in degraded RNA preparations from human tissue and cell samples. Clin Chem. 2010;56(6):998-1006.
86. Melman YF, Shah R, Das S. MicroRNAs in heart failure: is the picture becoming less miRky? Circ Heart Fail. 2014;7(1):203-214.
87. Krützfeldt J, Rajewsky N, Braich R, et al. Silencing of microRNAs in

vivo with 'antagomirs'. Nature. 2005;438(7068):685-689.
88. Oliveira-Carvalho V, Carvalho VO, Silva MM, et al. MicroRNAs: a new paradigm in the treatment and diagnosis of heart failure? Arq Bras Cardiol. 2012;98(4):362-369.
89. Wang HR, Wu M, Yu H, et al. Selective inhibition of the K(ir)2 family of inward rectifier potassium channels by a small molecule probe: the discovery, SAR, and pharmacological characterization of ML133. ACS Chem Biol. 2011;6(8):845-856..
90. Bonneau E, Neveu B, Kostantin E, et al. How close are miRNAs from clinical practice? A perspective on the diagnostic and therapeutic market. EJIFCC. 2019;30(2):114-127.
91. Schulte C, Zeller T. microRNA-based diagnostics and therapy in cardiovascular disease-Summing up the facts. Cardiovasc Diagn Ther. 2015;5(1):17-36.
92. Ebert MS, Neilson JR, Sharp PA. MicroRNA sponges: competitive inhibitors of small RNAs in mammalian cells. Nat Methods. 2007;4(9):721-726.
93. Ebert MS, Sharp PA. MicroRNA sponges: progress and possibilities. RNA. 2010;16(11):2043-2050.
94. Caroli A, Cardillo MT, Galea R, et al. Potential therapeutic role of microRNAs in ischemic heart disease. J Cardiol. 2013;61(5):315-320.
95. Xiao J, Luo X, Lin H, et al. MicroRNA miR-133 represses HERG K+ channel expression contributing to QT prolongation in diabetic hearts. J Biol Chem. 2011;286(32):28656.
96. Lu Y, Xiao J, Lin H, et al. A single anti-microRNA antisense oligodeoxyribonucleotide (AMO) targeting multiple microRNAs offers an improved approach for microRNA interference. Nucleic Acids Res. 2009;37(3):e24.
97. Wang S, Li J, He Y, et al. Protective effect of melatonin entrapped PLGA nanoparticles on radiation-induced lung injury through the miR-21/TGF-β1/Smad3 pathway. Int J Pharm. 2021;602:120584.
98. Löffler D, Brocke-Heidrich K, Pfeifer G, et al. Interleukin-6 dependent survival of multiple myeloma cells involves the Stat3-mediated induction of microRNA-21 through a highly conserved enhancer. Blood. 2007;110(4):1330-1333.
99. Talotta F, Cimmino A, Matarazzo MR, et al. An autoregulatory loop mediated by miR-21 and PDCD4 controls the AP-1 activity in RAS transformation. Oncogene. 2009;28(1):73-84.
100. Huang GL, Zhang XH, Guo GL, et al. Expression of microRNA-21 in invasive ductal carcinoma of the breast and its association with phosphatase and tensin homolog deleted from chromosome expression and clinicopathologic features. Zhonghua Yi Xue Za Zhi. 2008;88(40):2833-2837.
101. Seike M, Goto A, Okano T, et al. MiR-21 is an EGFR-regulated anti-apoptotic factor in lung cancer in never-smokers. Proc Natl Acad Sci USA. 2009;106(29):12085-12090.
102. Velu CS, Baktula AM, Grimes HL. Gfi1 regulates miR-21 and miR-196b to control myelopoiesis. Blood. 2009;113(19):4720-4728.
103. Wickramasinghe NS, Manavalan TT, Dougherty SM, et al. Estradiol downregulates miR-21 expression and increases miR-21 target gene expression in MCF-7 breast cancer cells. Nucleic Acids Res. 2009;37(8):2584-2595 .
104. Miranda KC, Huynh T, Tay Y, et al. A pattern-based method for the identification of MicroRNA binding sites and their corresponding heteroduplexes. Cell. 2006;126(6):1203-1217.
105. Huang CK, Bär C, Thum T. miR-21, mediator, and potential therapeutic target in the cardiorenal syndrome. Front Pharmacol. 2020;11:726.
106. Nag AC. Study of non-muscle cells of the adult mammalian heart: a fine structural analysis and distribution. Cytobios. 1980;28(109):41-61.
107. Zhou P, Pu WT. Recounting cardiac cellular composition. Circ Res. 2016;118(3):368-370.
108. Bronze-da-Rocha E. MicroRNAs expression profiles in cardiovascular diseases. Biomed Res Int. 2014;2014:985408.
109. Bonci D. MicroRNA-21 as therapeutic target in cancer and cardiovascular disease. Recent Pat Cardiovasc Drug Discov. 2010;5(3):156-161.
110. Kukreja RC, Yin C, Salloum FN. MicroRNAs: new players in cardiac injury and protection. Mol Pharmacol. 2011;80(4):558-564.
111. Wang B, Wang H, Zhang M, et al. Radiation-induced myocardial fibrosis: Mechanisms underlying its pathogenesis and therapeutic strategies. J Cell Mol Med. 2020;24(14):7717-7729.
112. Lang A, Grether-Beck S, Singh M, et al. MicroRNA-15b regulates mitochondrial ROS production and the senescence-associated secretory phenotype through sirtuin 4/SIRT4. Aging (Albany NY). 2016;8(3):484-505.
113. Rawal S, Manning P, Katare R. Cardiovascular microRNAs: as modulators and diagnostic biomarkers of diabetic heart disease. Cardiovasc Diabetol. 2014;13:44.

DOI 10.1007/s10330-023-0625-5
Cite this article as: Fan ZJ, Motuma Yigezu Daba, Xiao LY, et al. Role of miRNA-21 in radiation-induced heart disease. Oncol Transl Med. 2023;9(2):56-65.

Oncology and Translational Medicine
DOI 10.1007/s10330-023-0639-9
2023, Vol. 9, No. 2, 66–72

CASE REPORT

Successful surgical resection of large hepatocellular carcinoma with portal vein tumor thrombus after conversion therapy with mFOLFOX-HAIC combined with donafenib and sintilimab: two case reports and a literature review*

Zhitang Guo[1] (✉), Ming Zhang[2], Ang Liu[3], Zhihong Zhang[1], Kejia Li[4], Jiayun Ge[4] (✉)

[1] Department of Hepatobiliary and Pancreatic Surgery, Second Affiliated Hospital, Kunming Medical University, Kunming 650106, China
[2] Department of Surgery, Yunnan Maternal and Child Health Care Hospital, Kunming 650021, China
[3] Department of Surgery, Shiping County People's Hospital, Shiping 662299, China
[4] Department of Surgery, Third Affiliated Hospital, Yunnan University of Traditional Chinese Medicine, Kunming 650599, China

Abstract

The aim of our study was to evaluate the clinical efficacy of mFOLFOX-HAIC combined with donafenib and sintilimab conversion therapy followed by surgical resection of large hepatocellular carcinoma with portal vein tumor thrombus (PVTT). The clinical data of two patients with large hepatocellular carcinoma who were admitted to the Second Affiliated Hospital of Kunming Medical University were retrospectively collected. Both patients received mFOLFOX-HAIC combined with donafenib and sintilimab conversion therapy, followed by hepatectomy. Clinical data were reported, and clinical efficacy was evaluated. One patient had a 14.5 × 11.1 cm tumor with a tumor thrombus in the right portal vein. The other patient had a 12.1 × 8.3 cm tumor with portal and hepatic vein tumor thrombi. Both patients had CNLC stage IIIa prior to conversion therapy, which was reduced to stage Ib after conversion therapy. Subsequently, the patient underwent open and laparoscopic right hemihepatectomies. Short-term high-intensity conversion therapy with mFOLFOX-HAIC combined with donafenib and sintilimab is a feasible and effective treatment for patients with large hepatocellular carcinoma with PVTT.

Received: 7 April 2023
Revised: 12 April 2023
Accepted: 23 April 2023

Key words: hepatocellular carcinoma; portal vein tumor thrombus; immunotherapy; targeted therapy; mFOLFOX-HAIC

Hepatocellular carcinoma (HCC) is the third most common malignant tumor worldwide and the second leading cause of death from malignant tumors in China, seriously threatening human life and health [1, 2]. Radical surgery is the primary treatment option for patients with CNLC stage Ia, Ib, and IIa who meet the physical and tumor condition criteria and have good liver reserve function, with the goal of achieving long-term survival [3, 4]. However, the majority of HCC cases (approximately 80%) occur in developing countries, and unfortunately, most of these patients have tumors in the middle and late stages, which means they may have lost the opportunity for radical surgery [5]. The prognosis of these patients is extremely poor, with a median survival time of only approximately two years, and these patients can only receive non-surgical treatments, such as local and systemic treatments. However, the clinical effects of single treatment methods are poor.

✉ Correspondence to: Zhitang Guo. Email: xiaoguozhitang@163.com; Jiayun Ge. Email: gejy520@163.com
* Supported by grants from the Clinical Research Program of Kunming Medical University (No. ynIIT20211013) and the Joint Special Fund Project of Kunming Medical University (No. 202201AY070001-105).

Therefore, a multidisciplinary team approach and a combination of various methods have been explored for the comprehensive treatment of advanced HCC [6].

In recent years, transcatheter arterial chemoembolization (TACE), hepatic artery infusion chemotherapy (HAIC), and other interventional measures, combined with targeted therapy and immunotherapy, have achieved encouraging results in terms of tumor shrinkage, control, and elimination of tumor thrombi, and tumor downstaging. Simultaneously, with these methods, a higher objective response rate (ORR) is obtained during clinical treatment, and the median survival time of patients is significantly prolonged [7]. Here, two patients with large HCC with portal vein tumor thrombosis (PVTT) admitted to the Second Affiliated Hospital of Kunming Medical University were treated with mFOLFOX-HAIC combined with donafenib and sintilimab targeted therapies, as well as with immunotherapy. This combined treatment successfully down-staged the tumor, enabling the patients to undergo right hepatectomy with favorable therapeutic effects. The data is presented below, along with a review of related literature.

Patients and methods

Patient 1

Table 1 presents the data of the patient. A 57-year-old man was admitted to the hospital due to a liver mass detected by physical examination two days earlier. The patient had undergone open appendectomy for acute appendicitis 25 years previously and had a long history of chronic hepatitis B. Contrast-enhanced computerized tomography (CT) examination showed a 14.5×11.1-cm liver tumor in the right lobe and a tumor thrombus in the right branch of the portal vein (Fig. 1a). Other data included positive hepatitis B surface antigen, AFP 2.17 ng/mL, Eastern Cooperative Oncology Group (ECOG) score 0, Child–Pugh grade A, Barcelona Clinic Liver Cancer (BCLC) stage A, and CNLC stage IIIa.

Table 1 Clinical data of the patients

Indicators	Patient 1	Patient 2
Age (years)	57	62
Sex	Male	Male
Chronic hepatitis B	Yes	No
AFP (ng/mL)	2.17	285.04
ECOG score	0	0
ChildPugh	A	A
Before conversion therapy		
Tumor size (cm)	14.5 × 11.1	12.1 × 8.3
Portal vein tumor thrombus	Yes	Yes
Hepatic vein tumor thrombus	No	Yes
CNLC stage	IIIa	IIIa
After conversion therapy		
Tumor size (cm)	11.1 × 8.4	7.1 × 4.5
Portal vein tumor thrombus	No	No
Hepatic vein tumor thrombus	No	No
CNLC stage	Ib	Ib
ICG-R15 (%)	4.7	5.3

Patient 2

Table 1 presents the data of the patient. A 62-year-old man was admitted due to upper abdominal pain for three days. Their 10-year history of hypertension was well controlled with nifedipine and irbesartan. Their 5-year history of diabetes was well controlled with acarbose. The patient had undergone open cholecystectomy for gallstones with cholecystitis 20 years prior. Contrast-enhanced CT showed a tumor in the right lobe of the liver measuring approximately 12.1 × 8.3 cm in size. The portal and hepatic veins adjacent to the tumor were invaded, and a tumor thrombus was identified (Fig. 2a). Other data included AFP 285.04 ng/mL, ECOG score 0, Child–Pugh grade A, BCLC stage A, and CNLC stage IIIa.

Treatment

After examining the patients' liver and renal functions, blood cell analysis results, and coagulation function data, these two cases were treated with mFOLFOX-HAIC (oxaliplatin, 85 mg/m^2 intra-arterial infusion; formyltetrahydrofolate, 400 mg/m^2 intra-arterial infusion; fluorouracil, 400 mg/m2 intravenous injection, and 2400 mg/m^2 continuous intravenous drip) every 21 days. Donafenib tosilate tablets were administered orally at a dose of 200 mg twice a day. Sintilimab was administered intravenously at a dose of 200 mg with 100 mL of normal saline for the same 21-day treatment cycle. Contrast-enhanced CT data were reviewed every three cycles, and the patients' liver function, liver reserve, general condition, and tumor condition were comprehensively evaluated. Surgical treatment was performed if the patient's tumor shrank, the portal vein tumor thrombus disappeared, and the tumor was down-staged to meet the surgical conditions. Otherwise, the conversion therapy was continued.

Results

Patient 1

Table 1 presents the data of the patient. Contrast-enhanced CT showed that the tumor in the right lobe of the liver had shrunk to 11.1 × 8.4 cm, with multiple areas of necrosis within the tumor and no tumor thrombus in the portal vein, inferior vena cava, or hepatic artery (Fig. 1b). Other data included AFP 2.85 ng/mL, INR 1.14, PT 13.0 s, PLT 219 × 10^9/L, TBIL 14.2 μmol/L, no cirrhosis, body mass index (BMI): 24.39 kg/m^2, ICG 15 min retention test 4.7%, ECOG Score 0, Child–Pugh

grade A, BCLC stage A and CNLC stage Ib. An open right hemihepatectomy was successfully performed.

The postoperative pathological results revealed that the liver specimen had a 11.4 × 9.0 cm tumor with hemorrhage and massive necrosis (Fig. 1c). Pathological diagnosis: (right liver) hepatocellular carcinoma, grade II–III, trabecular type and mass type; significant necrosis after embolization (95%); and hepatic resection margins without tumor involvement (Fig. 1d).

Patient 2

Table 1 presents the data of the patient. Contrast-enhanced CT showed that the tumor in the right lobe of the liver had shrunk to 7.1×4.5 cm, with multiple areas of necrosis within the tumor and no tumor thrombus in the portal vein, inferior vena cava, or hepatic artery (Fig. 2b). Other data included AFP 76.26 ng/mL, INR 1.01, PT 13.1 s, PLT 125 × 10^9/L, TBIL 12.0 μmol/L, ICG 15-min retention test 5.3%, ECOG Score 0, Child–Pugh grade A, BCLC stage A and CNLC stage Ib. Laparoscopic right hemihepatectomy was successfully performed.

The postoperative pathological results showed a tumor in the liver specimen measuring 7.0 × 4.5 × 4.0 cm, with a soft texture and gray-brown cut surface, accompanied by significant necrosis (Fig. 2c). Pathological diagnosis: the right liver tumor tissue showed significant infarction and necrosis, and only cell remnants were observed; however, based on the immunohistochemical labeling results, it was diagnosed as hepatocellular carcinoma, and no cancer was found in the resection margin (Fig. 2d).

Discussion

Although the liver is supplied with blood by both the hepatic artery and portal vein, the blood supply to HCC tumor tissues primarily originates from the hepatic artery, while the portal vein is mainly involved in the blood supply to the tumor capsule and its surrounding area. This theory [8] has been the basis for the continuous development and improvement of transcatheter arterial embolization. In 1983, Yamada [9] first reported 120 cases of unresectable HCC treated with hepatic tumor arterial embolization combined with drug injection, which caused ischemia and hypoxia of the tumor tissue, produced cytotoxic effects, and induced tumor cell necrosis. This is called TACE, and the 1-year, 2-year, and 3-year survival rates for this treatment are 44%, 29%, and 15%, respectively. Since then, TACE has gradually become the standard treatment for medium-stage HCC (BCLC stage B) worldwide [10-15]. The Chinese guidelines for the diagnosis and treatment of HCC published in 2022 [3] suggest that all HCC patients with clinical stages from IB to IIIB should be included in the treatment indication range of TACE. As a palliative treatment, TACE has certain limitations, including a low complete necrosis rate and a high postoperative recurrence rate for HCC with

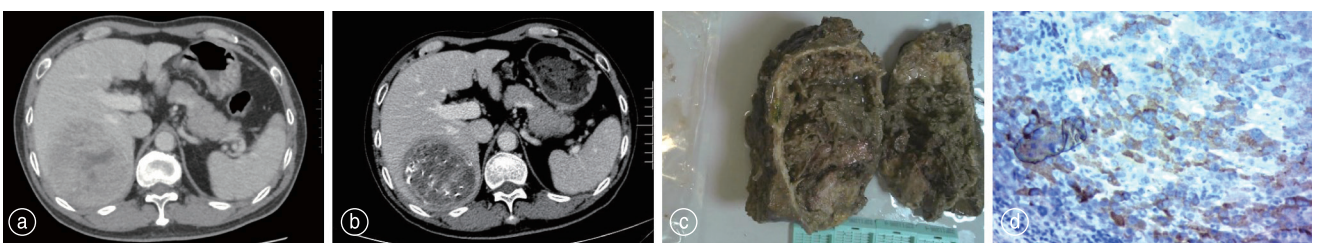

Fig. 1 Patient 1. (a) Preoperative computerized tomography (CT) showed a very large tumor in the right lobe of the liver, with invasion of the right branch of the portal vein and tumor thrombus formation; (b) After conversion therapy, the tumor was significantly reduced, and the portal vein tumor thrombus disappeared; (c) Surgically resected tumor specimen with a large amount of necrotic material inside the tumor; (d) Postoperative pathology (immunohistochemistry) showed hepatocellular carcinoma

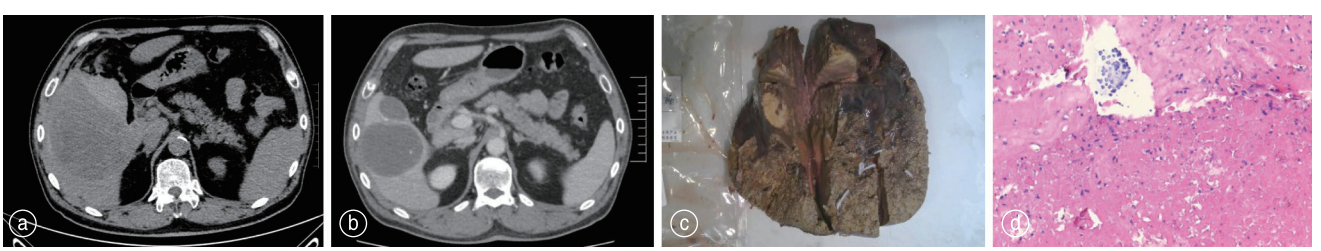

Fig. 2 Patient 2. (a) Preoperative computerized tomography (CT) showed a very large tumor in the right lobe of the liver, with invasion of the right branch of the portal vein and the inferior vena cava with tumor thrombus formation; (b) After conversion therapy, the tumor was significantly reduced, and the portal vein and inferior vena cava tumor thrombus disappeared; (c) Surgically resected tumor specimens; (d) Postoperative pathological results showed hepatocellular carcinoma

a large tumor burden. Additionally, owing to the strong heterogeneity of advanced HCC, its long-term efficacy is not ideal [16]. Therefore, there is an urgent need to develop improved treatment strategies for patients with advanced HCC.

There is no doubt that with the exploration of HCC treatment methods, TACE has also been continuously improved, and a variety of new treatment methods have been developed. As an example, conventional TACE (cTACE) is based on the use of an iodized oil drug emulsion assisted by gelatin sponge particles, microspheres, polyvinyl alcohol, or other solid particles for embolization to achieve tumor ischemic necrosis and cytotoxicity. Moreover, in recent years, drug-eluting bead-TACE (DEB-TACE), which uses pre-loaded chemotherapeutic drugs for continuous and slow release of chemotherapeutics in local tumors, has been developed. Through this method, a high local concentration of chemotherapeutic drugs can be maintained in the tumor, and the peak concentration of blood drugs entering the peripheral circulation can be reduced [10]. Notably, several studies have shown that DEB-TACE has better clinical efficacy than c-TACE [17, 18]. The technique was subsequently developed into transarterial radioembolization (TARE) using yttrium-90 microspheres. This method delivers high doses of β-rays at close range to kill tumor cells [19, 20]. However, the clinical efficacy of this technique remains unsatisfactory.

In recent years, an old technique called HAIC, which was proposed and performed by Japanese doctors in 1995, has received renewed attention [21]. Some studies have reported that HAIC is more effective in patients with advanced HCC who are suitable for TACE [7]. A phase III randomized controlled trial involving 315 patients [5] showed a median overall survival of 23.1 months (95% CI: 18.5–27.7) in the FOLFOX-HAIC group compared to 16.1 months in the control group (95% CI: 14.3–17.9) (hazard ratio 0.58; 95% CI: 0.45–0.75; $P < 0.001$). In addition, the ORR was higher with FOLFOX-HAIC than with TACE [73 (46%) *vs.* 28 (18%); $P < 0.001$], and longer median progression-free survival rates were also observed in the treatment group [9.6 months (95% CI: 7.4–11.9) *vs.* 5.4 months (95% CI: 3.8–7.0), $P < 0.001$]. In addition, the rate of serious adverse events was higher in the TACE group than in the FOLFOX-HAIC group (30% *vs.* 19%, $P = 0.03$). Therefore, compared with systemic chemotherapy, HAIC improves the local drug concentration and tumor uptake rate of drugs and minimizes chemotherapy toxicity [22].

Sorafenib, a tyrosine kinase inhibitor, was approved in 2007 as the first-line targeted therapy for unresectable HCC and showed an overall survival of 10.7 months. Since then, this drug has gradually been approved by the drug regulatory authorities of many countries and regions worldwide and has been recommended by HCC clinical treatment guidelines and expert consensus proceedings. Sorafenib has revolutionized the field of targeted therapy for advanced HCC, establishing its position as the first-line treatment for this condition [4, 23]. However, recent studies have highlighted the emergence of new, promising options for HCC treatment. For instance, lenvatinib has been found to achieve an overall survival (OS) of 13.6 months in the treatment of HCC, demonstrating the effectiveness of targeted therapy in managing advanced HCC [24]. Additionally, donafenib, a new multi-target, multi-kinase inhibitor, represents the latest class of small-molecule targeted drugs with therapeutic potential for HCC. This drug inhibits the RAF/MEK/ERK pathway and the tyrosine kinase activity of VEGFR/PDGFR in tumor cells. As a new deuterated derivative of sorafenib and lenvatinib, it has the advantages of reduced metabolism by hepatic drug enzymes, increased plasma exposure, and a longer half-life [25]. Moreover, it has better pharmacokinetic characteristics and stronger anti-tumor activity [26]. Finally, data from the ZGDH3 study [27] showed that patients with advanced HCC had significantly longer

Table 2 Results of studies related to local treatment, targeted therapy and immunotherapy for HCC

Study	Study type	Year	Treatment	Number of patients	ORR	PFS	DFS	OS
[17]	retrospective cohort study	2021	DEB-TACE or cTACE	71	60.0% *vs* 29.7%	3.3 *vs* 2.1 months	NR	7.8 *vs* 5.7 months
[20]	RCT phase II	2022	90-Y TARE or DEB-TACE	72	NR	NR	NR	30.2 *vs* 15.6 months
[7]	RCT phase III	2022	FOLFOX-HAIC or routine follow-up	315	NR	NR	20.3 *vs* 10 months	(3 years OS)80.4% *vs* 74.9%
[5]	RCT phase III	2022	FOLFOX-HAIC or TACE	315	NR	9.6 *vs* 5.4 months	NR	23.1 *vs* 16.1 months
[27]	RCT phase II-III	2021	Donafenib or Dorafenib	668	NR	3.7 *vs* 3.6 months	NR	12.1 *vs* 10.3 months
[29]	Clinical trial	2017	Nivolumab	262	20%	NR	NR	NR
[31]	retrospective cohort study	2022	pembrolizumab-lenvatinib-TACE or lenvatinib-TACE	142	NR	9.2 *vs* 5.5 months	NR	18.1 *vs* 14.1 months

NR: not reported

OS with donafinib than with sorafenib (12.1 months vs. 10.3 months, respectively; HR = 0.831. 95%CI: 0.699–0.988, $P = 0.0363$) [27, 28].

Based on tumor immunology research, the activation of T cells can upregulate the expression of programmed death receptor 1 (PD-1). However, the binding of PD-1 to PD-ligand 1 (PD-L1) on the surface of tumor cells inhibits the effect of effector T cells. Consequently, immune tolerance is induced, which promotes tumorigenesis. Based on this theory, PD-1/PD-L1 monoclonal antibody drugs have attracted considerable attention in tumor immunotherapy. The first PD-1/PD-L1 monoclonal antibody, pembrolizumab, was approved for marketing in the United States in 2014. Since then, 10 different drugs have been approved for the immunotherapy of various tumors worldwide. For instance, sintilimab, a PD-1/PD-L1 monoclonal antibody produced in China, was approved for marketing in 2018, which is of landmark significance in the "Chinese innovation era" of anti-tumor immunotherapy. This also brings new hope for the treatment of HCC. Furthermore, the CheckMate-040 study [29] showed that the PD-1 checkpoint inhibitor nivolumab showed good tolerance and safety in patients with advanced HCC.

The ORR of sintilimab combined with bevacizumab for the treatment of advanced HCC is 20% [30], and it should be noted that the effect of single-agent immunotherapy is poor. Nevertheless, the combination of immunotherapy and targeted therapy has shown good therapeutic effects [15, 30]. Although targeted therapy combined with immunotherapy has achieved certain clinical treatment effects, the overall ORR is not optimistic. On the other hand, TACE/HAIC is an important treatment method for patients with unresectable middle- and advanced-stage HCC. However, TACE/HAIC alone cannot completely eliminate tumor activity and often results in tumor progression and distant metastasis. Therefore, for unresectable advanced HCC, TACE/HAIC-based local treatment combined with targeted treatments and immunotherapy may demonstrate a "1+1 > 2" therapeutic effect [31]. Furthermore, numerous studies have demonstrated the superior efficacy of this combination therapy, with overall response rates (ORR) exceeding 60% in patients with advanced HCC, particularly in those with PVTT [32].

Since Hermann reported in the 1970s [33] that giant hepatoblastomas shrank after chemoradiotherapy and were successfully surgically resected, many studies have explored translational therapies for HCC [34]. In the Second Affiliated Hospital of Kunming Medical University, two patients with CNLC stage IIIb HCC achieved satisfactory therapeutic effects in terms of tumor shrinkage and tumor thrombus elimination through two cycles of mFOLFOX-HAIC combined targeted therapy and immunotherapy; following this treatment, the tumor descending stage (CNLC stage Ib) was achieved, and radical surgery was finally performed. Studies from many medical centers worldwide have also shown the excellent performance of HAIC combined with targeted therapy and immunotherapy for the treatment of HCC [31, 32, 35]. This combination therapy has been particularly effective in treating HCC patients with PVTT, who are classified as having CNLC stage IIIa, and for whom surgical resection is not the first choice. Therefore, this treatment approach can be considered as an alternative option for these patients.

Surgical operations often need to be combined with vascular thrombectomy, which is difficult to perform and can easily cause vascular embolism, massive bleeding, and even sudden death during and after surgery. During surgery, the risk of recurrence and metastasis is also high. However, through high-intensity conversion therapy using various methods and drugs, tumor shrinkage, tumor thrombus control or disappearance, and tumor downstaging can be achieved in a short time. Simultaneously, it can reduce the risk of surgery and increase the success rate of surgical resection to achieve longer survival times in patients. However, continuous follow-up is necessary to understand the prognosis of patients and ensure the timely implementation of relevant treatments. More data on patients who received such treatment will be collected to continuously understand the conversion therapy of patients with HCC with PVTT and explore better clinical treatment options.

In conclusion, in patients with large HCC complicated by PVTT, aggressive and high-intensity mFOLFOX-HAIC combined with donafenib and sintilimab can achieve tumor shrinkage, tumor thrombus control or disappearance, and tumor downstaging, reduce the risk of surgery, and increase the chance of surgical resection in a short time. However, these preliminary findings need to be further verified in large-sample randomized controlled trials and prospective clinical studies.

Acknowledgments

Not applicable.

Funding

Supported by grants from the Clinical Research Program of Kunming Medical University (No. ynIIT20211013) and the Joint Special Fund Project of Kunming Medical University (No. 202201AY070001-105).

Conflicts of interest

The authors indicated no potential conflicts of interest.

Author contributions

All authors contributed to data acquisition, data interpretation, and reviewed and approved the final version of this manuscript.

Data availability statement

Not applicable.

Ethical approval

The data that support the findings of this study are available from the corresponding author upon reasonable request.

References

1. Chen W, Zheng R, Zeng H, et al. The incidence and mortality of major cancers in China, 2012. Chin J Cancer (Chinese). 2016;35(1):73.
2. Zhou M, Wang H, Zeng X, et al. Mortality, morbidity, and risk factors in China and its provinces, 1990-2017: a systematic analysis for the Global Burden of Disease Study 2017. Lancet. 2019;394(10204):1145-1158.
3. Bureau of medical administration, national health commission of the People's Republic of China. Standardization for diagnosis and treatment of hepatocellular carcinoma (2022 edition). Zhonghua Gan Zang Bing Za Zhi (Chinese). 2022;30(4):367-388.
4. Govalan R, Lauzon M, Luu M, et al. Comparison of surgical resection and systemic treatment for hepatocellular carcinoma with vascular invasion: national cancer database analysis. Liver Cancer. 2021;10(5):407-418.
5. Li QJ, He MK, Chen HW, et al. Hepatic arterial infusion of Oxaliplatin, Fluorouracil, and Leucovorin versus transarterial chemoembolization for large hepatocellular carcinoma: a randomized phase III trial. J Clin Oncol. 2022;40(2):150-160.
6. Llovet JM, Villanueva A, Marrero JA, et al. Trial design and endpoints in hepatocellular carcinoma: AASLD consensus conference. Hepatology. 2021. 73 Suppl 1:158-191.
7. Li SH, Mei J, Cheng Y, et al. Postoperative adjuvant hepatic arterial infusion chemotherapy with FOLFOX in hepatocellular carcinoma with microvascular invasion: A multicenter, phase III, randomized study. J Clin Oncol. 2023;41(10):1898-1908.
8. Clinical Practice Guidelines Committee of Chinese College of Interventionalists. Chinese clinical practice guidelines for transarterial chemoembolization (TACE) for hepatocellular carcinoma (2021 edition). Nat Med J Chin (Chinese). 2021;101(24):1848-1862.
9. Yamada R, Sato M, Kawabata M, et al. Hepatic artery embolization in 120 patients with unresectable hepatoma. Radiology. 1983;148(2):397-401.
10. Heimbach JK, Kulik LM, Finn RS, et al. AASLD guidelines for the treatment of hepatocellular carcinoma. Hepatology. 2018;67(1):358-380.
11. European Association for the Study of the Liver. European association for the study of the liver. EASL clinical practice guidelines: management of hepatocellular carcinoma. J Hepatol. 2018;69(1):182-236.
12. Vogel A, Cervantes A, Chau I, et al. ESMO guidelines committee. hepatocellular carcinoma: ESMO clinical practice guidelines for diagnosis, treatment and follow-up. Ann Oncol. 2018;29(Suppl 4):iv238-iv255.
13. Kudo M, Han KH, Ye SL, et al. A changing paradigm for the treatment of intermediate-stage hepatocellular carcinoma: Asia-Pacific primary liver cancer expert consensus statements. Liver Cancer. 2020;9(3):245-260.
14. Xie DY, Ren ZG, Zhou J, et al. 2019 Chinese clinical guidelines for the management of hepatocellular carcinoma: updates and insights. Hepatobiliary Surg Nutr. 2020;9(4):452-463.
15. IMbrave150: Exploratory efficacy and safety results in patients with hepatocellular carcinoma without macrovascular invasion or extrahepatic spread treated with Atezolizumab + Bevacizumab or Sorafenib. Gastroenterol Hepatol (NY). 2021;17(11 Suppl 6):14-15.
16. He M, Li Q, Zou R, et al. Sorafenib plus hepatic arterial infusion of oxaliplatin, fluorouracil, and leucovorin vs sorafenib alone for hepatocellular carcinoma with portal vein invasion: A randomized clinical trial. JAMA Oncol. 2019;5(7):953-960.
17. Duan X, Liu J, Han X, et al. Comparison of treatment response, survival profiles, as well as safety profiles between CalliSpheres® microsphere transarterial chemoembolization and conventional transarterial chemoembolization in huge hepatocellular carcinoma. Front Oncol. 2022;11:793581.
18. Liu Y, Huang W, He M, et al. Efficacy and Safety of CalliSpheres® drug-eluting beads transarterial chemoembolization in barcelona clinic liver cancer stage C patients. Oncol Res. 2019;27(5):565-573.
19. Salem R, Gabr A, Riaz A, et al. Institutional decision to adopt Y90 as primary treatment for hepatocellular carcinoma informed by a 1,000-patient 15-year experience. Hepatology. 2018;68(4):1429-1440.
20. Dhondt E, Lambert B, Hermie L, et al. 90Y radioembolization versus drug-eluting bead chemoembolization for unresectable hepatocellular carcinoma: results from the TRACE phase II randomized controlled trial. Radiology. 2022;303(3):699-710.
21. Kudo M. Surveillance, diagnosis, and treatment outcomes of hepatocellular carcinoma in Japan: 2021 Update. Liver Cancer. 2021;10(3):167-180.
22. Hsu SJ, Xu X, Chen MP, et al. Hepatic arterial infusion chemotherapy with modified FOLFOX as an alternative treatment option in advanced hepatocellular carcinoma patients with failed or unsuitability for transarterial chemoembolization. Acad Radiol. 2021;28:S157-S166.
23. Llovet JM, Ricci S, Mazzaferro V, et al. SHARP Investigators Study Group. Sorafenib in advanced hepatocellular carcinoma. N Engl J Med. 2008;359(4):378-390.
24. Kudo M, Finn RS, Qin S, et al. Lenvatinib versus sorafenib in first-line treatment of patients with unresectable hepatocellular carcinoma: a randomised phase 3 non-inferiority trial. Lancet. 2018;391(10126):1163-1173.
25. Li X, Qiu M, Wang S, et al. A Phase I dose-escalation, pharmacokinetics and food-effect study of oral donafenib in patients with advanced solid tumours. Cancer Chemother Pharmacol. 2020;85(3):593-604.
26. Gong X, Qin S. Study progression of anti-angiogenetic therapy and its combination with other agents for the treatment of advanced hepatocellular carcinoma. Hepatobiliary Surg Nutr. 2018;7(6):466-474.
27. Qin S, Bi F, Gu S, et al. Donafenib versus sorafenib in first-line treatment of unresectable or metastatic hepatocellular carcinoma: A randomized, open-label, parallel-controlled phase II-III trial. J Clin Oncol. 2021;39(27):3002-3011.
28. Tan HY, Wang N, Lam W, et al. Targeting tumour microenvironment by tyrosine kinase inhibitor. Mol Cancer. 2018;17(1):43.
29. El-Khoueiry AB, Sangro B, Yau T, et al. Nivolumab in patients with advanced hepatocellular carcinoma (CheckMate 040): an open-label,

non-comparative, phase 1/2 dose escalation and expansion trial. Lancet. 2017;389(10088):2492-2502.
30. Ren Z, Xu J, Bai Y, et al. ORIENT-32 study group. Sintilimab plus a bevacizumab biosimilar (IBI305) versus sorafenib in unresectable hepatocellular carcinoma (ORIENT-32): a randomised, open-label, phase 2-3 study. Lancet Oncol. 2021;22(7):977-990.
31. Chen S, Wu Z, Shi F, et al. Lenvatinib plus TACE with or without pembrolizumab for the treatment of initially unresectable hepatocellular carcinoma harbouring PD-L1 expression: a retrospective study. J Cancer Res Clin Oncol. 2022;148(8):2115-2125.
32. Peng W, Zhang X, Li C, et al. Programmed cell death protein 1 and tyrosine kinase inhibition plus transcatheter arterial chemoembolization of advanced hepatocellular carcinoma. Br J Surg. 2022:znac334.
33. Hermann RE, Lonsdale D. Chemotherapy, radiotherapy, and hepatic lobectomy for hepatoblastoma in an infant: report of a survival. Surgery. 1970;68(2):383-388.
34. Sun HC, Zhou J, Wang Z, et al. Alliance of liver cancer conversion therapy, committee of liver cancer of the Chinese anti-cancer association. Chinese expert consensus on conversion therapy for hepatocellular carcinoma (2021 edition). Hepatobiliary Surg Nutr. 2022;11(2):227-252.
35. Qu S, Zhang X, Wu Y, et al. Efficacy and safety of TACE combined with lenvatinib Plus PD-1 inhibitors compared with TACE alone for unresectable hepatocellular carcinoma patients: A prospective Cohort study. Front Oncol. 2022;12:874473.

DOI 10.1007/s10330-023-0639-9
Cite this article as: Guo ZT, Zhang M, Liu A, et al. Successful surgical resection of large hepatocellular carcinoma with portal vein tumor thrombus after conversion therapy with mFOLFOX-HAIC combined with donafenib and sintilimab: two case reports and a literature review. Oncol Transl Med. 2023;9(2):66-72.

Oncology and Translational Medicine
DOI 10.1007/s10330-023-0637-7

April 2023, Vol. 9, No. 2, 73–81

ORIGINAL ARTICLE

The correlation between the hemoglobin-to-red cell distribution width ratio and all-cause mortality in patients with malignant tumors and sepsis: A retrospective cohort study using the MIMIC-IV database

Shu Zhang[1], Shan Xu[2] (✉), Rui Liao[1], Kaixiu Qin[2]

[1] Department of Hepatological Surgery, The First Affiliated Hospital of Chongqing Medical University, Chongqing 400013, China
[2] Department of Emergency, The Second Affiliated Hospital of Chongqing Medical University, Chongqing 400010, China

Abstract

Objective The aim of the study was to investigate the correlation between the hemoglobin-to-red cell distribution width ratio (HRR) and all-cause mortality in patients with malignant tumors and sepsis.

Methods All patients who met the inclusion criteria of the Medical Information Mart for Intensive Care (MIMIC)-IV were selected and divided into four groups according to the quartile range of HRR distribution. Kaplan-Meier (K-M) analysis was used to plot the 28-day survival curve, and the log-rank test was used to compare the prognosis in each HRR group. A Cox proportional hazards regression model was used to evaluate the prognosis of HRR as both a continuous and categorical variable, and a restricted cubic spline was used to study the effect of HRR, as a continuous variable, on the mortality in patients with malignant tumors and sepsis. Interaction and subgroup analyses were performed to evaluate the consistency of correlations.

Results A total of 3926 patients were included in the study, including 934 patients in the HRR ≤ 4.97 group, 988 patients in the 4.97 < HRR ≤ 6.26 group, 1005 patients in the 6.26 < HRR ≤ 7.84 group, and 999 patients in the HRR ≥ 7.84 group. According to the K-M analysis, the 28-day survival rate was the lowest in the HRR ≤ 4.97 group (59.53%), and there were significant differences in survival rates among different HRR levels ($P < 0.001$). The Cox proportional hazards regression model found that after adjusting for various potential confounding factors, HRR was negatively correlated with 28-day and 365-day mortality, and the risk of death in the HRR ≥ 7.84 group was significantly lower than that in the HRR ≤ 4.97 group ($P = 0.030$ and $P = 0.008$, respectively). The restricted cubic spline plot revealed a linear and negative relationship between the HRR and the 28-day and 365-day mortality rates. Subgroup analysis revealed an interaction between HRR, blood urea nitrogen, and SAPS II scores ($P = 0.010$ and $P = 0.048$, respectively).

Conclusion Low HRR is an independent risk factor for all-cause mortality in patients with malignant tumors and sepsis and could be used as a prognostic indicator for these patients.

Received: 1 April 2023
Revised: 11 April 2023
Accepted: 26 April 2023

Key words: Hemoglobin-to-red cell distribution width ratio (HRR); malignant tumors; sepsis; prognosis; the Medical Information Mart for Intensive Care (MIMIC)-IV

Over the past 30 years, substantial progress has been made in the prevention, diagnosis, and treatment of various types of malignant tumors, leading to improved survival rates in patients with malignancy [1, 2]. However, significant improvements in the care of patients with malignant tumors are often accompanied by an increased risk of life-threatening complications such as severe infections caused by surgery or immunotherapy, which have become major non-malignant causes of death [3–5]. Moreover, the specific involvement of malignant tumors

✉ Correspondence to: Shan Xu. Email: 601421954@qq.com

may directly alter the host defense against pathogens, leading to severe infections [6]. Sepsis is one of the leading causes of patients with cancer being admitted to the intensive care unit (ICU) [7]. It has been reported that the risk of sepsis is ten times higher in patients with cancer than in hospitalized non-cancer patients [8]. Moreover, the in-hospital mortality rate of patients with malignancy and sepsis exceeds 25%, which is significantly higher than that of non-malignant patients with sepsis [9, 10], especially in younger patients with malignancy [11, 12]. The treatment of critically ill patients with malignant tumors and sepsis is extremely challenging; thus, it is necessary to identify simple and sensitive clinical variables to predict the risk of death in these patients and provide a theoretical basis for personalized treatment.

Hemoglobin (Hb) and red blood cell distribution width (RDW) are markers derived from red blood cells and also are routine indicators in the complete blood cell count, which can reflect the nutritional, oxidative stress, and inflammatory status of the body [13–16]. As Hb and RDW are mutually influenced by each other, recent studies from various fields suggest that the ratio of Hb to RDW [Hb/RDW ratio (HRR)] could be used as a novel parameter to investigate its relationship with these diseases [17–19]. In particular, the predictive value of the HRR for the prognosis in patients with malignancy has been widely recognized [20–23]. Recent studies have shown that a decrease in HRR is also an independent predictor of an increased risk of all-cause mortality associated with sepsis, atrial fibrillation, and sepsis-related encephalopathy [24, 25]. Both malignant tumors and sepsis share many pathological and physiological features and are caused by the dysregulated host immune response to the initial injury, such as the transformation of malignant tumor cells and invasion of pathogens into the tissue, suggesting the possible existence of mutual effects [8, 26]. However, to date, no studies have been published on the use of a combined HRR index to evaluate the prognosis in patients with malignant tumors and sepsis.

This retrospective study aimed to investigate the correlation between HRR at admission and the prognosis in patients with malignancy and sepsis. A low HRR at ICU admission was shown to be associated with an increased mortality risk. In patients with malignant tumors and sepsis, the HRR could serve as a valuable indicator for predicting prognosis.

Methods

Data source

All relevant data in this study were obtained from the the Medical Information Mart for Intensive Care (MIMIC) (MIMIC-IV version 2.0) database [27]. The MIMIC-IV version 2.0 was updated on June 22, 2022, with additional death records after patient discharge, which can better facilitate the study of long-term prognosis in critically ill patients. The researchers accessed and extracted the data from the database after completing relevant training courses provided by the National Institutes of Health (NIH) in the United States and obtaining certification (Certification Number: 36743986).

Study population and diagnostic criteria

The study population included patients who met MIMIC-IV database criteria. The inclusion criteria were as follows: (1) patients with malignant tumors complicated by sepsis, with malignant tumors determined based on ICD-9 (140-208) or ICD-10 (C00-C96) codes; and (2) diagnosis of sepsis made according to the Sepsis-3.0 definition published jointly by the Society of Critical Care Medicine (SCCM) and the European Society of Intensive Care Medicine (ESICM) in 2016, which requires the presence of a new infection and a new organ dysfunction (SOFA score > 2) [28]. In this study, patients with a record of antibiotic use and a SOFA score > 2 were considered to have sepsis. The exclusion criteria were as follows: (1) age < 18 years, (2) ICU stay < 1 d, and (3) lack of HRR records within 24-hours of ICU admission. The HRR was calculated as follows: HRR = Hb (g/L) / RDW (%). Only the data from the first admission of patients with multiple admissions were included in the analysis.

Outcome variables

The main outcome variable was 28-day mortality, and the secondary outcome variables included ICU stay, hospital stay, ICU mortality, hospital mortality, and 365-day mortality.

Data extraction

All data were extracted using structured query language (SQL), including demographic data (age, sex, weight), laboratory test results (renal function, coagulation function, electrolytes), comorbidities [hypertension, diabetes, chronic obstructive pulmonary diseases (COPD), chronic heart failure], severity scores (SAPS II, SOFA), and prognosis (ICU mortality, hospital mortality, 28-day mortality, and 365-day mortality). Laboratory test results with > 5% missing values were excluded, and missing values were imputed with the mean or median.

Statistical analysis

All data were analyzed using STATA 16.0. Continuous variables were expressed as mean ± standard deviation ($\chi \pm s$) or median (interquartile range) [M (IQR)] based on their distribution and analyzed using one-way ANOVA or Kruskal-Wallis tests. Categorical variables were expressed as percentages and analyzed using the chi-square test. This study plotted the 28-day K-M curve of patients

with malignant tumors and sepsis at different HRR levels and performed a log-rank test. Cox proportional hazards regression models were used to determine the adjusted hazard ratios (HRs) and 95% confidence interval (CI) for 28-day and 365-day mortality, with HRR as a continuous and categorical variable, and a restricted cubic spline was used to evaluate the effect of HRR as a continuous variable on mortality in patients with malignancy and sepsis. Subgroup analyses were performed to eliminate the confounding factors. A P-value < 0.05 was considered statistically significant.

Results

Baseline characteristics of different HRR groups

Following a stepwise screening process, 3926 patients were included in the analysis after excluding those with duplicate hospitalizations, non-sepsis, non-malignant tumors, and ICU length of stay of less than 24 hours. The screening process is illustrated in Fig. 1. Based on the quartile distribution of HRR at ICU admission, patients were divided into four groups: HRR ≤ 4.97 group (n = 934), 4.97 < HRR ≤ 6.26 group (n = 988), 6.26 < HRR ≤ 7.84 group (n = 1005), and HRR ≥ 7.84 group (n = 999). The general characteristics, laboratory test results, vital signs, comorbidities, disease severity scores, and prognoses of the four groups are shown in Table 1. There were more male patients in the high-HRR group. In terms of laboratory indicators, as HRR increased, Hb, white blood cell (WBC) count, and platelet (PLT) count increased, whereas RDW decreased. Blood urea nitrogen (BUN) and creatinine levels were higher and prothrombin time (PT), activated partial thromboplastin time (APTT), and international normalized ratio (INR) were longer in the low HRR group. Serum potassium and calcium levels were lower in the low-HRR group. Additionally, patients in the low HRR group were more likely to have underlying comorbidities, such as hypertension and diabetes; had higher CCI, SOFA, and SAPS II scores; and had a higher continuous renal replacement therapy (CRRT) proportion during hospitalization (P < 0.05). However, there was no statistical difference among the four groups in terms of age, serum sodium and chloride levels, vital signs at admission, or invasive mechanical ventilation proportion.

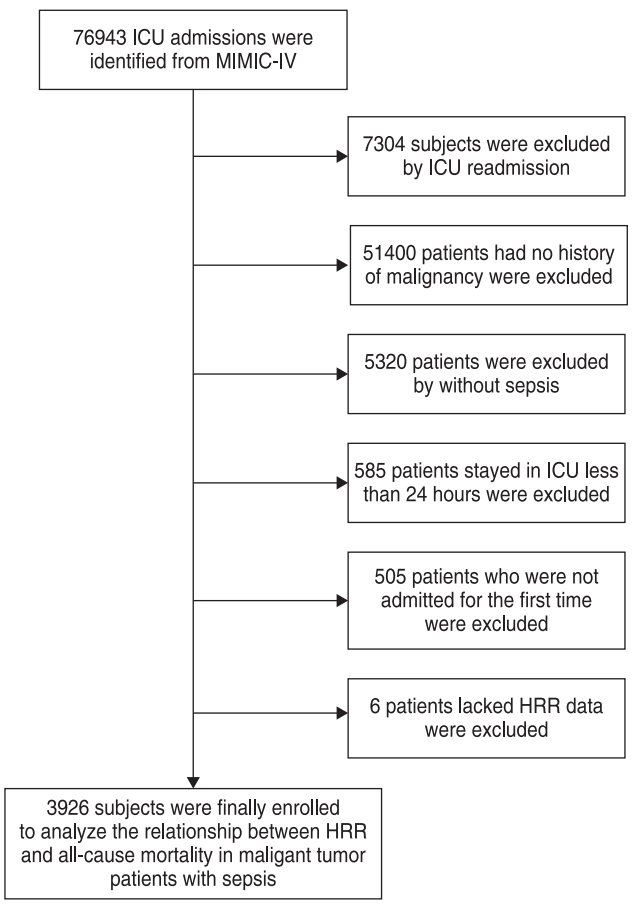

Fig. 1 Flow chart

Prognosis in different HRR groups

In this study, the K-M curve of 28-day mortality was plotted to investigate the prognostic differences among the different HRR groups. The results showed that patients in the different HRR groups had significantly different prognoses. The group with HRR ≤ 4.97 had the lowest 28-day survival rate of 59.53% (556/934), and the survival rate gradually increased with increasing HRR. The survival rates of 4.97 < HRR ≤ 6.26 group, 6.26 < HRR ≤ 7.84 group, and HRR ≥ 7.84 group were 63.46% (627/988), 68.65% (690/1005), and 79.18% (791/999), respectively. The log-rank test indicated that the differences among the four groups were statistically significant (P < 0.001; Fig. 2).

The primary outcomes of this study are summarized in Table 2. There were no significant differences in the length of ICU stay between the groups. The low HRR group had a longer hospital stay and higher ICU, in-hospital, 28-day, and 365-day mortality rates. Moreover, the mortality rates decreased gradually with increasing HRR, and the differences among the four groups were statistically significant (P < 0.05).

The relationship between HRR and mortality in patients with malignant tumors and sepsis

A Cox proportional hazards regression model was used to determine the relationship between HRR level and 28-day and 365-day mortality in patients with malignant tumors and sepsis. Model I was not adjusted for any parameters; Model II was adjusted for sex and age only; and Model III was adjusted for potential confounding

Table 1 Demographic characteristics of study population in each group

Variables	HRR ≤ 4.97 (*n* = 934)	4.97 < HRR ≤ 6.26 (*n* = 988)	6.26 < HRR ≤ 7.84 (*n* = 1005)	HRR ≥ 7.84 (*n* = 999)	H/F/χ^2-value	*P*-value
Demographic						
Age (year)	68.2 ± 13.1	69.4 ± 13.2	70.0 ± 12.5	68.1 ± 13.5	6.812	0.078
Male [*n* (%)]	538 (57.6)	563 (57.0)	611 (60.8)	680 (68.1)	32.198	< 0.001
Weight (kg)	77.8 ± 22.1	78.4 ± 21.7	78.2 ± 20.4	81.3 ± 21.8	7.612	0.055
Laboratory indexes						
Hb (g/dL)	7.7 ± 1.2	9.3 ± 1.1	10.6 ± 1.1	12.9 ± 1.5	121.164	< 0.001
WBC (× 10^{12}/L)	9.8 (5.1–16.9)	11.0 (6.4–17.0)	10.9 (7.1–16.1)	11.9 (8.2–16.2)	29.423	< 0.001
PLT (× 10^9/L)	141 (62–245)	187 (107–296)	201 (129–305)	207 (150–275)	159.580	< 0.001
RDW (%)	19.2 ± 2.9	16.8 ± 2.1	15.3 ± 1.6	13.9 ± 1.2	865.188	< 0.001
Creatine (mg/dL)	1.2 (0.8–2.0)	1.1 (0.7–1.8)	1.0 (0.7–1.6)	1.0 (0.7–1.3)	46.398	< 0.001
BUN (mg/dL)	28 (18–46)	24 (16–41)	22 (15–35)	19 (14–27)	152.044	< 0.001
PT (S)	15.7 (13.6–18.7)	14.9 (13.3–17.8)	14.3 (12.8–16.8)	13.4 (12.1–15.2)	237.138	< 0.001
APTT (S)	31.5 (27.8–39.0)	31.3 (27.4–37.7)	30.6 (26.7–37.2)	29.6 (26.1–34.2)	56.197	< 0.001
INR	1.4 (1.2–1.7)	1.3 (1.2–1.6)	1.3 (1.1–1.5)	1.2 (1.1–1.4)	238.756	< 0.001
Serum potassium (mmol/L)	4.3 ± 0.9	4.3 ± 0.9	4.3 ± 0.8	4.3 ± 0.9	10.234	0.017
Serum sodium (mmol/L)	137.3 ± 5.7	137.1 ± 5.6	137.3 ± 5.7	137.6 ± 6.0	5.012	0.171
Serum chlorine (mmol/L)	102.8 ± 6.9	102.3 ± 7.0	102.3 ± 6.8	101.8 ± 6.8	0.833	0.841
Serum calcium (mg/dL)	8.1 ± 1.0	8.3 ± 1.1	8.4 ± 1.0	8.6 ± 0.9	32.410	< 0.001
Glucose (mg/dL)	125.0 (103.0–162.0)	127.0 (103.0–164.0)	130.5 (105.0–167.0)	135.0 (111.0–168.0)	28.440	< 0.001
Serum anion gap (mmol/L)	16.2 ± 5.0	15.7 ± 4.9	15.5 ± 4.4	16.1 ± 4.7	16.765	< 0.001
Bicarbonate (μmol/L)	22 (18–25)	23 (19–26)	23 (20–26)	23 (21–26)	75.878	< 0.001
Vital signs						
HR (BPM)	97.9 ± 21.0	97.1 ± 21.9	94.7 ± 20.9	93.1 ± 21.8	3.613	0.306
RR (BPM)	21.6 ± 6.9	21.1 ± 6.6	20.3 ± 6.7	20.2 ± 6.6	2.450	0.484
T (°C)	36.8 ± 0.8	36.8 ± 0.8	36.8 ± 0.9	36.8 ± 0.9	2.518	0.472
MBP (mmHg)	76 (66–87)	78 (67–90)	80 (70–91)	84 (73–97)	12.798	0.005
SpO_2 (%)	98 (95–100)	98 (95–100)	98 (94–100)	97 (95–100)	0.604	0.896
Complication						
COPD [*n* (%)]	74 (7.9)	58 (5.9)	79 (7.9)	43 (4.3)	14.801	0.002
Chronic heart failure [*n* (%)]	86 (9.2)	75 (7.6)	69 (6.9)	48 (4.8)	14.749	0.002
Diabetes [*n* (%)]	283 (30.3)	291 (29.5)	274 (27.3)	238 (23.8)	12.267	0.007
Hypertension [*n* (%)]	336 (36.0)	375 (38.0)	421 (41.9)	445 (44.5)	18.050	< 0.001
HIV [*n* (%)]	15 (1.6)	15 (1.5)	15 (1.5)	20 (2.0)	1.029	0.794
CCI	9 (7–11)	9 (7–11)	9 (7–11)	8 (6–10)	88.791	< 0.001
Severity score						
SAPS II	47 (39–57)	45 (37–56)	44 (35–54)	41 (32–50)	114.215	< 0.001
SOFA	7 (5–10)	6 (4–9)	6 (4–8)	5 (3–7)	148.832	< 0.001
Organ support [*n* (%)]						
CRRT	66 (7.1)	42 (4.3)	44 (4.4)	26 (2.6)	22.687	< 0.001
mechanical ventilation	349 (37.4)	423 (42.8)	455 (45.3)	483 (48.4)	25.316	< 0.001
vasoactive agent	468 (50.1)	460 (46.6)	493 (49.1)	394 (39.4)	27.448	< 0.001

Note: WBC: white blood cell; PLT: platelet; BUN: blood urea nitrogen; PT: prothrombin time; APTT: activated partial thromboplastin time; INR: international normalized ratio; HR: heart rate; RR: respiratory rate; MBP: mean blood pressure; COPD: chronic obstructive pulmonary diseases; CCI: chronic disease index; CRRT: continuous renal replacement therapy

factors such as age, weight, sex, Hb, PLT, WBC, creatinine, INR, PT, anion gap, bicarbonate, SAPS II, and SOFA. The results showed that higher HRR was associated with a lower risk of death [HR (95% CI): 0.7 (0.6–0.8), P < 0.001], and the difference was statistically significant (P < 0.001) after adjusting for potential confounding factors in Model III. As a categorical variable, it was also found that compared with the HRR ≤ 4.97 group, the HRR ≥ 7.84 group had a significantly reduced risk of death [HR (95% CI): 0.6 (0.4–1.0)], and the difference was statistically significant (P = 0.030). The 365-day mortality rates were also similar (Table 3).

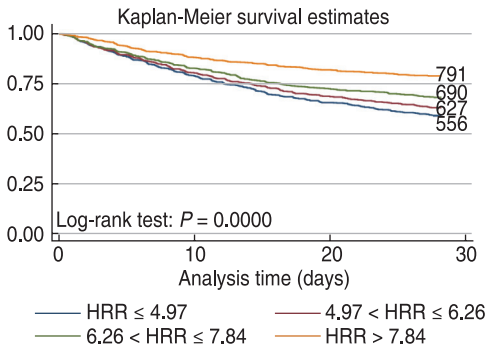

Fig. 2 Kaplan-Meier survival curves of 28-day mortality classified into four groups according to HRR level

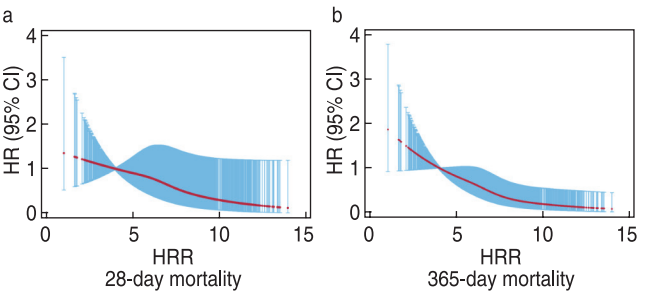

Fig. 3 Restricted cubic splines of the relationship between HRR and mortality in malignancy-associated sepsis patients. (a) HRR and 28-day mortality; (b) HRR and 365-day mortality

Table 2 Comparison of outcomes among different HRR groups

Variables	HRR ≤ 4.97 (*n* = 934)	4.97 < HRR ≤ 6.26 (*n* = 988)	6.26 < HRR ≤ 7.84 (*n* = 1005)	HRR ≥ 7.84 (*n* = 999)	Statistical value	*P*-value
ICU los (d)	3.0 (1.9–5.8)	3.1 (1.8–5.7)	3.0 (1.9–5.4)	3.1 (1.8–6.3)	1.551	0.670
Hospital los (d)	10.12 (5.8–20.0)	9.7 (5.7–17.1)	9.3 (5.6–15.9)	9.1 (5.8–14.9)	13.953	0.003
ICU-mortality [*n* (%)]	209 (22.4)	194 (19.6)	168 (16.7)	122 (12.2)	37.962	< 0.001
In hospital-mortality [*n* (%)]	329 (35.2)	308 (31.2)	253 (25.1)	171 (17.1)	91.940	< 0.001
28 d-mortality [*n* (%)]	378 (40.5)	361 (36.5)	315 (31.3)	208 (20.8)	97.458	< 0.001
365 d-mortality [*n* (%)]	697 (74.6)	677 (68.5)	587 (58.4)	448 (44.8)	209.314	< 0.001

Table 3 Correlation analysis of HRR and its grouping with mortality in patients with malignant tumor and sepsis in different Cox regression models

	Model-I		Modle-II		Modle-III	
	HR (95% CI)	*P* value	HR (95% CI)	*P* value	HR (95% CI)	*P* value
28 d-mortality						
HRR	0.9 (0.8–0.9)	< 0.001	0.9 (0.8–0.9)	< 0.001	0.7 (0.6–0.8)	< 0.001
HRR ≤ 4.97	1		1		1	
4.97 < HRR ≤ 6.26	0.9 (0.8–1.0)	0.093	0.9 (0.8–1.0)	0.066	1.1 (0.9–1.3)	0.585
6.26 < HRR ≤ 7.84	0.7 (0.6–0.9)	< 0.001	0.7 (0.6–0.8)	< 0.001	0.9 (0.7–1.3)	0.714
HRR ≥ 7.84	0.5 (0.4–0.5)	< 0.001	0.5 (0.4–0.5)	< 0.001	0.6 (0.4–1.0)	0.030
365 d-mortality						
HRR	0.9 (0.8–0.9)	< 0.001	0.9 (0.8-0.9)	< 0.001	0.7 (0.6–0.8)	< 0.001
HRR ≤ 4.97	1		1		1	
4.97 < HRR ≤ 6.26	0.9 (0.8–1.0)	0.004	0.8 (0.8–0.9)	0.002	1.1 (0.9–1.2)	0.472
6.26 < HRR ≤ 7.84	0.7 (0.6–0.7)	< 0.001	0.7 (0.6–0.7)	< 0.001	0.9 (0.7–1.1)	0.280
HRR ≥ 7.84	0.4 (0.4–0.5)	< 0.001	0.4 (0.4–0.5)	< 0.001	0.7 (0.5–0.9)	0.008

Note: Model I: no other parameter adjustments were made; Model II: adjusted for gender and age; Model III: adjusted for age, gender, hemoglobin, platelets, white blood cells, creatinine, blood urea nitrogen, prothrombin time, international normalized ratio, activated partial thromboplastin time, anion gap, bicarbonate, potassium, sodium, hypertension, chronic obstructive pulmonary disease, diabetes mellitus, chronic heart failure, chronic respiratory failure, SAPS II, SOFA, and initial vital signs at admission

Relationship between HRR as a continuous variable and the mortality of patients with malignant tumors and sepsis

This study investigated the relationship between HRR as a continuous variable and mortality in patients with malignant tumors and sepsis using restricted cubic splines. The results showed that HRR had a linear and negative correlation with 28-day and 365-day mortality in patients with malignant tumors and sepsis. Specifically, a higher HRR was associated with lower mortality risk in these patients (Fig. 3).

Subgroup analysis

To further investigate the relationship between HRR and mortality in patients with malignant tumors and sepsis, a subgroup analysis was conducted. The results showed that there was an interaction between HRR and BUN, as well as the SAPS II score (P = 0.010, and P = 0.048; Fig. 4).

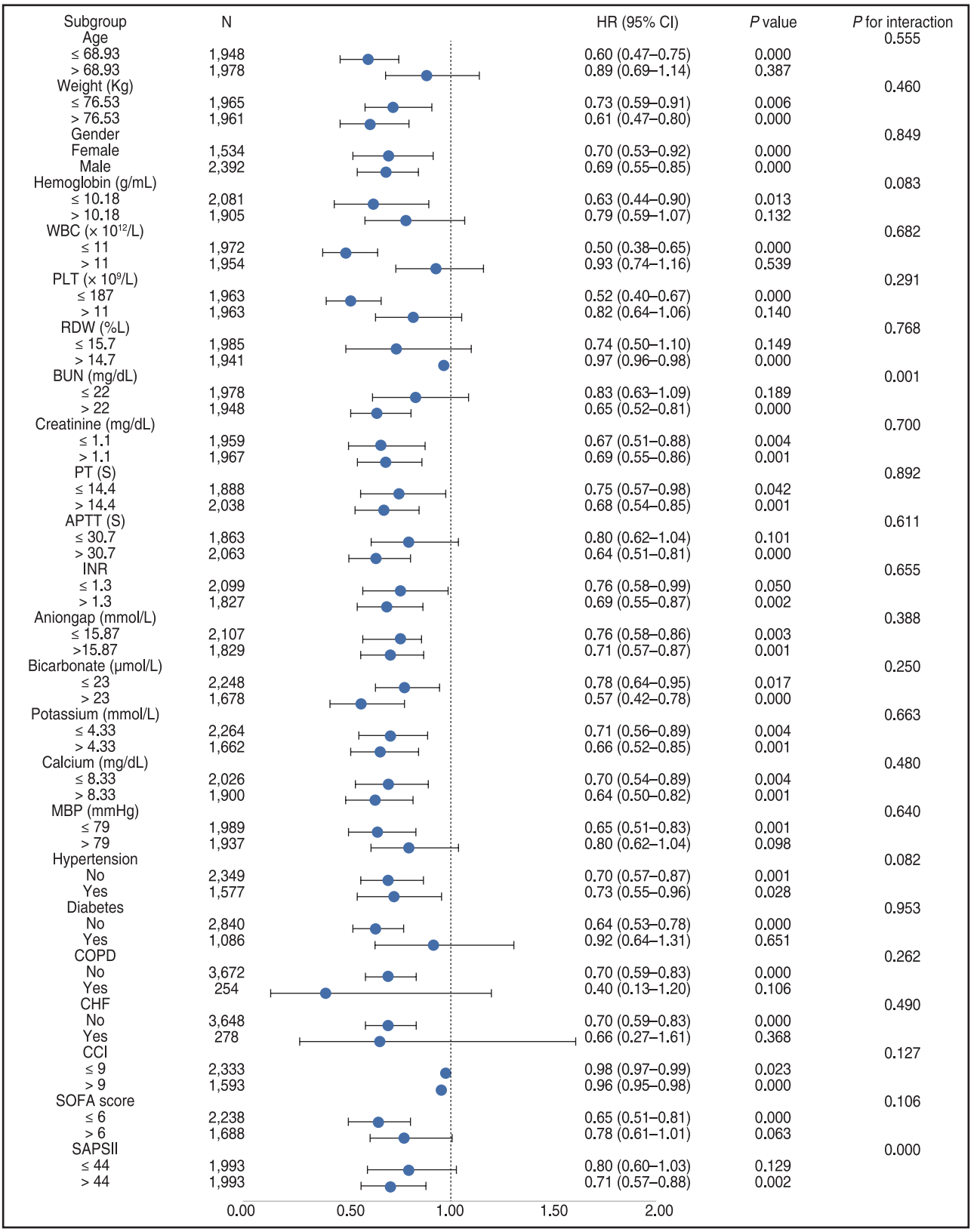

Fig. 4 Subgroup analysis

Discussion

A total of 3926 patients from the MIMIC-IV database were included in this study. The results showed that among patients with malignant tumors and sepsis, the 28-day mortality rate was 33.01% (1262/3926) and the 365-day mortality rate was as high as 61.36% (2409/3926), consistent with other studies [29, 30]. The HRR at ICU admission is related to the prognosis in patients with malignant tumors and sepsis. As HRR levels increase, the length of hospital stay, 28-day mortality, and 365-day mortality of patients with malignant tumors and sepsis decrease. Multivariate Cox proportional hazards regression analysis showed that after adjusting for potential confounding factors, a lower HRR was an independent risk factor for 28-day mortality and 365-mortality ($P < 0.05$). As a categorical variable, it indicated that compared to patients with lower HRR levels (HRR ≤ 4.97 group), those with higher HRR levels (HRR ≥ 7.84 group) had a significantly lower risk of mortality.

The HRR has emerged as a novel comprehensive biomarker for predicting overall and disease-free survival in patients with malignant tumors [20]. A low HRR is closely associated with a poor prognosis in small cell lung cancer [31], and a similar result has been reported in studies on non-small cell lung cancer [32]. As a simple, easy-to-obtain, and reproducible hematological parameter, HRR can also be used for the prognosis in patients with lung large-cell neuroendocrine carcinoma [33]. Additionally, HRR levels have shown good predictive value for survival among patients with gastric cancer treated with neoadjuvant [23]. Su *et al* found that HRR levels were associated with disease progression and poor prognosis in upper tract urothelial carcinoma [21], and the combination of HRR and platelet-lymphocyte ratio could predict the prognosis in patients with liver metastases from gastric cancer. Recent studies have found that the HRR has excellent predictive value for the prognosis in patients with sepsis [34]. A study using the MIMIC-IV database found that a low HRR was associated with increased all-cause mortality among patients with sepsis. Another MIMIC database study found that low HRR levels were associated with poor prognosis in patients with sepsis-associated encephalopathy [25]. This study confirmed that a low HRR at ICU admission was associated with an increased risk of mortality. The HRR can be used to assess the severity and prognosis in patients with malignant tumors and sepsis.

The HRR is a valuable indicator, obtained by calculating the Hb/RDW ratio, that can effectively predict the prognosis in patients with malignant tumors and sepsis. Low Hb levels are usually associated with malnutrition and decreased immune response. Low hematocrit and anemia are independent risk factors for poor prognosis in sepsis [35, 36]. RDW is an essential parameter of complete blood count, representing the variability in red blood cell counts, and has been widely studied in patients with sepsis. A series of studies have confirmed that elevated RDW is closely related to the poor prognosis of sepsis [37–40]. However, while the HRR can be used to predict the prognosis in patients with malignant tumors and sepsis, it is not simply a combination of Hb and RDW, as these two factors may influence each other in the following ways: first, malnutrition usually results in low levels of Hb in patients with malignant tumors, and the body undergoes an inflammatory response and oxidative stress after suffering from sepsis. As a result, both the number of red blood cells and the Hb level decrease [41, 42]. The reduction in Hb shortens the lifespan of red blood cells, releases a large number of immature red blood cells into the circulation, and leads to an increase in RDW. Second, cytokine production induced by oxidative stress in patients with sepsis can reduce erythrocyte survival time and increase RDW [43]. In summary, the HRR reflects changes in both Hb and RDW simultaneously and can provide more predictive information than a single indicator.

In this study, an interaction between HRR and blood urea nitrogen was observed. A low HRR was closely associated with a higher risk of mortality in patients with BUN levels > 22 mg/dL. This is consistent with a study by Huang *et al*, which found that in patients with septic encephalopathy who had a history of dialysis, a low HRR was strongly associated with a high mortality risk [25]. This study also found an interaction between the HRR and SAPS II scores.

This study has several limitations. First, as it was a retrospective study, unavoidable bias may have affected the authenticity of the research results. Second, owing to the lack of data in public databases, some information, such as blood gas analysis, was missing. Third, only a single HRR level at ICU admission was selected to evaluate its relationship with the prognosis in patients with malignant tumors and sepsis. Since the impact of dynamic changes on the outcome was unable to be assessed, dynamic monitoring during hospitalization may be more valuable for prognostic prediction in patients with malignant tumors and sepsis.

Conclusion

In summary, early clinical diagnosis and appropriate interventions are crucial. The HRR is an effective predictor of prognosis in patients with malignant tumors and sepsis. Thus, a decrease in HRR could indicate a poor prognosis in patients with malignant tumors and sepsis. These results should be validated in prospective clinical studies.

Acknowledgments
Not applicable.

Funding
Not applicable.

Conflicts of interest
The authors indicated no potential conflicts of interest.

Author contributions
Shu Zhang contributed to the statistical analysis and manuscript writing. Shan Xu contributed to data acquisition and interpretation. Rui Liao and Kaixiu Qin reviewed and approved the final manuscript.

Data availability statement
The datasets used and analyzed during the current study are available from the corresponding author on reasonable request.

Ethical approval
Not applicable.

References

1. Edwards BK, Noone AM, Mariotto AB, et al. Annual report to the nation on the status of cancer, 1975–2010, featuring prevalence of comorbidity and impact on survival among persons with lung, colorectal, breast, or prostate cancer. Cancer. 2014;120(9):1290-1314.
2. Coleman MP, Gatta G, Verdecchia A, et al. EUROCARE-3 summary: cancer survival in Europe at the end of the 20th century. Ann Oncol. 2003;14 Suppl 5:v128-v149.
3. Hiong A, Thursky KA, Teh BW, et al. Sepsis following cancer surgery: the need for early recognition and standardised clinical care. Expert Rev Anti Infect Ther. 2016;14(4):425-433.
4. Zaorsky NG, Churilla TM, Egleston BL, et al. Causes of death among cancer patients. Ann Oncol. 2017;28(2):400-407.
5. Anderson C, Lund JL, Weaver MA, et al. Noncancer mortality among adolescents and young adults with cancer. Cancer. 2019;125(12):2107-2114.
6. Toma A, Fenaux P, Dreyfus F, et al. Infections in myelodysplastic syndromes. Haematologica. 2012;97(10):1459-1470.
7. Hawari FI, Nazer LH, Addassi A, et al. Predictors of ICU admission in patients with cancer and the related characteristics and outcomes: A 5-year registry-based study. Crit Care Med. 2016;44(3):548-553.
8. Mirouse A, Vigneron C, Llitjos JF, et al. Sepsis and cancer: An interplay of friends and foes. Am J Respir Crit Care Med. 2020;202(12):1625-1635.
9. Lemiale V, Pons S, Mirouse A, et al. Sepsis and septic shock in patients with malignancies: A groupe de recherche respiratoire en réanimation onco-hématologique study. Crit Care Med. 2020;48(6):822-829.
10. Torres VB, Azevedo LC, Silva UV, et al. Sepsis-associated outcomes in critically Ill patients with malignancies. Ann Am Thorac Soc. 2015;12(8):1185-1192.
11. Hensley MK, Donnelly JP, Carlton EF, et al. Epidemiology and outcomes of cancer-related versus non-cancer-related sepsis hospitalizations. Crit Care Med. 2019;47(10):1310-1316.
12. Nazer L, Lopez-Olivo MA, Cuenca JA, et al. All-cause mortality in cancer patients treated for sepsis in intensive care units: a systematic review and meta-analysis. Support Care Cancer. 2022;30(12):10099-10109.
13. Friedman JS, Lopez MF, Fleming MD, et al. SOD2-deficiency anemia: protein oxidation and altered protein expression reveal targets of damage, stress response, and antioxidant responsiveness. Blood. 2004;104(8):2565-2573.
14. Patel KV, Semba RD, Ferrucci L, et al. Red cell distribution width and mortality in older adults: a meta-analysis. J Gerontol A Biol Sci Med Sci. 2010;65(3):258-265.
15. Lippi G, Targher G, Montagnana M, et al. Relation between red blood cell distribution width and inflammatory biomarkers in a large cohort of unselected outpatients. Arch Pathol Lab Med. 2009;133(4):628-632.
16. Ganz T. Anemia of inflammation. N Engl J Med. 2019;381(12):1148-1157.
17. Yildiz D, Cakir U, Tugcu AU, et al. Hemoglobin/red cell distribution width ratio (HRR): A novel and promising red cell parameter in ductal closure. Arq Bras Cardiol. 2023;120(2):e20220339.
18. Qu J, Zhou T, Xue M, et al. Correlation analysis of hemoglobin-to-red blood cell distribution width ratio and frailty in elderly patients with coronary heart disease. Front Cardiovasc Med. 2021;8:728800.
19. Yu Z, Zhang T, Shen J. Low hemoglobin-to-red cell distribution width ratio is associated with mortality in patients with HBV-related decompensated cirrhosis. Biomed Res Int. 2022;2022:5754790.
20. Chi G, Lee JJ, Montazerin SM, et al. Prognostic value of hemoglobin-to-red cell distribution width ratio in cancer: a systematic review and meta-analysis. Biomark Med. 2022;16(6):473-482.
21. Su YC, Wen SC, Li CC, et al. Low hemoglobin-to-red cell distribution width ratio is associated with disease progression and poor prognosis in upper tract urothelial carcinoma. Biomedicines. 2021;9(6):672.
22. Yılmaz H, Yılmaz A, Demirağ G. Prognostic significance of hemoglobin-to-red cell distribution width ratio in patients with metastatic renal cancer. Future Oncol. 2021;17(29):3853-3864.
23. Yılmaz A, Mirili C, Tekin SB, et al. The ratio of hemoglobin to red cell distribution width predicts survival in patients with gastric cancer treated by neoadjuvant FLOT: a retrospective study. Ir J Med Sci. 2020;189(1):91-102.
24. Wang J, Chen Z, Yang H, et al. Relationship between the hemoglobin-to-red cell distribution width ratio and all-cause mortality in septic patients with atrial fibrillation: based on propensity score matching method. J Cardiovasc Dev Dis. 2022;9(11):400.
25. Huang X, Yuan S, Ling Y, et al. The hemoglobin-to-red cell distribution width ratio to predict all-cause mortality in patients with sepsis-associated encephalopathy in the MIMIC-IV database. Int J Clin Pract. 2022;2022:7141216.
26. Hotchkiss RS, Moldawer LL. Parallels between cancer and infectious disease. N Engl J Med. 2014;371(4):380-383.
27. Johnson A, Bulgarelli L, Pollard T, et al. MIMIC-IV (version 0.4). PhysioNet. https://doi.org/10.13026/a3wn-hq05. 2020.
28. Rhodes A, Evans LE, Alhazzani W, et al. Surviving sepsis campaign: International guidelines for management of sepsis and septic shock: 2016. Intensive Care Med. 2017;43(3):304-377.
29. Vesteinsdottir E, Sigurdsson MI, Gottfredsson M, et al. A nationwide study on characteristics and outcome of cancer patients with sepsis requiring intensive care. Acta Oncol. 2022;61(8):946-954.
30. Awad WB, Nazer L, Elfarr S, et al. A 12-year study evaluating the outcomes and predictors of mortality in critically ill cancer patients

admitted with septic shock. BMC Cancer. 2021;21(1):709.
31. Wu F, Yang S, Tang X, et al. Prognostic value of baseline hemoglobin-to-red blood cell distribution width ratio in small cell lung cancer: A retrospective analysis. Thorac Cancer. 2020;11(4):888-897.
32. Bozkaya Y, Kurt B, Gürler F. A prognostic parameter in advanced non-small cell lung cancer: the ratio of hemoglobin-to-red cell distribution width. Int J Clin Oncol. 2019;24(7):798-806.
33. Zhao W, Shi M, Zhang J. Preoperative hemoglobin-to-red cell distribution width ratio as a prognostic factor in pulmonary large cell neuroendocrine carcinoma: a retrospective cohort study. Ann Transl Med. 2022;10(2):42.
34. Zhai Z, Gao J, Zhu Z, et al. The ratio of the hemoglobin to red cell distribution width combined with the ratio of platelets to lymphocytes can predict the survival of patients with gastric cancer liver metastasis. Biomed Res Int. 2021;2021:8729869.
35. Apple CG, Kelly LS, Kannan KB, et al. Ineffective erythropoietin response to anemia in sepsis. Surg Infect (Larchmt). 2022;23(2):142-149.
36. Luo M, Chen Y, Cheng Y, et al. Association between hematocrit and the 30-day mortality of patients with sepsis: A retrospective analysis based on the large-scale clinical database MIMIC-IV. PLoS One. 2022;17(3):e0265758.
37. Hu ZD, Lippi G, Montagnana M. Diagnostic and prognostic value of red blood cell distribution width in sepsis: A narrative review. Clin Biochem. 2020;77:1-6.
38. Moreno-Torres V, Royuela A, Múñez-Rubio E, et al. Red blood cell distribution width as prognostic factor in sepsis: A new use for a classical parameter. J Crit Care. 2022;71:154069.
39. Li Y, She Y, Fu L, et al. Association between red cell distribution width and hospital mortality in patients with sepsis. J Int Med Res. 2021;49(4):3000605211004221.
40. Ramires MLV, Leite MFB, Lo DZY, et al. Relation between red blood cell distribution width and acute kidney injury in patients with sepsis. Einstein (Sao Paulo). 2022;20:eAO6828.
41. Fagerberg SK, Patel P, Andersen LW, et al. Erythrocyte P2X1 receptor expression is correlated with change in haematocrit in patients admitted to the ICU with blood pathogen-positive sepsis. Crit Care. 2018;22(1):181.
42. Janz DR, Bastarache JA, Peterson JF, et al. Association between cell-free hemoglobin, acetaminophen, and mortality in patients with sepsis: an observational study. Crit Care Med. 2013;41(3):784-790.
43. Semba RD, Patel KV, Ferrucci L, et al. Serum antioxidants and inflammation predict red cell distribution width in older women: the Women's Health and Aging Study I. Clin Nutr. 2010;29(5):600-604.

DOI 10.1007/s10330-023-0637-7
Cite this article as: Zhang S, Xu S, Liao R, et al. The correlation between the hemoglobin-to-red cell distribution width ratio and all-cause mortality in patients with malignant tumors and sepsis: A retrospective cohort study using the MIMIC-IV database. Oncol Transl Med. 2023;9(2):73-81.

Oncology and Translational Medicine
DOI 10.1007/s10330-022-0594-4

April 2023, Vol. 9, No. 2, 82–92

ORIGINAL ARTICLE

Development of a redox-related prognostic signature for predicting biochemical-recurrence-free survival of prostate cancer*

Peng Hu[1], Guoda Song[1,2], Bingliang Chen[1,2], Jianping Miao[3] (✉)

[1] Department of Urology, Tongji Hospital, Tongji Medical College, Huazhong University of Science and Technology, Wuhan 430030, China
[2] Second Clinical College, Tongji Medical College, Huazhong University of Science and Technology, Wuhan 430030, China
[3] Department of Geriatrics, Tongji Hospital, Tongji Medical College, Huazhong University of Science and Technology, Wuhan 430030, China

Abstract

Objective Prostate cancer (PCa) is one of the most common malignancies among elderly males. However, effective prognostic biomarkers are currently lacking. Bioinformatic analysis was used to identify patients at high risk of biochemical recurrence (BCR).

Methods In our study, RNA sequencing and clinical data were downloaded from The Cancer Genome Atlas (TCGA) dataset to serve as the training and internal validation sets. The GSE84042 dataset was used as the external validation set. Batch effects were removed and normalized for the two datasets using "sva" package. Univariate Cox, least absolute shrinkage and selection operator (LASSO) Cox, and multivariate Cox regression analyses were successively performed to identify the redox-related gene (RRG) signature. After performing univariate Cox, LASSO Cox, and multivariate Cox regression analyses, a signature consisting of seven RRGs was established to predict BCR of patients with PCa, which included *TP53, ADH5, SRRT, SLC24A2, COL1A1, CSF3R*, and *TEX19*. Kaplan-Meier and receiver operating characteristic curve analyses showed good performance for the prognostic signature in the training and validation datasets.

Results Univariate and multivariate Cox analyses showed that the RRG signature was an independent prognostic factor for BCR of patients with PCa. Thereafter, the nomogram results revealed that it was able to predict BCR of patients with PCa with high efficiency.

Conclusion This study identified an independent prognostic signature and established a nomogram to predict BCR in PCa. This signature can be used to identify patients with PCa with a high risk of BCR, and personalized treatment can be applied.

Received: 28 August 2022
Revised: 11 February 2023
Accepted: 27 March 2023

Key words: prostate cancer (PCa); redox; prognostic signature; prognosis; bioinformatic

Prostate cancer (PCa) is one of the most commonly diagnosed urogenital cancers in the elderly (age > 65 years) [1] and has the second highest male cancer-related mortality rate in the United States, accounting for approximately 20% of newly diagnosed cases in 2019 [2]. With advances in diagnosis and therapy, the clinical survival of patients with PCa has significantly increased. However, 20%–30% of patients experience biochemical recurrence (BCR) without clinical or radiographic metastases [3]. Without secondary treatment, the interval time from BCR to clinical progression is approximately 5–8 years, and 32%–45% of patients die of PCa within 15 years [4]. Therefore, a prognostic signature that can predict BCR-free survival is of tremendous clinical value.

Redox (reduction and oxidation) reactions are a series of reactions that transfer electrons between molecules. Redox reactions occur extensively throughout the body in response to both endogenous and exogenous stimuli. Redox reactions have important physiological functions such as transcriptional regulation, direct

✉ Correspondence to: Jianping Miao. Email: miaojianping888@hotmail.com
* Supported by grants from the National Natural Science Foundation of China (No. 81902619) and National Natural Science Foundation of Hubei Province (No: 2020CFB591).

oxidative modification, regulation of redox-sensitive interacting proteins, regulation of redox-sensitive modifying proteins, and regulation of protein turnover [5]. The homeostasis of redox reactions refers to a delicate balance between the generation and removal of reactive oxygen species (ROS). Reactive oxidizing molecules are strongly oxidizing molecules that include free radicals. The excessive accumulation of these molecules is called "oxidative stress," which can destroy proteins, DNA and lipid macromolecules, and lead to DNA damage, signal transduction abnormalities and remodeling of the extracellular matrix [6]. Studies have shown that the imbalance of redox reactions is closely related to the development of many diseases, such as cancer, cardiovascular diseases, diabetes mellitus, and neurodegenerative diseases [7–9]. The accumulation of ROS has been linked to the occurrence and progression of various malignancies such as bladder, breast, liver, lung, ovarian, and prostate cancers [10–12]. The possible mechanisms of oxidative stress-induced cancers include the induction of genomic instability, abnormal epigenetic modifications, uncontrolled proliferation of initiated cells, and failure of apoptosis [10]. However, no studies have explored the association between redox-related genes (RRGs) and PCa prognosis.

In this study, The Cancer Genome Atlas (TCGA) and Gene Expression Omnibus (GEO) databases were used to analyze the association between RRGs and the prognosis of patients with PCa. Potential biomarkers were identified to improve the clinical outcome of patients with PCa.

Materials and methods

Data acquisition and processing

The RRGs were searched using the Genecard database (https://www.genecards.org/), NCBI gene function module (https://www.ncbi.nlm.nih.gov/gene/), OMIM database (https://www.oncomine.org/resource/), and GSEA-MsigDB (https://www.gsea-msigdb.org/gsea/msigdb) with the keyword "redox," and 4087 genes were obtained. We downloaded the transcriptomic data and associated clinical information for 499 PCa tumors from TCGA (https://portal.gdc.cancer.gov/), which contained 499 tumors and 52 surrounding normal tissues. Background correction and normalization of the RNA-seq data were performed using fragments per kilobase million (FPKM) [13]. The patients in TCGA cohort were randomly split into training and internal validation cohorts. Normalized mRNA expression data of the GSE84042 dataset with 73 PCa samples were downloaded from the GEO database, and clinicopathological data were obtained from the supplementary material of the original literature [14]. The GSE84042 dataset was used as the external validation cohort. Genes with expression values of 0 in more than half of the samples were deleted. The batch effect was eliminated by using the "sva" package in R (Version 4.1.0).

Construction and validation of RRG prognostic signature

To identify prognosis-related RRGs, we used data from TCGA cohort to perform univariate Cox proportional regression to evaluate the correlation between RRGs and BCR-free survival. The RRGs with P value < 0.00001 were selected, and then the better prognostic RRGs were screened by the least absolute shrinkage and selection operator (LASSO) regression analysis using the "glmnet" package. Finally, a prognostic signature was constructed using a multivariate Cox regression analysis. In order to reveal the biological functions of the selected RRGs, Gene Ontology (GO) and Kyoto Gene and Genome Encyclopedia (KEGG) enrichment analysis were performed by R packages "ggplot2" with P-value of < 0.05. The GO enrichment results are described in terms of three aspects: biological process (BP), cellular component (CP), and molecular function (MF). The following formula was used to compute the risk score of each patient: risk score = (exp Gene1 × coef Gene1) + (exp Gene2 × coef Gene2) +…+ (exp GeneN × coef GeneN). Here, exp represents the expression value of the selected genes, and coef represents the computed multivariate Cox regression coefficients.

The median risk score of the training cohort was used as the cut-off value for the training and validation cohorts. Patients were separated into high- and low-risk subgroups based on the cutoff values. The prognostic capacity of the gene signature was assessed using Kaplan-Meier curve analysis (using the "survival" package) and area under the receiver operating characteristic (ROC) curve (AUC) analysis (using the "timeROC" package). In addition, the internal validation dataset and GSE84042 cohort were employed as validation sets to verify the stability and correctness of the signature. The risk score for each patient in the validation set was calculated using the formula described above. Kaplan-Meier and ROC curve analyses were also performed on the validation set. The prognostic signature results were used to perform a principal component analysis (PCA). Statistical significance was set at $P < 0.05$.

Clinical relevance of RRG signature

Clinicopathological parameters including age at diagnosis, pathologic T stage (pT), Gleason grade score (GGS), and preoperative prostate-specific antigen (PSA) levels were used to stratify patients with PCa. Using the Kaplan-Meier "survival" package, Kaplan-Meier curve analysis was performed to evaluate the prognostic value of the signature in different subgroups. In addition,

we analyzed the differences in the signature-based risk score distribution between subgroups stratified by clinicopathological parameters. Statistical significance was set at $P < 0.05$.

Construction and validation of a nomogram

To identify independent prognostic indicators for PCa related to BCR-free survival, we used univariate and multivariate Cox analyses based on the prognostic gene signature and clinicopathological data such as age at diagnosis and pT, GGS, and PSA values. Then, using the "rms" package, we created a nomogram combining clinicopathological data and the gene signature to produce a quantitative strategy to predict the prognosis of patients with PCa. Finally, Kaplan-Meier survival analysis, AUC under the ROC curve analysis, and the C-index were performed to assess the accuracy and stability of the nomogram. The performances of the nomogram and clinical models were compared using decision curve analysis (DCA). Statistical significance was set at $P < 0.05$.

Results

Construction and validation of RRG prognostic signature

A flowchart of the process used in this study is shown in Fig. 1. In TCGA dataset, 429 patients with BCR-free survival status and time were collected to construct the RRGs signature. After performing univariate Cox proportional regression analysis, 19 RRGs were found to be significantly related to BCR-free survival ($P < 0.00001$). Next, LASSO Cox regression and multivariate Cox regression analyses were performed, and seven genes were identified: *TP53*, *ADH5*, *SRRT*, *SLC24A2*, *COL1A1*, *CSF3R*, and *TEX19*. The results are shown in Fig. 2 and 3. The results of GO and KEGG showed RRGs were mainly involved in cellular response to environmental stimulus, cellular response to abiotic stimulus and production of miRNAs involved in gene silencing by miRNA. Molecular functions of the differentially expressed RRGs were enriched for protease binding. KEGG analysis showed that these RRGs mainly enriched in the pathways of PI3K-Akt signaling pathway. The results were showed in Fig. 4. The risk score of each patient was calculated as follows: Risk score = (–0.3239 × TP53 exp) + (–0.6248 × ADH5 exp) + (1.4499 × SRRT exp) + (0.9269 × SLC24A2 exp) + (0.3841 × COL1A1 exp) + (1.5398 × CSF3R exp) + (1.5942 × TEX19 exp).

Patients were separated into high- and low-risk subgroups based on the cutoff values. Kaplan-Meier curve analysis of the TCGA training cohort revealed that patients in the high-risk group had a worse prognosis than those in the low-risk group ($P < 0.001$; Fig. 5a). The AUC under the ROC curve of different time points were calculated using the ROC curve. The AUC values for the first year were 0.837, 0.754 for the second year, 0.837 for the third year, 0.820 for the fourth year, and 0.846 for the fifth year, indicating that this model can accurately predict the BCR-free survival prognosis of patients with PCa (Fig. 5d). The TCGA validation cohort and GSE84042

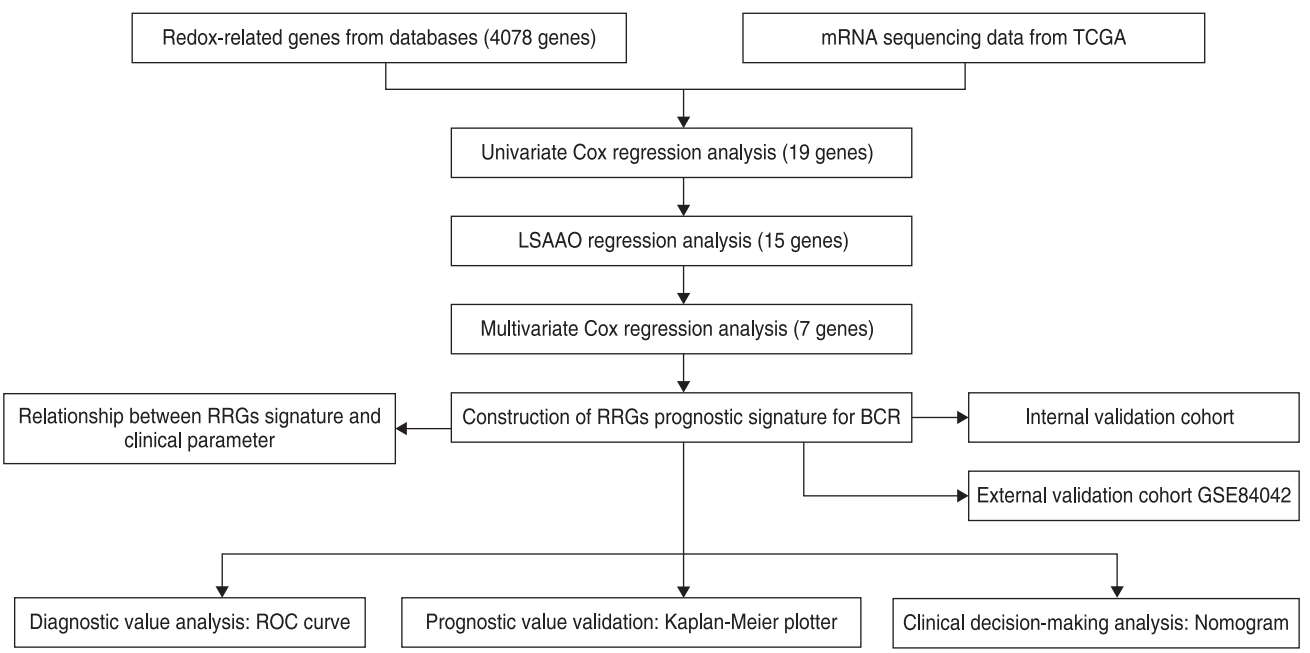

Fig. 1 Flowchart of the procedures performed in the study. TCGA: The Cancer Genome Atlas; PCa: prostate cancer; LASSO: the least absolute shrinkage and selection operator; ROC: receiver operating characteristic; RRGs: redox-related genes; BCR: biochemical recurrence

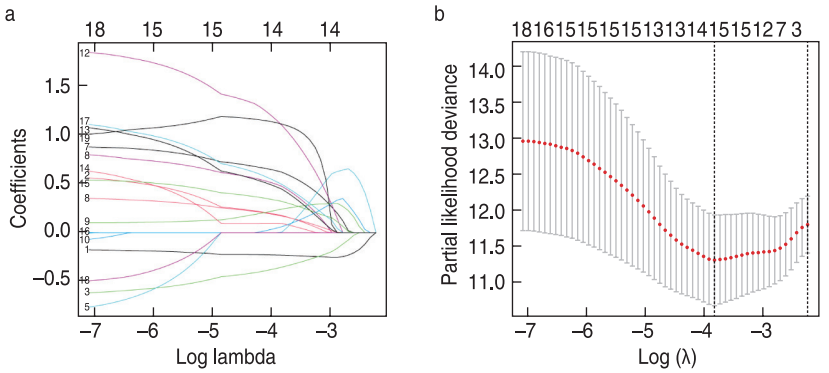

Fig. 2 Selection of prognostic RRGs by LASSO regression. (a) LASSO coefficient profiles of the prognostic RRGs. (b) Parameter selection in the LASSO model. RRGs: redox-related genes; LASSO: least absolute shrinkage and selection operator

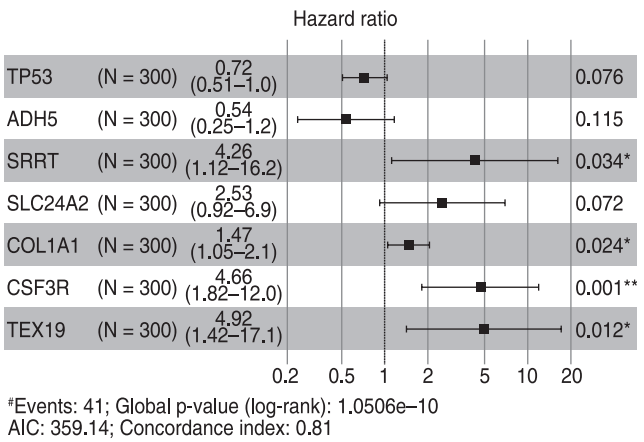

Fig. 3 Identification of prognostic RRGs by multivariate Cox regression analysis. RRGs: redox-related genes; * $P < 0.05$, ** $P < 0.001$

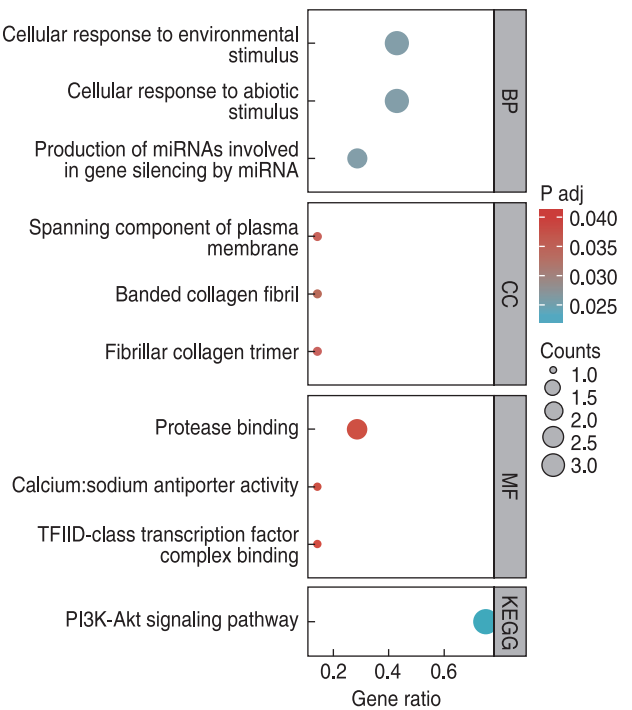

Fig. 4 GO and KEGG enrichment analysis. GO: Gene Ontology; KEGG: Kyoto Gene and Genome Encyclopedia; BP: biological process; CP: cellular component; MF: molecular function

cohort were used as validation sets to test the performance of the RRG signature. The results of the Kaplan-Meier survival analysis revealed that patients in the high-risk group had a worse BCR-free survival prognosis than those in the low-risk group (P = 0.015 in the TCGA validation cohort, Fig. 5b; P = 0.022 in the GSE84042 dataset, Fig. 5c). The AUC values of the 1st, 2nd, 3rd, 4th and 5th years were 0.762, 0.786, 0.849, 0.665, and 0.662, respectively, in the TCGA validation cohort (Fig. 5e) and 0.806, 0.742, 0.684, 0.713, and 0.722, respectively, in the GSE84042 dataset (Fig. 5f). The risk score curve, survival status, and gene expression heat maps of each patient in the TCGA training cohort, TCGA validation cohort, and GSE84042 dataset are shown in Fig. 5g–5o. Subsequently, the PCA results demonstrated that the RRGs signature could effectively distinguish patients with PCa with different BCR risks in the training and validation cohorts (Fig. 6). In addition, we used ROC analysis to compare the clinical performance of the prognostic signature and clinical parameters, including age, pT, GGS, and PSA. The AUC values of the prognostic signature, age, pT, GGS, and PSA levels were 0.803, 0.482, 0.682, 0.720, and 0.654, respectively (Fig. 7). This showed that the RRGs signature was a better model for predicting BCR of patients with PCa.

Clinical relevance of RRG signature

We used the Kaplan-Meier survival analysis of different clinicopathological stratifications to investigate the relationship between RRG-related prognostic signature and clinicopathological characteristics. Except for individuals with PSA > 4, the results showed that all high-risk groups had worse BCR-free survival outcomes

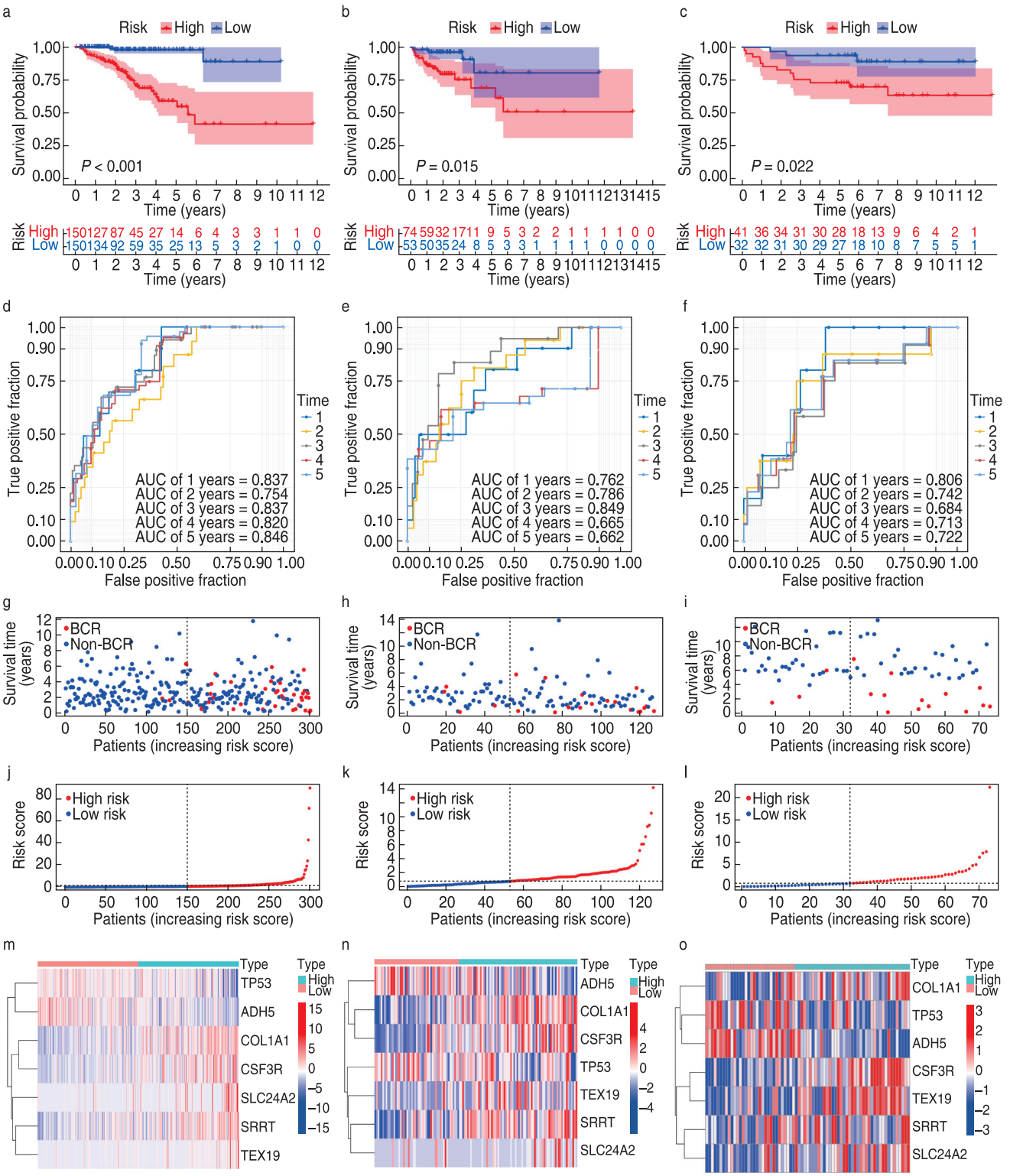

Fig. 5 Evaluation of the prognostic performance of the seven-RRG signature in the TCGA training cohort, TCGA internal validation cohort and GSE84042 external validation cohort. (a–c): Kaplan-Meier curve analysis in the high-risk and low-risk subgroups of the TCGA training cohort, TCGA internal validation cohort and GSE84042 external validation cohort. (d–f): The time-dependent ROC for 1st-, 2nd-, 3rd-, 4th- and 5th-year BCR predictions based on the RRG signature in the TCGA training cohort, TCGA internal validation cohort and GSE84042 external validation cohort. (g–o) The distribution of survival status, risk scores and expression of prognostic RRGs in the TCGA training cohort, TCGA internal validation cohort and GSE84042 external validation cohort

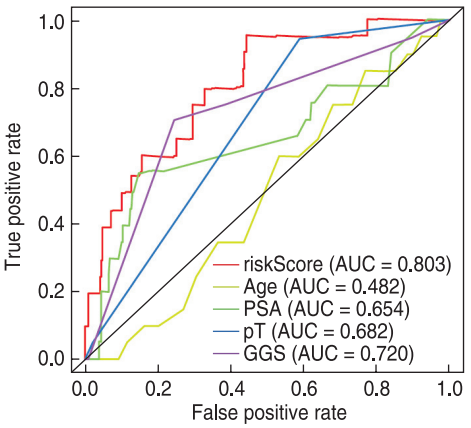

Fig. 6 The AUCs under ROC for comparing the diagnostic value among RRG signature, age, PSA, pT and GGS. AUC: area under ROC curve; ROC: receiver operating characteristic; RRG: redox-related gene; PSA: prostate specific antigen; pT: pathological T stage; GGS: Gleason grade score

than the low-risk groups (Fig. 8a–8h). We conclude that the RRGs-related prognostic signature could predict the prognosis of patients with PCa of different clinicopathological stratifications.

In addition, risk scores were compared based on clinicopathological status. The results showed that high pathological T stage, PSA value, and Gleason score were all linked to considerably higher RRG signature risk scores. The distribution of risk scores in the subgroups divided by age was not statistically different (P = 0.17, Fig. 9).

Identification of independent prognostic parameters

Univariate and multivariate Cox regression models were used to investigate the predictive value of different clinicopathological characteristics and RRG signature (Fig. 10). In the TCGA cohort, the Gleason score, pathological T stage, PSA value, and RRGs signature were significantly correlated with BCR-free survival. However, multiple regression analysis revealed that Gleason score, pathological T stage, and RRG signature were independent prognostic factors associated with BCR-free survival. In the GSE84042 cohort, the pathological T stage and the RRG signature were significantly correlated with BCR-free survival. After performing multivariate Cox regression analysis, these factors were identified as independent prognostic factors.

Construction and validation of a nomogram

We established a nomogram as a quantitative approach for predicting the prognosis of patients with PCa. In the TCGA cohort, the clinical parameters, age, and PSA were excluded from the nomogram because of their insignificant prognostic value. Gleason score, pathological T stage, and RRG signature were used to construct a nomogram (Fig. 11a). In both the TCGA and GSE84042 cohorts, the median risk score of the TCGA cohort was chosen as the cutoff value. The TCGA cohort was separated into high- and low-risk groups, and the high-risk group had a worse BCR-free survival outcome (P < 0.001; Fig. 11b). Patients in the GSE84042 cohort were similarly divided into two groups based on the same cut-off value, and the results revealed that those in the high-risk group had a worse prognosis (P < 0.001; Fig. 11c). Thereafter, we validated the clinical usefulness and availability of the nomogram using TCGA and GSE84042 cohorts. The AUCs for the first, second, third, fourth, and fifth years were 0.816, 0.775, 0.818, 0.806, and 0.850, respectively (Fig. 11d), and the C-index was 0.837 in the TCGA cohort (95% CI: 0.774–0.0.899, P < 0.0001). The AUCs were 0.919, 0.732, 0.776, 0.770 and 0.775 (Fig. 11e), and the C index was 0.808 in the GSE84042 cohort (95% CI: 0.728–0.888, P < 0.0001). The DCA curves demonstrated that the nomogram model was more effective than the clinical model in predicting BCR-free survival in patients with PCa (Fig. 11f and 11g).

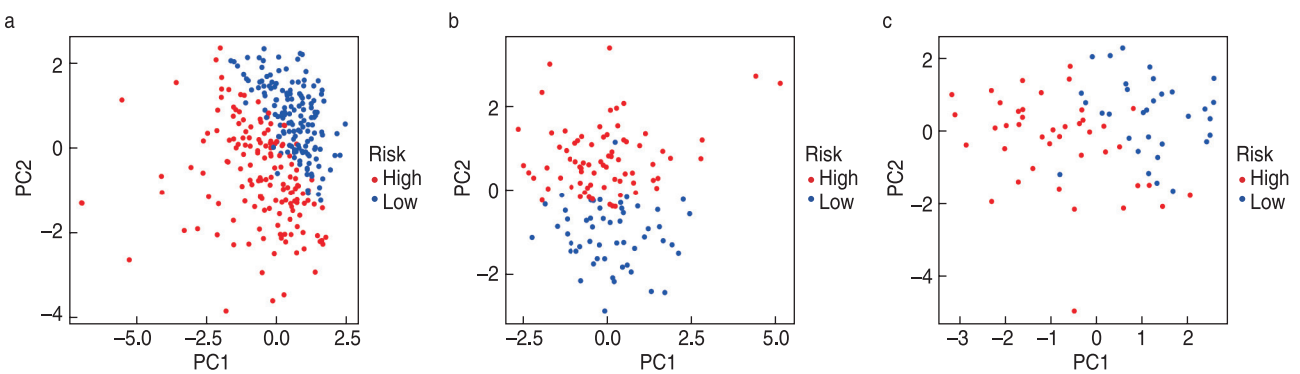

Fig. 7 (a) The results of PCA in the TCGA training cohort; (b) The results of PCA in the TCGA internal validation cohort; (c) The results of PCA in the GSE84042 external validation cohort. PCA: principal component analysis. TCGA: The Cancer Genome Atlas

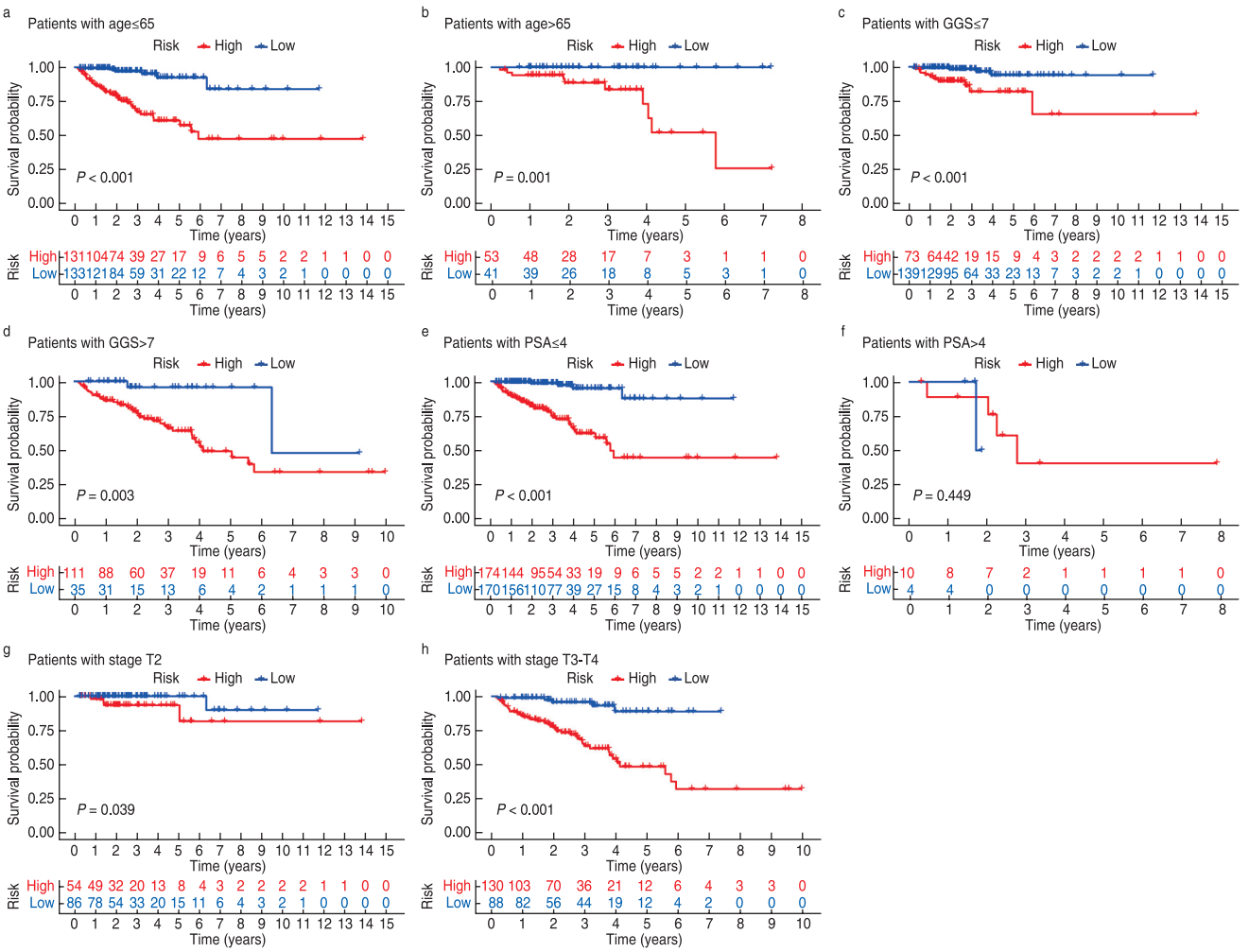

Fig. 8 Kaplan-Meier curve analysis of patients with PCa stratified by different clinicopathological stratifications. (a) Age ≤ 65 years; (b) Age > 65 years; (c) GGS ≤ 7; (d) GGS > 7; (e) pT: T2; (f) pT: T3–T4; (g) PSA value ≤ 4; (h): PSA value > 4. PCa: prostate cancer; GGS: Gleason grade score; pT: pathological T stage; PSA: prostate specific antigen

Discussion

In our study, we used the TCGA and GEO databases to retrieve transcriptome and clinicopathological data. Prognostic RRGs were identified by univariate, LASSO, and multivariate Cox regression analyses. Next, an RRGs signature was created to predict the BCR-free survival prognosis of patients with PCa. These genes included *TP53*, *ADH5*, *SRRT*, *SLC24A2*, *COL1A1*, *CSF3R*, and *TEX19*. The tumor suppressor gene *TP53* plays an important role in genomic integrity, cell cycle arrest, and other vital signaling pathways [15]. The wild-type *TP53* gene is lost in more than 50% of human cancers, and *TP53* mutations affect half of all metastatic PCa cases [16]. TP53 status has been shown to predict the clinical prognosis of castration-resistant prostate cancer and can be used as a biomarker for poor hormonal therapy responses [17]. *ADH5*, also known as S-nitrosoglutathione reductase (GSNOR), is a cellular denitrosylase that catalyzes the breakdown of SNOs to balance the intracellular thiol redox state [18, 19]. Studies have demonstrated that dysregulation of *ADH5* contributes to diseases such as asthma and breast cancer [18]. *SRRT*, also known as Ars2, plays a key role in sodium arsenite resistance [20]. It has been revealed that *SRRT* participates in the proliferation and migration of glioblastoma [21]. *SLC24A2* is a member of the solute carrier (SLC) family and is responsible for transporting compounds across biological molecules into cells [22]. SLC family members have been demonstrated to play roles in the carcinogenesis and prognosis of various cancers [23]. *COL1A1* participates in the encoding of type I collagen and belongs to the collagen family, which contributes to intercellular adhesion, cell differentiation and components of the extracellular matrix [24]. Gene dysfunction plays a critical role in the tumor development, metastasis, and prognosis of breast, lung,

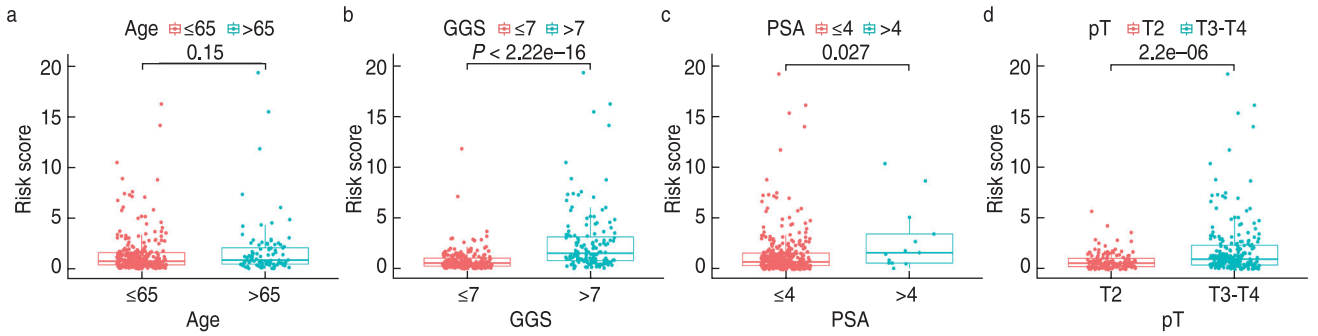

Fig. 9 The differential distribution of RRG signature risk scores between subgroups stratified by different clinical parameters and survival status. (a) Age; (b) GGS; (c) PSA; (d) pT. RRG: redox-related gene; GGS: Gleason grade score; PSA: prostate specific antigen; pT: Pathological T stage

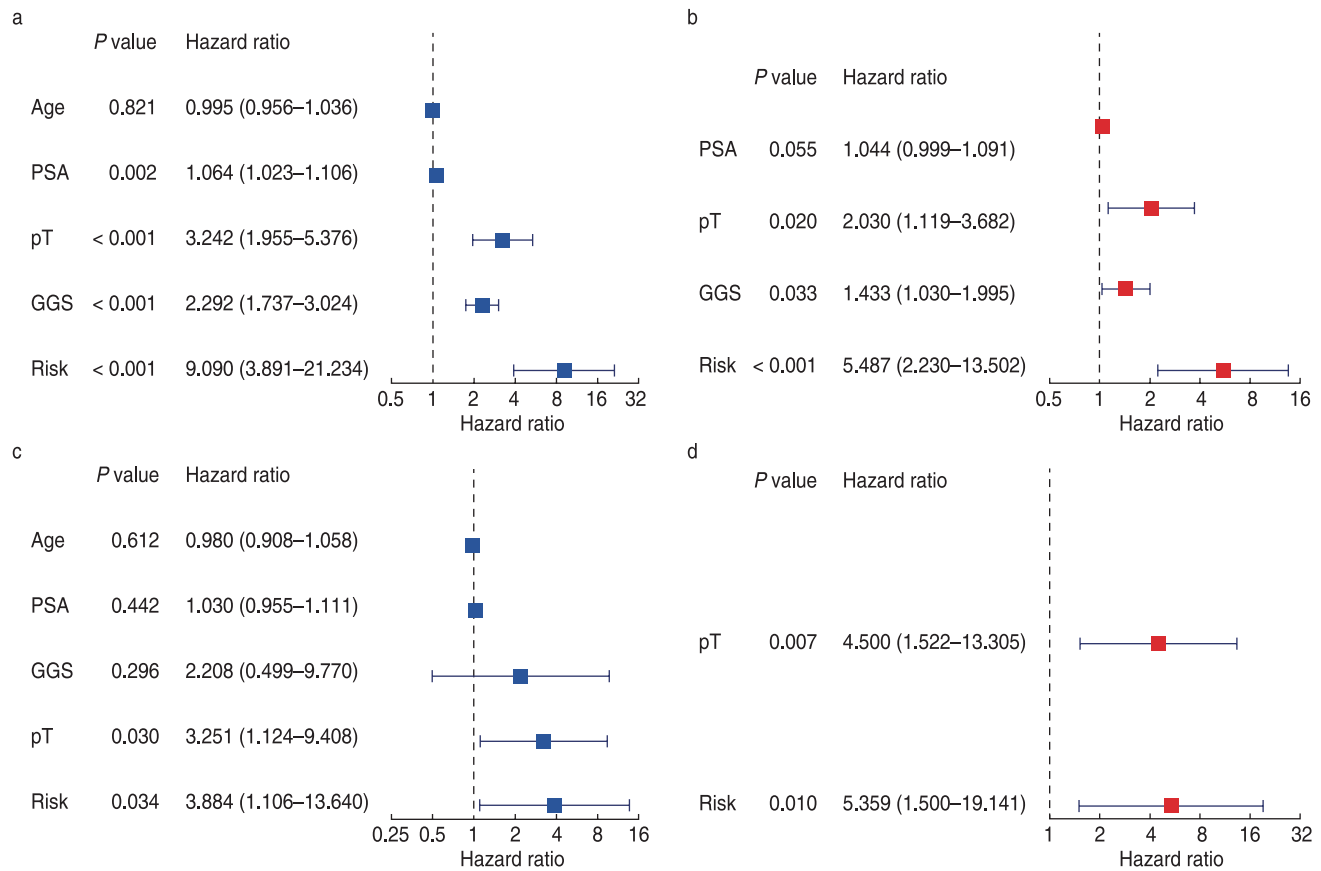

Fig. 10 Evaluation of independent prognostic factors based on clinicopathological parameters and the RRG signature in the TCGA and GSE84042 cohorts. (a) Univariate Cox regression analysis and (b) multivariate Cox regression analysis for evaluating independent prognostic factors in the TCGA cohort. (c) Univariate Cox regression analysis and (d) multivariate Cox regression analysis for evaluating independent prognostic factors in the GSE84042 cohort. RRGs: redox-related genes; TCGA: The Cancer Genome Atlas; PSA: prostate specific antigen; pT: pathological T stage; GGS: Gleason grade score

and hepatocellular cancers [24–26]. *CSF3R* is the colony-stimulating factor 3 receptor, and the encoded protein regulates the growth and differentiation of granulocytes [27]. A long-term survey revealed that patients with *CSF3R* mutations developed acute myeloid leukemia [28]. *TEX19* is an orphan gene expressed in adult testes, undifferentiated embryonic stem cells, and primordial germ cells [29]. *TEX19* has an impact on cancer cell proliferation and the initiation and prognosis of tumors [30].

We performed Kaplan-Meier and ROC curve analyses in the training and testing cohorts based on the RRGs signature, and the findings showed that the signature had an excellent prognostic ability to identify patients with a high risk for BCR. The patients were classified

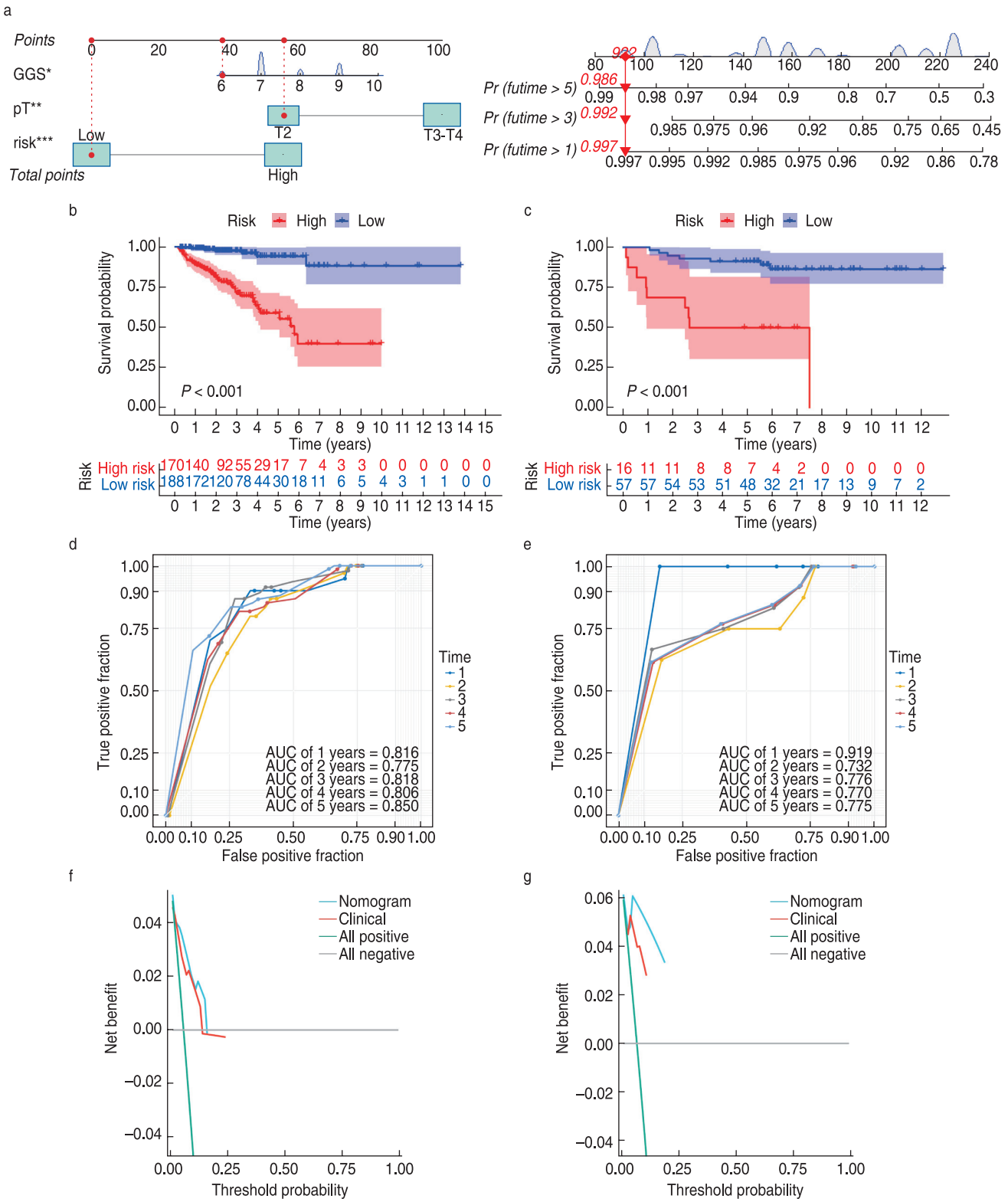

Fig. 11 The construction and validation of a nomogram. (a) Nomogram for predicting the 1st-, 3rd- and 5th-year BCR-free survival of patients with PCa in the TCGA cohort. (b and c) Kaplan-Meier curve analysis of the nomogram between high-risk and low-risk subgroups stratified by the cut-off value for the risk scores based on the nomogram model in the TCGA cohort and GSE84042 cohort, respectively. (d and e) The time-dependent ROC for 1st-, 2nd-, 3rd-, 4th- and 5th-year BCR predictions based on the nomogram model in the TCGA cohort and GSE84042 cohort, respectively. (f and g) The DCA curve of the nomogram in the TCGA cohort and GSE84042 cohort, respectively. *: $P < 0.05$, **: $P < 0.001$, ***: $P < 0.0001$; BCR: biochemical recurrence; PCa: prostate cancer; TCGA: The Cancer Genome Atlas; ROC: receiver operating characteristic; DCA: decision curve analysis

based on several clinical characteristics to investigate the relationship between the RRGs signature and clinical variables. We discovered that the RRGs signature could predict the prognosis of patients with PCa, except for those with PSA > 4 and that the signature was highly linked with clinical prognosis. It is possible that there were too few patients with PSA levels of > 4.

Additionally, a nomogram was developed to expand the clinical applications of the RRGs signature by combining clinical parameters. To verify the accuracy of the model in predicting PCa patient prognosis, Kaplan-Meier survival and ROC curve analyses were applied to TCGA and GSE84042 cohorts, and the results suggested that the model had good performance and efficiency in predicting prognosis.

Gene signatures based on different gene sets have been constructed to predict the prognosis of PCa. The Genomic Prostate Score (GPS) was based on 12 genes involved in PCa aggressiveness and 5 reference genes [31]. This score can evaluate the aggressiveness of PCa and help physicians to select the best therapy for patients [32]. Furthermore, GPS has significant predictive value for PCa recurrence [33]. The Prolaris Score is another polygenic genomic assay containing 31 genes involved in cell cycle progression that was established and confirmed to independently predict the BCR of PCa [34]. The Decipher genomic classifier is a gene profile comprising 22 genes created at the mRNA level to predict early metastasis and disease-specific mortality following radical prostatectomy [35].

In summary, our study provides new insights for the development of a novel signature based on RRGs to predict the clinical prognosis of patients with PCa. It has good predictive ability and clinical value and could help clinicians screen patients with a high probability of BCR and choose better treatment. However, our study has some limitations. First, the majority of patients in the training and validation cohorts were from North America; thus, caution should be taken when using the model for other nations. Secondly, the model was constructed and validated based on online data and should be validated using a prospective clinical cohort. However, the regulatory mechanisms underlying these prognostic RRGs require further investigation.

Conclusion

We established a novel RRGs prognostic prediction model using bioinformatic methods. This RRGs signature is an independent prognostic factor for assessing BCR survival in patients with PCa and could serve as a method for individualized risk stratification of patients with PCa. A nomogram was constructed to predict BCR survival, which would be useful for selecting personalized treatment.

Acknowledgements

Not applicable.

Funding

This work was supported by grants from the National Natural Science Foundation of China (No. 81902619) and National Natural Science Foundation of Hubei Province (No: 2020CFB591).

Conflict of interest

The authors have no conflicts of interest to disclose.

Author contributions

Conception and design: PH and GS; Data curation and methodology: PH, BC, and GS; data analysis and interpretation: PH, BC, and GS; manuscript preparation: PH and GS; manuscript review: JM; Study supervision: JM.

Data availability statement

Data used to support the findings of this study are available from the corresponding author upon request.

Ethical approval

Not applicable.

References

1. Salinas CA, Tsodikov A, Ishak-Howard M, et al. Prostate cancer in young men: an important clinical entity. Nat Rev Urol. 2014;11(6):317-323.
2. Siegel RL, Miller KD, Jemal A. Cancer statistics, 2019. CA Cancer J Clin. 2019;69(1):7-34.
3. Simmons MN, Stephenson AJ, Klein EA. Natural history of biochemical recurrence after radical prostatectomy: risk assessment for secondary therapy. Eur Urol. 2007;51(5):1175-1184.
4. Brockman JA, Alanee S, Vickers AJ, et al. Nomogram predicting prostate cancer-specific mortality for men with biochemical recurrence after radical prostatectomy. Eur Urol. 2015;67(6):1160-1167.
5. Dawane JS, Pandit VA. Understanding redox homeostasis and its role in cancer. J Clin Diagn Res. 2012;6(10):1796-1802.
6. Trachootham D, Lu W, Ogasawara MA, et al. Redox regulation of cell survival. Antioxid Redox Signal. 2008;10(8):1343-1374.
7. Singh A, Kukreti R, Saso L, et al. Oxidative stress: A key modulator in neurodegenerative diseases. Molecules. 2019;24(8):1583.
8. Dhalla NS, Temsah RM, Netticadan T. Role of oxidative stress in cardiovascular diseases. J Hypertens. 2000;18(6):655-673.
9. Valko M, Leibfritz D, Moncol J, et al. Free radicals and antioxidants in normal physiological functions and human disease. Int J Biochem Cell Biol. 2007;39(1):44-84.
10. Reuter S, Gupta SC, Chaturvedi MM, et al. Oxidative stress, inflammation, and cancer: how are they linked? Free Radic Biol Med. 2010;49(11):1603-1616.
11. Zhou D, Shao L, Spitz DR. Reactive oxygen species in normal and tumor stem cells. Adv Cancer Res. 2014;122:1-67.
12. Gupta-Elera G, Garrett AR, Robison RA, et al. The role of oxidative stress in prostate cancer. Eur J Cancer Prev. 2012;21(2):155-162.

13. Mortazavi A, Williams BA, McCue K, et al. Mapping and quantifying mammalian transcriptomes by RNA-Seq. Nat Methods. 2008;5(7):621-628.
14. Fraser M, Sabelnykova VY, Yamaguchi TN, et al. Genomic hallmarks of localized, non-indolent prostate cancer. Nature. 2017;541(7637):359-364.
15. Muller PA, Vousden KH. Mutant p53 in cancer: new functions and therapeutic opportunities. Cancer Cell. 2014;25(3):304-317.
16. Robinson D, Van Allen EM, Wu YM, et al. Integrative clinical genomics of advanced prostate cancer. Cell. 2015;161(5):1215-1228.
17. Hamid AA, Gray KP, Shaw G, et al. Compound genomic alterations of TP53, PTEN, and RB1 tumor suppressors in localized and metastatic prostate cancer. Eur Urol. 2019;76(1):89-97.
18. Barnett SD, Buxton ILO. The role of S-nitrosoglutathione reductase (GSNOR) in human disease and therapy. Crit Rev Biochem Mol Biol. 2017;52(3):340-354.
19. Benhar M, Forrester MT, Stamler JS. Protein denitrosylation: enzymatic mechanisms and cellular functions. Nat Rev Mol Cell Biol. 2009;10(10):721-732.
20. Elahi S, Egan SM, Holling GA, et al. The RNA binding protein Ars2 supports hematopoiesis at multiple levels. Exp Hematol. 2018;64:45-58.e9.
21. Ke XX, Pang Y, Chen K, et al. Knockdown of arsenic resistance protein 2 inhibits human glioblastoma cell proliferation through the MAPK/ERK pathway. Oncol Rep. 2018;40(6):3313-3322.
22. Lin L, Yee SW, Kim RB, et al. SLC transporters as therapeutic targets: emerging opportunities. Nat Rev Drug Discov. 2015;14(8):543-560.
23. Bhutia YD, Babu E, Ramachandran S, et al. SLC transporters as a novel class of tumour suppressors: identity, function and molecular mechanisms. Biochem J. 2016;473(9):1113-1124.
24. Geng Q, Shen Z, Li L, et al. COL1A1 is a prognostic biomarker and correlated with immune infiltrates in lung cancer. PeerJ. 2021;9:e11145.
25. Liu J, Shen JX, Wu HT, et al. Collagen 1A1 (COL1A1) promotes metastasis of breast cancer and is a potential therapeutic target. Discov Med. 2018;25(139):211-223.
26. Ma HP, Chang HL, Bamodu OA, et al. Collagen 1A1 (COL1A1) is a reliable biomarker and putative therapeutic target for hepatocellular carcinogenesis and metastasis. Cancers (Basel). 2019;11(6):786.
27. Beekman R, Touw IP. G-CSF and its receptor in myeloid malignancy. Blood. 2010;115(25):5131-5136.
28. Germeshausen M, Ballmaier M, Welte K. Incidence of CSF3R mutations in severe congenital neutropenia and relevance for leukemogenesis: Results of a long-term survey. Blood. 2007;109(1):93-99.
29. Xu Z, Tang H, Zhang T, et al. TEX19 promotes ovarian carcinoma progression and is a potential target for epitope vaccine immunotherapy. Life Sci. 2020;241:117171.
30. Planells-Palop V, Hazazi A, Feichtinger J, et al. Human germ/stem cell-specific gene TEX19 influences cancer cell proliferation and cancer prognosis. Mol Cancer. 2017;16(1):84.
31. Nguyen HG, Welty CJ, Cooperberg MR. Diagnostic associations of gene expression signatures in prostate cancer tissue. Curr Opin Urol. 2015;25(1):65-70.
32. Knezevic D, Goddard AD, Natraj N, et al. Analytical validation of the Oncotype DX prostate cancer assay – a clinical RT-PCR assay optimized for prostate needle biopsies. BMC Genomics. 2013;14:690.
33. Cullen J, Rosner IL, Brand TC, et al. A biopsy-based 17-gene genomic prostate score predicts recurrence after radical prostatectomy and adverse surgical pathology in a racially diverse population of men with clinically low- and intermediate-risk prostate cancer. Eur Urol. 2015;68(1):123-131.
34. Cuzick J, Swanson GP, Fisher G, et al. Prognostic value of an RNA expression signature derived from cell cycle proliferation genes in patients with prostate cancer: a retrospective study. Lancet Oncol. 2011;12(3):245-255.
35. Erho N, Crisan A, Vergara IA, et al. Discovery and validation of a prostate cancer genomic classifier that predicts early metastasis following radical prostatectomy. PLoS One. 2013;8(6):e66855.

DOI 10.1007/s10330-022-0594-4
Cite this article as: Hu P, Song GD, Chen BL, et al. Development of a redox-related prognostic signature for predicting biochemical-recurrence-free survival of prostate cancer. Oncol Transl Med. 2023;9(2):82-92.

Oncology and Translational Medicine
DOI 10.1007/s10330-022-0603-3

April 2023, Vol. 9, No. 2, 93–98

ORIGINAL ARTICLE

Preliminary security investigation and short-time follow-up of intraoperative intraperitoneal chemotherapy with lobaplatin for advanced colorectal cancer

Qin Li, Xianrong Li, Libo Feng, Xiaolong Chen, Dong Xia, Linxia Xu (✉)

Department of Gastrointestinal Surgery, The Affiliated Hospital, Southwest Medical University, Luzhou 646000, China

Abstract

Objective The aim of this study was to conduct a security assessment of intraoperative intraperitoneal chemotherapy using lobaplatin for advanced colorectal cancer.

Methods From February 2015 to February 2016, 143 patients with colorectal cancer who underwent surgery in our department were selected prospectively. All patients were randomly screened and enrolled into the intraperitoneal chemotherapy (IPC) (74 cases) and control (69 cases) groups, depending on the distribution of cases in the random table. In the trial group, patients were administered 40 mg lobaplatin by intraperitoneal implantation intraoperatively, together with intravenous chemotherapy post-operatively using a typical FOLFOX strategy with oxaliplatin, fluorouracil, and leucovorin. In the control group, only FOLFOX was administered. Bowel function recovery time, adverse reactions and complications, and pre- and post-chemotherapy laboratory examinations were compared. In addition, a 5-year-long follow-up was performed.

Results Recovery times of bowel function were 73.5 ± 9.7 h and 74.8 ± 10.3 h respectively, and the difference was not significant ($P > 0.05$). Wound fat liquefaction was observed in five cases in both groups (6.8% *vs*. 7.2%, $P > 0.05$). The outcomes of nausea and vomiting (57 cases, 77.0% *vs*. 50 cases, 72.5%), constipation (43 cases, 58.1% *vs*. 36 cases, 52.2%), and diarrhea (5 cases, 6.8% *vs*. 5 cases, 7.2%) were not statistically significant (all $P > 0.05$). Indices of white blood cell count, blood platelet count, and hepatorenal function were not significantly different (all $P>0.05$) neither post-operatively nor post-chemotherapy. The 5-year survival rate was not significantly different between the groups (58.1% *vs*. 56.5%, $P > 0.05$).

Conclusion Intraoperative chemotherapy with lobaplatin for advanced colorectal cancer is safe and tolerable.

Received: 22 October 2022
Revised: 3 November 2022
Accepted: 13 February 2023

Key words: intraoperative intraperitoneal chemotherapy; lobaplatin; colorectal cancer

Chemotherapy can be divided into systemic and loco-regional therapies, based on the method of administration. Intraperitoneal chemotherapy (IPC) is a local application that has received increasing attention at home and abroad for advanced gastrointestinal malignancies [1-3]. The theoretical rationale of IPC was first described in 1978, which demonstrated that intraperitoneal administration of chemotherapeutic drugs for ovarian cancer led to a higher drug concentration and longer half-life in the peritoneal cavity than intravenous administration [4]. Intraperitoneal chemotherapy presents an exciting consequence in the field of gynecological oncology as it promotes both progression-free survival and overall survival in advanced ovarian malignant tumors [5]. Due to this delightful condition, the National Comprehensive Cancer Network (NCCN) guidelines now recommend IPC for patients with stage III epithelial ovarian cancer after optimal debulking surgery [6]. Intraperitoneal administration of antitumor drugs is also performed in gastrointestinal oncology, and IPC for gastric and

✉ Correspondence to: Linxia Xu. Email: 14369372@qq.com

rectal cancers has been researched in full swing [7, 8]. IPC can expose free tumor cells or residual tumor tissue to therapeutic drugs directly and immediately, which would not only enhance the anti-cancer efficiency but also relieve the systemic adverse reactions due to the peritoneum-plasma barrier [9]. Currently, a few drugs commonly used in IPC primarily include cyclophosphamide, platinum, mitomycin, and fluorouracil sustained-release preparations [10] for abdominal malignant tumors. Lobaplatin is one of the third-generation platinum drugs, which is used in gynecologic and thoracic tumors by serous-cavity injection in lung cancers and oophoromas, but few investigations have been conducted on gastrointestinal carcinomas. The efficacy of this treatment is not known. Hence, security assessment data are limited. This study was mainly aimed at observing the safety of intraoperative IPC with lobaplatin in advanced colorectal cancer, and the 5-year survival rate was also observed to speculate whether this strategy plays a role in improving survival time.

Materials and methods

Patients

A total of 143 colorectal cancer patients (Table 1) undergoing surgical operations were enrolled in this study between February 2015 and February 2016 in the Department of Gastrointestinal Surgery, the Affiliated Hospital, Southwest Medical University. After signing informed consent, they were randomly allocated into an experimental group of 74 patients and a control group of 69 patients, according to the case distribution random table. This study was approved by the Ethics Committee of our hospital. Tumor stage classification was performed according to the 8th edition of the AJCC Cancer Staging Manual [11]. The inclusion criteria were as follows:

(1) The patients had not undergone abdominal surgery before, and did not have diabetes, hyperthyroidism, hypothyroidism, post-operative hypokalemia, or any other diseases that could affect gastrointestinal function.

(2) Tumors affected or penetrated the serous membrane layer and could undergo radical or palliative resection.

(3) Blood indicators met the basic requirement for chemotherapy: white blood cell count (WBC) > 3.0×10^9/L, blood platelet count (PLT) > 100×10^9/L, hemoglobin (Hb) > 100 g/L, and indices of hepato-renal function, such as alanine aminotransferase (ALT), aspartate transaminase (AST), and creatinine (Cr.) were normal.

(4) The age range was from 55 to 80 years.

Table 1 The general materials of this 143 patients, [*n* (%)]

	Group A	Group B	*P* value
No. of patients	74	69	
Gender			
Male	42 (56.8)	40 (58.0)	> 0.05
Female	32 (43.2)	29 (42.0)	
Age (years)	59.4 ± 10.8	56.9 ± 10.2	> 0.05
Site			
Colon	31 (41.9)	28 (40.6)	> 0.05
Rectum	43 (58.1)	41 (59.4)	
Stage			
III	68 (91.9)	64 (92.8)	> 0.05
IV	6 (8.1)	5 (7.2)	
Time (min)	136.8 ± 14.7	134.5 ± 15.8	> 0.05
Operation selection			
Radically	67 (90.5)	63 (91.3)	> 0.05
Palliatively	7 (9.5)	6 (8.7)	

Group A means intraperitoneal chemotherapy group, Group B means the control group

Protocol treatment

All the patients underwent surgical resection. The operations were performed by the same set of surgeons who possessed the necessary qualifications and ample experience. Various methods were carried out according to the practical situation during the operation, such as left, right-half, and transverse colon resection, low anterior resection (LAR, Dixon), abdominoperineal resection (APR, Miles) for rectal cancers, as well as Hartmann and colostomy.

In the IPC group, 40 mg lobaplatin (Hainan Changan International Pharmaceutical Co., Ltd.) was mixed with 20 mL 5% glucose at room temperature. The mixed solution was then extensively infused into the washed cavity in the IPC group. In the control group, the same quantity of room-temperature 5% glucose, with no other composition, was infused into the peritoneal cavity. In both groups, the drainage tube was fixed at the proper site of the abdominal wall and kept off for 4 to 6 h after the operation. As soon as the operated patient exhausted, defecated, and could have some liquid diet, he or she would receive systemic chemotherapy using the FOLFOX scheme with oxaliplatin (Jinghua Pharmaceutical Group Co., Ltd.), fluorouracil, and leucovorin (Jiangsu Hengrui Medicine Co., Ltd.), according to the NNCN guidelines for colorectal cancer [12].

Observation indices

Immediately after the operation, daily observations were conducted including temperature monitoring, bowel sound auscultation, exhaust and defecation inquiry, and observation of drainage condition. Early in the morning before and after intravenous chemotherapy, hematological indices, including ALT, AST, and Cr, were retested hollowly.

Statistical analysis

All data were analyzed using the professional statistical software SPSS 20.0. If the data were not normally distributed, we used the median (quarterback spacing) [M (P25, P75)] for description and using rank and inspection, we used an inspection level of α= 0.05. If the data was normally distributed, we used the mean ± standard deviation ($\bar{\chi} \pm s$) to represent the parametric test using the *t*-test and Fisher's exact probability method.

Results

Bowel function recovery time

The recovery times of bowel function in the IPC and control group were 73.5 ± 9.7 h and 74.8 ± 10.3 h, respectively, with no significant difference ($P > 0.05$). The drainage volume was not significantly different until the tubes were pulled out (160 ± 20 mL *vs.* 150 ± 30 mL, $P > 0.05$). Tubes were pulled out after bowel function recovery and patients defecated without fistula, and the time to abandon the tubes were 96 ± 12 h post-operatively.

Complications of surgery plus IPC (Table 2)

Each group had six cases of incisional fat liquefaction (6.8% *vs.* 7.2%, $P > 0.05$), some of which developed into infection (three cases vs. two cases). These complications were controlled and cured by squeezing the incisions, taking out sutures, enlarging the incisions, debriding necrotic tissues, draining liquid, and finally placing a secondary suture. Fortunately, no IP or systemic infections occurred. Some patients in the two groups experienced abdominal distension, nausea, and vomiting (three cases vs. two cases), and the symptoms disappeared after removal of the nasogastric tube one to three days after surgery. Five patients (three cases vs. two cases) who were not exhausting and defecating five days after surgery in the two groups were considered to have bowel obstruction. One patient in the therapy group underwent exploratory laparotomy because of the invalidation of expectant treatments, which ultimately proved to be an adhesive intestinal obstruction. However, the rest were cured via non-surgical treatments and recuperated three to four days after treatment.

Side effects and adverse reactions (Table 3)

During intravenous chemotherapy in the IPC and control groups, there was occurrence of nausea and vomiting (57 cases, 77.0% *vs.* 50 cases, 72.5%), constipation (43 cases, 58.1% *vs.* 36 cases, 52.2%), and diarrhea (5 cases, 6.8% *vs.* 5 cases, 7.2%), and there was no statistical significance (all $P > 0.05$). All of these side effects vanished after chemotherapy or were cured by

Table 2 Postoperative complications, [*n* (%)]

Group	Patients (*n*)	Nausea and vomiting	Constipation	Diarrhea	Poor wound healing		Bowel obstruction	Anastomotic fistula
					Fat liquefaction	Infection		
Group A	74	57 (77.0)	43 (58.1)	5 (6.8)	5 (6.8)	3 (4.1)	3 (4.1)	0
Group B	69	50 (72.5)	36 (52.2)	5 (7.2)	5 (7.2)	2 (4.3)	2 (2.9)	0

Group A means intraperitoneal chemotherapy group, Group B means the control group

Table 3 Haematological indexes before and after IPC and IV chemotherapy

Group	*n*	WBC (× 10^9/L)	PLT (× 10^9/L)	AST (U/L)	ALT (U/L)	GR (μmol/L)
Preoperative						
Group A	74	6.56 (4.7–8.3)	137 (118–183)	22.4 (9.7–29.5)	15.8 (9.3–19.4)	67.1 ± 10.6
Group B	69	6.9 (5.4–7.9)	140 (120–197)	20.2 (11.8–28.4)	16.2 (11.3–21.7)	66.6 ± 9.8
P value		> 0.05	> 0.05	> 0.05	> 0.05	> 0.05
Postoperative[a]						
Group A	74	9.3 (8.1–12.9)	135 (128–207)[b]	27.8 (12.8–33.1)[b]	31.1 (14.3–38.5)[b]	50.5 ± 12.4
Group B	69	9.6 (6.7–13.8)	152 (130–217)[b]	26.2 (13.4–33.6)[b]	28.2 (15.4–36.2)[b]	54.9 ± 14.6
P value		> 0.05	> 0.05	> 0.05	> 0.05	> 0.05
Post-chemotherapy						
Group A	74	5.1 (4.2–6.7)	114 (100–167)[b]	33.7 (19.7–49.8)[b]	37.8 (23.2–45.2)[b]	86.2 ± 10.6[b]
Group B	69	5.3 (3.8–6.1)	115 (104–171)[b]	35.6 (22.6–51.1)[b]	38.2 (24.5–52.1)[b]	91.4 ± 9.4[b]
P value		> 0.05	> 0.05	> 0.05	> 0.05	> 0.05

Group A means intraperitoneal chemotherapy group, Group B means the control group; [a] These data were recorded just the day before intravenous chemotherapy, that was also pre-chemotherapy; [b] Compared with preoperative data in each group internally *P* value < 0.05

symptomatic treatment. In each group, when compared with pre-operative levels, the post-operative levels of ALT, AST, Cr, WBC, and PLT were significantly increased, and the difference was statistically significant ($P < 0.05$). However, the difference between the two groups was insignificant ($P > 0.05$).

Follow-up results (Table 4)

A few patients missed follow-up and died every year since the second year post-operatively during the 5-year follow-up period. The 1-, 3-, and 5-year survival rates were similar, but the differences were not significant (all $P > 0.05$).

Discussion

The most common reason why intestinal tumors plant, metastasize, and recur after operation is that malignant cells fall into the abdominal cavity and microscopic cancer remains in the cavity [13, 14]. Cancer cells can drop into the abdominal cavity when they invade the serosa of the intestinal tract as the adhesive force among the cells weakens. In addition, they can also come from micrometastases in the lymphatic or blood circulation system. Exfoliation and spreading of tumor cells can be intraperitoneal and transperitoneal and tend to follow the circulatory path of the peritoneal fluid. These behaviors lead to peritoneal carcinomatosis (PC) or peritoneal metastasis (PM), which is detected synchronously during primary resection in approximately 5% of patients and develops metachronously in 4%–19% of patients with colorectal cancer [15–17]. The reported incidence of PC at autopsy in patients who died from CRC ranges from 40% to 80% [15]. In peritoneal carcinomatosis from non-gynecologic malignancies, including gastric, colorectal, and pancreatic cancer, the median survival time is less than six months [18]. In China, most patients with colorectal cancer are confirmed to be at an advanced stage, which means that there might be many more free cancer cells and micrometastases existing and/or retained in the abdominal cavity. It is impossible to clear all the tumor cells, even by accepted radical resection. However, most of the cells can be eliminated by perioperative chemotherapy and rinsed repeatedly with distilled water.

IPC is a highly selective regional chemotherapy compared with systemic chemotherapy, which has the following advantages: [19–23] (1) It can improve the local drug concentration remarkably and enhance the lethal effect on residual microscopic lesions and cells directly. (2) It can strengthen local anti-cancer effects, since IP drugs are difficult to transit through the peritoneum-plasma barrier, which can also slow down the rapid entry of drugs through the peritoneum and portal system. (3) Drugs are mostly absorbed into the liver via the portal vein system, but only a small part diverts into the systemic circulation, thereby relieving systemic toxicity and reaching the maximum tolerance dose of chemotherapeutic drugs. (4) Drugs can be absorbed through the lymphatic system, which plays a positive role in microscopic metastases remaining in this system. Because of these specific characteristics, IPC has been studied as a third approach to prevent the relapse and metastasis of gastrointestinal malignancies.

Effective drugs used for IPC must have low peritoneal permeability and irritation, strong penetrating power into tumoral tissue, fast plasma ablation rate, high water solubility, and heavy molecular mass. Lobaplatin (D-19466) is a diastereomeric mixture of platinum complexes containing a stable 1, 2-bis (aminomethyl) cyclobutane ligand with lactic acid as the leaving group. Lobaplatin influences the expression of the *c-myc* gene, which is involved in oncogenesis, apoptosis, and proliferation. Lobaplatin is a third-generation platinum with a heavy molecular mass and better peritoneal permeability and irritation. Compared with cisplatin, lobaplatin is considered less toxic, more soluble, and stable in water [24–26]. It possesses the requisite factors to be a useful IP anticancer drug. In January 2003, lobaplatin was licensed to Hainan Tianwang International Pharmaceutical in China [27] and approved for use in clinical anti-tumor therapy for lung cancer, breast cancer, and chronic myelogenous leukemia by the China State Food and Drug Administration (CFDA). Before being approved clinically, lobaplatin was investigated in a series of phase I and II trials overseas [27–29]. The trials demonstrated that lobaplatin was a dose-dependent drug, and it was safer

Table 4 5-year follow-up data

Time post-operatively (years)	Group A				Group B				Anastomotic fistula
	Recurrence/ Metastasis (*n*)	Loss of follow-up (*n*)	Death (*n*)	SR (%)	Recurrence/ Metastasis (*n*)	Loss of follow-up (*n*)	Death (*n*)	SR (%)	
1	0	0	0	100	0	0	0	100	> 0.05
2	3	2	4	94.6	2	2	5	92.8	> 0.05
3	14	3	7	85.1	12	3	6	84.1	> 0.05
4	7	2	9	73.0	9	3	9	71.0	> 0.05
5	10	6	11	58.1	8	5	10	56.5	> 0.05

to administer 5 days of continuous IV push or 72 h of continuous pumping every four weeks with doses ranging from 30 to 60 mg/m^2. The recommended dose was 50mg/m^2, and the maximum tolerated dose was 60 mg/m^2. These studies also revealed that the most common complication was thrombocytopenia, while nausea, vomiting, appetite loss, and leukocytopenia were less frequent.

An increasing number of tumors have been treated with lobaplatin since it was permitted in China, and abdominal cancers, such as gynecological cancers and gastrointestinal cancers, have been treated with lobaplatin. As for gastrointestinal tumors, lobaplatin is effective and has less side effects [27–33]. The reason why we chose lobaplatin as the research object was that this drug was much more stable and was verified to be effective, with fewer side effects for treating colorectal cancer in many trials both in vitro and *in vivo* [27-33].

This research was a randomized control study. The patients who were included strictly agreed with the formulated inclusion criteria, and they were randomly divided into treatment and control groups. The general clinical data had no statistical difference, so they could be comparable. The major observation items, which were also the probable complications that might be caused by IPC and systemic chemotherapy, included post-operative bowel function recovery complications such as abdominal distention, nausea, vomiting, anastomotic fistula, infection of incision, and systemic toxic reactions, (e.g., abnormalities in liver and kidney function, white blood cell count, and platelet count). The main purpose was to investigate whether patients could tolerate the toxic and side effects and whether any increase in adverse reactions would occur when IPC using lobaplatin was used at a prescribed dosage. By comparison, we found no statistical differences between the two groups with respect to intestinal function recovery time, post-operative complications, and toxic reactions of other systems. This suggests that IP lobaplatin does not cause any serious complications in patients with advanced CRC. Changes in hematologic indices in the investigation were considered to be caused by systemic chemotherapy.

These findings suggest that the technique using lobaplatin for IPC causes no serious toxic reactions and side effects and will not affect the normal recovery and systemic chemotherapy process post-operatively. However, this study did not compare the differences in various surgical procedures, especially radical and palliative resections. Although the follow-up data were recorded, there were unexpected absent cases. Therefore, the data may not be completely accurate. A better follow-up management mechanism and data-collection system are required. Because of the small sample size and the limited study items, larger multi-center randomized controlled clinical trials should be carried out to explore the optimal concentration and dose of lobaplatin on treating gastrointestinal malignant tumors that will be necessary to cause a significant change. In addition, survival time must be considered as an endpoint to determine the efficacy of the process.

Conclusion

Although it cannot improve survival time, intraoperative IPC with lobaplatin for elective surgeries is safe and tolerant, and when combined with intravenous chemotherapy, it does not increase the incidence of hepato-renal function damage or induce bone marrow suppression or other side effects.

Acknowledgments

Not applicable.

Funding

Not applicable.

Conflicts of interest

The authors indicated no potential conflicts of interest.

Author contributions

All authors contributed to data acquisition, data interpretation, and reviewed and approved the final version of this manuscript.

Data availability statement

The data supporting the findings of this study are available from the corresponding author upon reasonable request.

Ethical approval

The study has been reviewed and approved by the ethics committee.

References

1. Coccolini F, Cotte E, Glehen O, et al. Intraperitoneal chemotherapy in advanced gastric cancer. Meta-analysis of randomized trials. Eur J Surg Oncol. 2014;40(1):12-26.
2. Huang XE, Wei GL, Huo JG, et al. Intrapleural or intraperitoneal lobaplatin for treatment of patients with malignant pleural effusion or ascites. Asian Pac J Cancer Prev. 2013;14(4):2611-2614.
3. Kitayama J. Intraperitoneal chemotherapy against peritoneal carcinomatosis: current status and future perspective. Surg Oncol. 2014;23(2):99-106.
4. Dedrick RL, Myers CE, Bungay PM, et al. Pharmacokinetic rationale for peritoneal drug administration in the treatment of ovarian cancer. Cancer Treat Rep. 1978;62(1):1-11.
5. Jaaback K, Johnson N, Lawrie TA. Intraperitoneal chemotherapy for the initial management of primary epithelial ovarian cancer. Cochrane Database Syst Rev. 2016;2016(1):CD005340.
6. Lheureux S, Gourley C, Vergote I, et al. Epithelial ovarian cancer. Lancet. 2019;393(10177):1240-1253.

7. Coccolini F, Fugazzola P, Ansaloni L, et al. Advanced gastric cancer: the value of systemic and intraperitoneal chemotherapy. Acta Biomed. 2018;89(8-S):104-109.
8. Eng OS, Turaga KK. Cytoreduction and hyperthermic intraperitoneal chemotherapy in metastatic colorectal cancer. J Surg Oncol. 2019;119(5):613-615.
9. Amira G, Morsi A, Fayek IS, et al. Hyperthermic intraperitoneal chemotherapy versus systemic chemotherapy in recurrent platinum-sensitive ovarian cancer NCI case control study. Asian Pac J Cancer Prev. 2019;20(2):621-627.
10. Emoto S, Sunami E, Yamaguchi H, et al. Drug development for intraperitoneal chemotherapy against peritoneal carcinomatosis from gastrointestinal cancer. Surg Today. 2014;44(12):2209-2220.
11. Amin MB, Greene FL, Edge SB, et al. The Eighth Edition AJCC Cancer Staging Manual: Continuing to build a bridge from a population-based to a more "personalized" approach to cancer staging. CA Cancer J Clin. 2017;67(2):93-99.
12. Benson AB, Venook AP, Al-Hawary MM, et al. Colon cancer, version 2.2021, NCCN clinical practice guidelines in oncology. J Natl Compr Canc Netw. 2021;19(3):329-359.
13. Franko J. Therapeutic efficacy of systemic therapy for colorectal peritoneal carcinomatosis: Surgeon's perspective. Pleura Peritoneum. 2018;3(1):20180102.
14. Canda AE, Arslan C, Terzi C, et al. Treatment of intraoperatively detected peritoneal carcinomatosis of colorectal origin with cytoreductive surgery and intraperitoneal chemotherapy. World J Surg Oncol. 2018;16(1):70.
15. Razenberg LG, van Gestel YR, Lemmens VE, et al. Bevacizumab in addition to palliative chemotherapy for patients with peritoneal carcinomatosis of colorectal origin: a nationwide population-based study. Clin Colorectal Cancer. 2016;15(2):e41-46.
16. Enblad M, Graf W, Birgisson H. Risk factors for appendiceal and colorectal peritoneal metastases. Eur J Surg Oncol. 2018;44(7):997-1005.
17. Sadeghi B, Arvieux C, Glehen O, et al. Peritoneal carcinomatosis from non-gynecologic malignancies: results of the EVOCAPE 1 multicentric prospective study. Cancer. 2000;88(2):358-363.
18. Gelli M, Huguenin JF, Cerebelli C, et al. Strategies to prevent peritoneal carcinomatosis arising from colorectal cancer. Future Oncol. 2017;13(10):907-918.
19. Cavaliere F, De Simone M, Virzì S, et al. Prognostic factors and oncologic outcome in 146 patients with colorectal peritoneal carcinomatosis treated with cytoreductive surgery combined with hyperthermic intraperitoneal chemotherapy: Italian multicenter study S.I.T.I.L.O. Eur J Surg Oncol. 2011;37(2):148-154.
20. Miller EM, Tymon-Rosario J, Xie X, et al. Utilization of intraperitoneal chemotherapy for optimally cytoreduced advanced stage epithelial ovarian cancer: A 10-year single institution experience with a racially diverse urban population. Gynecol Oncol. 2017;147(1):36-40.
21. Sloothaak DA, Mirck B, Punt CJ, et al. Intraperitoneal chemotherapy as adjuvant treatment to prevent peritoneal carcinomatosis of colorectal cancer origin: a systematic review. Br J Cancer. 20149;111(6):1112-1121.
22. Eveno C, Haidara A, Ali I, et al. Experimental pharmacokinetics evaluation of chemotherapy delivery by PIPAC for colon cancer: first evidence for efficacy. Pleura Peritoneum. 2017;2(2):103-109.
23. Bouchard-Fortier G, Rosen B, Vyarvelska I, et al. A comparison of the toxicity and tolerability of two intraperitoneal chemotherapy regimens for advanced-stage epithelial ovarian cancer. Gynecol Oncol. 2016;140(1):36-41.
24. Voegeli R, Schumacher W, Engel J, et al. D-19466, a new cyclobutane-platinum complex with antitumor activity. J Cancer Res Clin Oncol. 1990;116(5):439-442.
25. McKeage MJ. Lobaplatin: a new antitumour platinum drug. Expert Opin Investig Drugs. 2001;10(1):119-128.
26. Lobaplatin: D 19466. Drugs R D. 2003;4(6):369-372.
27. Gietema JA, Guchelaar HJ, de Vries EG, et al. A phase I study of lobaplatin (D-19466) administered by 72 h continuous infusion. Anticancer Drugs. 1993;4(1):51-55.
28. Gietema JA, de Vries EG, Sleijfer DT, et al. A phase I study of 1,2-diamminomethyl-cyclobutane-platinum (II)-lactate (D-19466; lobaplatin) administered daily for 5 days. Br J Cancer. 1993;67(2):396-401.
29. Langdon SP, Hendriks HR, Braakhuis BJ, et al. Preclinical phase II studies in human tumor xenografts: a European multicenter follow-up study. Ann Oncol. 1994;5(5):415-422.
30. Li Y, Liu B, Yang F, et al. Lobaplatin induces BGC-823 human gastric carcinoma cell apoptosis via ROS- mitochondrial apoptotic pathway and impairs cell migration and invasion. Biomed Pharmacother. 2016;83:1239-1246.
31. Harstrick A, Bokemeyer C, Scharnofkse M, et al. Preclinical activity of a new platinum analogue, lobaplatin, in cisplatin-sensitive and -resistant human testicular, ovarian, and gastric carcinoma cell lines. Cancer Chemother Pharmacol. 1993;33(1):43-47.
32. Dai HY, Liu L, Qin SK, et al. Lobaplatin suppresses proliferation and induces apoptosis in the human colorectal carcinoma cell Line LOVO in vitro. Biomed Pharmacother. 2011;65(3):137-141.
33. Wei W, Liu Z, Chen X, et al. Chemosensitivity of resistant colon cancer cell lines to lobaplatin, heptaplatin, and dicycloplatin. Int J Clin Pharmacol Ther. 2014;52(8):702-707.

DOI 10.1007/s10330-022-0603-3
Cite this article as: Li Q, Li XR, Feng LB, *et al*. Preliminary security investigation and short-time follow-up of intraoperative intraperitoneal chemotherapy with lobaplatin for advanced colorectal cancer. Oncol Transl Med. 2023;9(2):93-98.

Oncology and Translational Medicine

Volume 9 • Number 2 • April 2023

Aims & Scope

Oncology and Translational Medicine (OTM) is an international, open-access, peer-reviewed academic journal that aims to promote research in oncology and translational medicine as well as levels of service in clinical practice. It publishes the results of novel research investigations which bridge the laboratory and clinical settings including risk assessment, cellular and molecular characterization, prevention, detection, diagnosis and treatment of human cancers with the overall goal of improving the clinical care of oncology patients. OTM covers the types of Original research, Review articles, Consensus and Guideline, Perspectives, Letters to the Editor, Editorials, Commentary, Personage Column, Case Report, etc.

Copyright

Supervised by

Ministry of Education of the People's Republic of China.

Administered by

Tongji Medical College, Huazhong University of Science and Technology.

Submission Information

Manuscripts should be submitted to:
http://otm.tjh.com.cn
otm.office@tjh.tjmu.edu.cn

Subscription Information

ISSN edition: 2095-9621
CN: 42-1865/R

■ Subscription rates

Subscription may begin at any time. Remittances made by check, draft or express money order should be made payable to this journal. The price for 2023 is as follows: US $ 30 per issue; RMB ¥28.00 per issue.

Database

Oncology and Translational Medicine is abstracted and indexed in EMBASE, Index Copernicus, Chinese Science and Technology Paper Citation Database (CSTPCD), Chinese Core Journals Database, Chinese Journal Full-text Database (CJFD), Wanfang Data; Weipu Data; Chinese Academic Journal Comprehensive Evaluation Database.

Business Correspondence

All matters relating to orders, subscriptions, back issues, offprints, advertisement booking and general enquiries should be addressed to the editorial office.

Mailing address
Editorial office of
Oncology and Translational Medicine
Tongji Hospital
Tongji Medical College
Huazhong University of Science and Technology
Jie Fang Da Dao 1095
430030 Wuhan, China
Tel.: +86-27-83662395
Email: otm.office@tjh.tjmu.edu.cn

Printer
Changjiang Spatial Information Technology Engineering Co., Ltd. (Wuhan) Hangce Information Cartorgraphy Printing Filial, Wuhan, China
Printed in People's Republic of China

Editors-in-Chief

Managing Director

Executive Editors